UNIVERSITY OF CALIFORNIA SAN DIEGO
SAN DIEGO STATE UNIVERSITY

Data-supported modeling of climate change impacts on coastal water infrastructure for developing community-based adaptation strategies

A Dissertation submitted in partial satisfaction of the requirements for the degree
Doctor of Philosophy

in

Engineering Sciences (Mechanical and Aerospace Engineering)

by

Yousef Sangsefidi

Committee in charge:

University of California San Diego

Professor Jan Kleissl, Co-chair
Professor Mark Merrifield
Professor Oliver T. Schmidt

San Diego State University

Professor Hassan Davani, Co-chair
Professor Megan Welsh

2023

The Dissertation of Yousef Sangsefidi is approved, and it is acceptable in quality and form for publication on microfilm and electronically.

University of California San Diego
San Diego State University

2023

DEDICATION

This dissertation is dedicated to:

- My best friend, Parvaneh, whose love and both her internal and external beauty sustain me.
- My amazing parents who have been raising their children to think for themselves and have been supporting all their endeavors with indescribable sacrifice, steadfastness, and patience.
- My beloved siblings, especially my twin brother, Younes, for always being there for me and being with me even before the birth.
- My supportive in-laws for their encouragement and trust in me to pursue my goals and not give up on my dreams.
- My sweet nieces for their heart-melting presence.

TABLE OF CONTENTS

LIST OF FIGURES

LIST OF TABLES

LIST OF ABBREVIATIONS

A	Tidal efficiency;
A_{eff}	Effective area of a conduit for groundwater infiltration (L^2);
C1, C2, C3, and C4	Abbreviations used for specifying conduits;
C_d	Discharge coefficient of a circular orifice;
CCTV	Closed-circuit television;
D	Circular conduit diameter (L);
d	Circular defect diameter (L);
EGL	Energy Grade Level (L);
EL_d	Rim elevation of the downstream node of a conduit (L);
EL_u	Rim elevation of the upstream node of a conduit (L);
GI	Green Infrustructure;
GMSL	Global Mean Sea Level (L);
GMW	Groundwater Monitoring Well;
GWD	Groundwater Depth (L);
GWI	GroundWater Infiltration (L^3/T);
GWI_i	GWI in the presence of SWI (L^3/T);
GWI_j	GWI in the absence of SWI (L^3/T);
GWI_k	GWI in the absence of SWI when GWT = sea level (L^3/T);
GWT	GroundWater Table (L);
GWT_{ave}	Average GWT on a conduit (L);
g	Gravity acceleration (≈ 9.81 L/T^2);
H_G	Groundwater head on a conduit (L);
HGL	Hydraulic Grade Line;
h	Groundwater hydraulic head (m);
IB	City of Imperial Beach;
K	Diagonal tensor of hydraulic conductivity (L/T);
L	Conduit length (L);
L_{eff}	Effective length of a conduit for groundwater infiltration (L);
LECZ	Low-Elevation Coastal Zone;

MI	Marine Inundation;
L	Conduit length (m);
L_{eff}	Effective length of a conduit for groundwater infiltration (m);
LECZ	Low-Elevation Coastal Zone;
MHHW	Mean Higher High Water (L);
MI	Marine Inundation;
MSL	Mean Sea Level (L);
N	Number of defects;
NERRS	National Estuarine Research Reserve System;
NOAA	National Oceanic and Atmospheric Administration;
P	System porosity (%);
PCSWMM	Personal Computer Storm Water Management Model
POC	Point of connection between sewer systems;
Q_d	Groundwater infiltration rate through a single defect (L^3/T);
R	Hydraulic radius of a non-circular conduit (L);
RB	Rain barrel;
RDII	Rainfall-Derived Inflow and Infiltration (L^3/T);
RG	Rain Garden;
RWH	RainWater Harvesting;
SANDAG	San Diego Association of Governments
SFM	Sewer Flow Monitoring;
SLR	Sea-Level Rise (L);
SSF	Sanitary Sewage Flow (L^3/T);
SSO	Sanitary Sewer Overflow
SSVI	Sanitary Sewer Vulnerability Index;
SWI	SeaWater Intrusion;
T_{lag}	Tidal phase lag (T);
USGS	United States Geological Survey;
W	Groundwater source and/or sink (T^{-1});
WWI	WasteWater Inflow (L^3/T);
ε	Soil void ratio.

ACKNOWLEDGEMENTS

I am deeply thankful to my doctoral committee who patiently and generously provided their constructive feedback during all stages of this research, especially Dr. Davani for his motivational supervision in this long journey. My sincere thanks also go to Dr. Welsh and Prof. Merrifield (and their research groups) for their continuous and intellectual support during this project. In addition, I deeply appreciate all students who have supported this interdisciplinary study by exchanging their ideas and sharing their research outputs with me. In this regard, I specifically acknowledge the efforts of Austin Barnes (for the installation of groundwater wells and collection of monitoring data under Prof. Merrifield's supervision), Kian Bagheri (for his help in developing the preliminary version of stormdarin model), Adriana Rios (for designing and distributing social surveys under Dr. Welsh's supervision), Giovanna Zampa and Jacey Domingsil (for classifying responses to survey questions), and Jaeda Cook-Wallace and Asuka Koga (for their community outreach activities along with Adriana, Austin, Giovanna, and Jacey under Dr. Welsh's supervision).

I appreciate the support of The City of Imperial Beach (particularly Mr. Chris Helmer), John Wood Group PLC, Computational Hydraulics Int. (CHI), and Waterloo Hydrogeologic, for providing me with access to spatial data on stormwater and wastewater systems as well as monitoring data on sewage flow, monitoring data on stormdrain flow and depth, PCSWMM license, and stormwater measurements, respectively. I also acknowledge that this research has been supported by the National Science Foundation (under Grants No. 2113987, 2113984, and 2239602). Additionally, the second resulting paper has been produced with support from the National Sea Grant College Program, National Oceanic and Atmospheric Administration, U.S.

Department of Commerce (under grant number A22OAR4170104).

Chapter 2, in full, is a reprint of the material as it appears in the Journal of Hydrology, 2023, Sangsefidi, Yousef; Bagheri, Kian; Davani, Hassan; Merrifield, Mark, Elsevier, 2023. The dissertation author was the primary investigator and author of this paper.

Chapter 3, in full, has been submitted for publication of the material as it may appear in Sustainable Cities and Society, 2023, Sangsefidi, Yousef; Austin, Barnes; Merrifield, Mark; Davani, Hassan, Elsevier BV, 2023. The dissertation author was the primary researcher and author of this paper. The material describing methods and results of groundwater monitoring (mentioned in sections 3.2.3.1 and 3.3.1) is drafted by Austin Barnes and edited by the dissertation author.

Chapter 4, in full, is currently being prepared for submission for publication of the material. Sangsefidi, Yousef; Rios, Adriana; Welsh, Megan; Davani, Hassan. The dissertation author was the primary researcher of the engineering component of the research. The social-science component was led by Dr. Welsh. Specifically, the material in section 4.2.3.3 describes the methods for development, distribution, and collection of the social survey, which has been originally drafted by Dr. Welsh (and/or other students working under her supervision) and then edited/extended by the dissertation author. Section 4.3.1 presents the dissertation author's analyses of the survey responses that have been collected by Dr. Welsh's research group. These sections are reviewed by Dr. Welsh.

VITA

2011 Bachelor of Science in Water Engineering, Gorgan University, Iran.

2014 Master of Science in Civil Engineering-Hydraulic Structures, Tarbiat Modares University, Iran.

2023 Doctor of Philosophy in Engineering Sciences (Mechanical and Aerospace Engineering), University of California San Diego, CA, USA.

PUBLICATIONS

Listed in Google Scholar Profile of the dissertation author.

ABSTRACT OF THE DISSERTATION

Data-supported modeling of climate change impacts on coastal water infrastructure systems for developing community-based adaptation strategies

by

Yousef Sangsefidi

Doctor of Philosophy in Engineering Sciences (Mechanical and Aerospace Engineering)

University of California San Diego, 2023
San Diego State University, 2023

Jan Kleissl, Co-Chair
Hassan Davani, Co-Chair

Low-lying coastal areas are susceptible to multiple flooding pathways from seawater, groundwater, and stormwater sources. Focusing on Imperial Beach California, USA, this research studies the vulnerability of coastal stormwater and wastewater systems to compound impacts of changing climate [i.e., Sea-Level Rise (SLR), groundwater shoaling, and precipitation intensification], the capability of decentralized water infrastructure in flood mitigation, and their adoptability by the community.

After presenting the background information and research goals in Chapter 1, Chapter 2

evaluates compound flooding of the stormdrain system under a changing climate. Here, the obtained results for current and high sea-level conditions are presented (SLR = 0 and 2 m). The result illustrates that seawater may intrude into 2/3 of the stormdrain system length by a 2 m rise in current sea level. SLR consequences can be exacerbated by GroundWater Infiltration (GWI) such that the flooding volume may increase six-fold with 0.25% porosity systemwide and impact areas kilometers away from the coastline.

Chapter 3 shows that defect flows currently increase hydraulic loading on the sewer system by 21% and 49% in dry- and wet-weather conditions, respectively. These numbers can be elevated to 84% and 120% at SLR = 2 m placing ~ $3 M cost on the system every year. The excess hydraulic loading also increases the potential of sanitary sewer overflows (i.e., exposing the community and environment to raw sewage pollution). Finally, by involving structural, hydrological, and hydraulic criteria, a holistic approach is presented to prioritize sewer rehabilitation.

Chapter 4 first analyzes a social survey, whose results show that homeowners are more likely to adopt decentralized infrastructure. In addition, gardeners with the intention of reducing water usage should be targeted as the most prevalent adopters. Moreover, appropriate outreach activities are essential for enhancing public awareness in areas at the future risk of flooding. The engineering model outputs reveal that for a system with 0.25% porosity working under SLR = 0 m and a 1-year rainfall, the flood volume may decrease 56%−99% after implementing an RB system and adding an RG system. Although the RB system implementation can reduce the flood volume only by 24% at future conditions (SLR = 2 m and 25% increase in rainfall intensity), this value can be improved to 77% by adding an RG system. Additionally, the value of harvested rainwater over the lifetime of the RB system is estimated to be 60^{+} M while its cost will be 4^{-} M. The RG system is also estimated to cost $15 M and occupy 2.4% of the city area.

CHAPTER 1 INTRODUCTION

1.1 Problem statement

Global warming, attributed to greenhouse gas emissions, is changing the natural water cycle on the earth. An unequivocal sign of global climate change has been a 13.8 ± 1.5 cm rise in Global Mean Sea Level (GMSL) over the 20th century, which is more than that of the previous 27 centuries (Kopp et al. 2016). In the wake of melting glaciers and ice sheets as well as the thermal expansion of ocean water, the rate of sea-level rise (SLR) has accelerated to 3.7 ± 0.5 mm/yr for the period 2006-2018 (Masson-Delmotte et al. 2021). Recent climate studies warn that depending on future greenhouse gas emissions, relative sea levels along the continental US coastline are projected to rise by ∼0.6−2.2 m by the end of the century (Sweet et al. 2022). Besides the increasing exposure of coastal communities to marine flooding, SLR may also raise groundwater tables, posing a further threat to subterranean urban infrastructure systems and natural resources (Befus et al. 2020).

Climate projections also raise concerns about how precipitation will respond in a warming world. While longer droughts are expected in most regions due to rising temperatures (attributed to higher surface evaporation), global models project a 16-24% increase in heavy precipitation intensity by 2100 (associated with the larger water-holding capacity of the warmer air) (Fischer et al. 2014; Trenberth 2011). As shown in Figure 1.1, due to the interactions of oceanographic, hydrological, and meteorological processes, low-lying coastal areas are susceptible to different sources of marine, subsurface, and surface inundation, especially after considering climate change effects on water resources (Befus et al. 2020; Bevacqua et al. 2019).

By taking the above points into account, efficient management of coastal drainage systems

requires immediate attention to

(i) current and future interactions between marine-subsurface-surface water resources and their compound impacts on coastal infrastructure systems; and

(ii) sustainable and community-based solutions for vulnerable coastal areas and assets to adapt to climate change (i.e., SLR, shallow groundwater, and precipitation intensification).

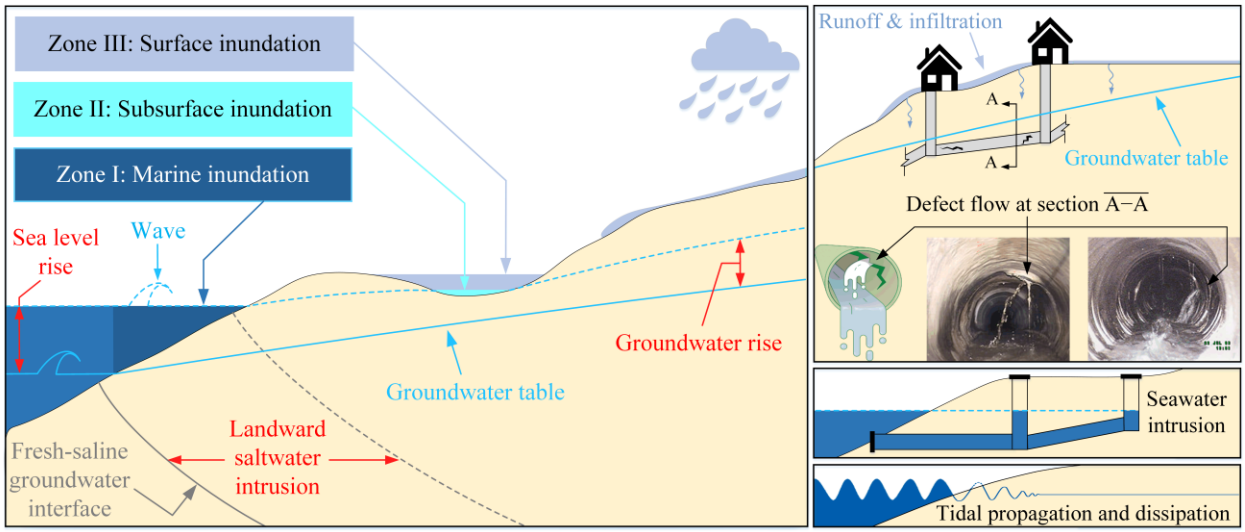

Figure 1.1 Schematic view of: (left) different sources of inundation along with current [solid line] and future [dashed line] conditions of sea level, groundwater table, and fresh-saline groundwater interface; (right-top) defect flows into system defects; (right-middle) seawater intrusion into system outfalls; (right-bottom) tidal propagation and dissipation in aquifers

1.2 Background information

1.2.1 Marine flooding

Currently, over 20 million people of the world's population are permanently exposed to marine inundation while more than 200 million people are vulnerable to marine flooding during temporary extreme high sea-level events (Nicholls 2011). SLR will exacerbate coastal marine inundation (Zone I in Figure 1.1), which has been projected to impact ~13 million people directly in the United States by 2100 [assuming 1.8 m of SLR, Hauer et al. (2016)].

SLR also will magnify the impacts of extreme sea-level events as their frequency and magnitude follow a sharply escalating pattern (Thompson et al. 2021; Vitousek et al. 2017). A relatively small SLR of 0.1−0.2 m may double the frequency of elevated sea-level events; therefore, a 1-m rise in GMSL could cause an increase of ~50% of the global population, assets, and land areas at risk of marine flooding (Kirezci et al. 2020; Vitousek et al. 2017). Over the current century, the projected SLR will dramatically threaten coastal communities and ecosystems such that it may shift the coastline landward, accelerate cliff failure and beach erosion, degrade groundwater quality in coastal aquifers through saltwater intrusion (i.e., raising the fresh–saline groundwater interface shown in Figure 1.1), and potentially damage coastal infrastructure systems (Arkema et al. 2013; Dawson et al. 2009; Nicholls and Cazenave 2010; Rotzoll and Fletcher 2013).

1.2.2 Subsurface flooding

Coastal groundwater is dynamically connected to sea levels (Figure 1.1). Although flood control measures may protect Low-Elevation Coastal Zones (LECZ: areas with 0−10 m elevation above sea level) from marine flooding, coastal groundwater may respond to high sea-level events in the form of groundwater emergence and shoaling (Befus et al. 2020; Bevacqua et al. 2019). While the majority of previous studies on coastal aquifers [such as Watson et al. (2010), Lu et al. (2013), Mehdizadeh et al. (2014), and Badaruddin et al. (2015)] have focused on groundwater salinization due to landward seawater intrusion, there is growing interest in studying subsurface flooding (Zone II in Figure 1.1) and its potential threats to infrastructure systems and coastal aquifers in recent years [such as Sangsefidi et al. (2023), Su et al. (2022), Teimoori et al. (2021), McKenzie et al. (2021), and Befus et al. (2020)]. Numerical simulations of Su et al. (2022) for the city of Hoboken (New Jersey, USA) indicated that groundwater starts to emerge for SLR = 0.4 m, and one third of the city will experience subsurface flooding for a 1-meter SLR scenario. The

increased risk of groundwater inundation has been confirmed for other areas such as Miami, Honolulu, San Francisco Bay Area, and Philadelphia (Cooper et al. 2015; Habel et al. 2017; Plane et al. 2019; Rossi and Toran 2019).

In metropolitan areas, the existence of shallow groundwater (having a depth of 0−2 m) can intensify chemical corrosion and deterioration of subterranean infrastructure systems (e.g., water supply and drainage networks, road and building foundations, and electric substations) and cause serious problems to their operation and maintenance (Habel et al. 2020; Rotzoll and Fletcher 2013). As visualized in Figure 1.1, high-level groundwater can intrude into urban drainage networks through their defects (e.g., holes, cracks, and misaligned joints) and increase their hydraulic loading (Dirckx et al. 2016; Karpf and Krebs 2011; Su et al. 2022). Previous studies indicate that groundwater infiltration into sanitary sewer systems ranges from 30 to 72% of total sewage flow (Zhao et al. 2020), which may triple in LECZs with 1 m SLR (Fung and Babcock 2020). Excessive GWI leads to higher costs of wastewater treatment and system maintenance, and potentially more Sanitary Sewer Overflow (SSO) incidents (Liu et al. 2018). A previous research studied the sensitivity of various inputs and found that compared to pipe geometries and surrounding soil characteristics, the parameter with the greatest effect on GWI is the groundwater table elevation (i.e., groundwater head over pipes) (Liu et al. 2021). It is worth noting that groundwater pumping and extraction as a temporary and unsustainable response to shallow groundwater tables may cause additional problems like ground fractures, infrastructure damages, and saltwater intrusion (Habel et al. 2020).

1.2.3 Compound seawater-groundwater-stormwater stressors

A rainfall-runoff event can be another source of inundation (i.e., surface inundation; Zone

III in Figure 1.1) during wet-weather conditions. In these circumstances, Rainfall-Derived Inflow and Infiltration (RDII) can also increase defect flows into aged sewer systems (top-left part of Figure 1.1) causing a further reduction in their hydraulic capacity (Rezaee and Tabesh 2022). Therefore, LECZs are critically exposed to compound flooding where multiple flooding pathways co-occur (Jang and Chang 2022; Rahimi et al. 2020).

In compound events when heavy precipitation coincides with an extreme sea-level event, the flooding extent substantially increases compared to that of either in isolation (Moftakhari et al. 2019; Saharia et al. 2021; Wahl et al. 2015). For example, by coupling heavy rainfall and high sea-level events, around 80% of The City of New Orleans in the United States was inundated for several weeks in 2005 (Moghimi et al. 2021). The vulnerability of coastal communities to compound flooding is expected to critically exacerbate over the century due to SLR and climate change effects on heavy rainfall patterns, which lead to further reductions in terrestrial infiltration, ponding, and drainage capacity (Davtalab et al. 2020; Karamouz et al. 2015).

In recent years, the enhanced awareness of potentially catastrophic impacts of compound events on human lives and properties has motivated new assessments of their multiple and interconnected drivers in different natural and urbanized areas. Table 1.1 presents a summary of selected recent studies on compound flooding. Using MIKE Urban 1D model and focusing on the number of flooded junctions and flood frequency, Laster Grip et al. (2021) simulated the performance of a coastal stormdrain system under coupled events of SLR, storm surge, and rainfall. While the model was neither calibrated nor validated, their comparative studies reported that although the impact of SLR is not evident today, a tipping point will occur in 2075-2100, after which storm surges become a major driver for stormdrain system failure. While rainfall-induced stormwater flooding was not included in the studies of Gold et al. (2022) and Habel et al. (2020),

their evaluation of stormdrain system performance under high tides showed that the system may flood due to seawater backflow (even in the absence of precipitation). By studying coupled storm surge and rainfall events, Tahvildari et al. (2022) and Khanam et al. (2021) quantified the flooding extent as a measure of the potential threat to roadway networks and electric infrastructure during compound events. Davtalab et al. (2020) and Rahimi et al. (2020) reported higher risks of flooding in retention ponds and riverine streams during SLR-induced groundwater rise associated with the reduction in their infiltration and discharge capacity, respectively.

Table 1.1 Selected studies on compound flooding

Study	Case Study	Flooding component	Main insight
Laster Grip et al. (2021)	Stormdrain system (Trelleborg, Sweden)	Storm surge, SLR, and rainfall	Dominance of storm surges for drainage flooding frequency in the last quarter of this century
Gold et al. (2022)	Stormdrain system (Beaufort, Wilmington, New Bern, and Nags Head, NC, USA)	High tide	Stormdrain backflow flooding in the absence of precipitation
Habel et al. (2020)	Stormdrain system (Honolulu, HI, USA)		
Tahvildari et al. (2022)	Roadway networks (Hampton Roads, VA, USA)	Storm surge and rainfall	Larger flooding extent as a measure of the potential threat to urban infrastructure systems
Khanam et al. (2021)	Electric infrastructure (Connecticut, CT, USA)	Storm surge, SLR, and rainfall	
Davtalab et al. (2020)	Stormwater retention pond (Tampa Bay, FL, USA)	SLR-driven groundwater rise	Poor performance of retention pond due to the infiltration reduction
Rahimi et al. (2020)	Riverine stream (Oakland Flatlands, CA, USA)	SLR-driven groundwater rise and rainfall	Larger extent of river flooding due to reduction in its discharge capacity

1.2.4 Decentralized water infrastructure

According to Figure 1.2, the growth in impervious surfaces associated with urbanization can reduce infiltration and evapotranspiration processes. As a result, stormwater runoff may increase twofold, threefold, and more than fivefold by extending impervious surfaces to 10–20%, 35–50%, and 75–100% of a catchment area, respectively (Paul and Meyer 2001). In addition, it is estimated that 1-2 percent of the United States land area is currently impervious surfaces (e.g., rooftops, parking lots, roads), and its construction companies approximately add one million single-family homes and twenty thousand kilometers of new roads each year (Elvidge et al. 2004; Gao et al. 2016). As a result of the rapid urban expansion in the last decades, higher runoff volumes

and peak flows have substantially increased burdens on existing centralized infrastructure systems (Qi and Barclay 2021).

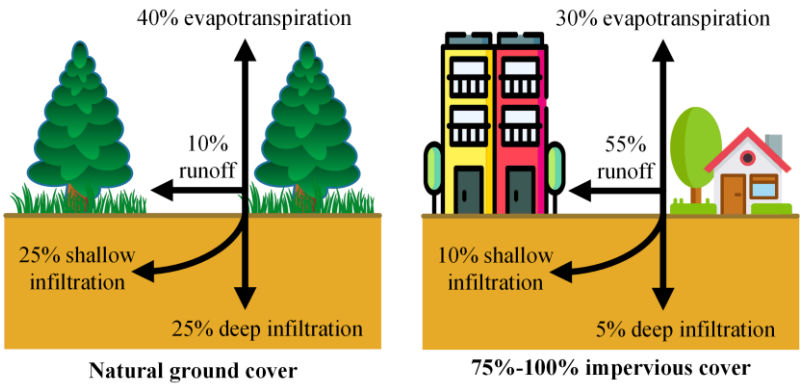

Figure 1.2 Variations of hydrologic flows with changes in ground cover [plotted based on the data from Paul and Meyer (2001)]

Decentralized water infrastructure is being increasingly deployed for stormwater and wastewater management because the development potential of centralized water infrastructure may not keep up with the urbanization growth (Chelleri et al. 2015; Piratla and Goverdhanam 2015; Tavakol-Davani et al. 2018). RainWater Harvesting (RWH) and Green Infrastructure (GI) are two popular techniques for decentralization, which can mitigate flood impacts and combined sewer overflow potentials by reducing the magnitude of precipitation-based runoff (Ahiablame and Shakya 2016; Ahiablame et al. 2013; Boening-Ulman et al. 2022; Snir et al. 2022). RWH mostly refers to rain barrels connected to building gutter systems, which collect and store rainwater for future use (Ferreira et al. 2023). Thus, in addition to runoff reduction, RWH can adjust the water budget on a local scale (i.e., providing new water sources and reducing water stresses) (Hernandez Rosales and Lutz 2023). As an environmentally-friendly technique, GI includes a variety of techniques (e.g., rain garden, infiltration basin, green roof) to mimic natural or pre-development hydrologic processes including stormwater retention, infiltration, and evapotranspiration (Khodadad et al. 2023). Besides capturing stormwater from a variety of

impervious urban surfaces, GI can remove various stormwater pollutants (e.g., oil & grease, nutrients, heavy metals, and microplastic particles) before discharging into major water bodies (McDowell 2022; Smith et al. 2023; Smyth et al. 2021).

According to the number of scientific publications shown in Figure 1.3, there had been a rapidly rising interest in studying decentralized infrastructure systems by different research groups in the two last decades. However, regardless of their high potential for addressing both stormwater quantity and quality issues, the number of publications has declined in recent years, which might be due to a slow increase in the implementation of RWH and GI by municipalities and government agencies (Gao et al. 2016; Qi and Barclay 2021; Qi and Barclay 2022). In this regard, the literature review suggests that besides engineering aspects, social and human dimensions of water infrastructure systems are equally essential components to be considered for their successful design and management (discussed in the flowing section).

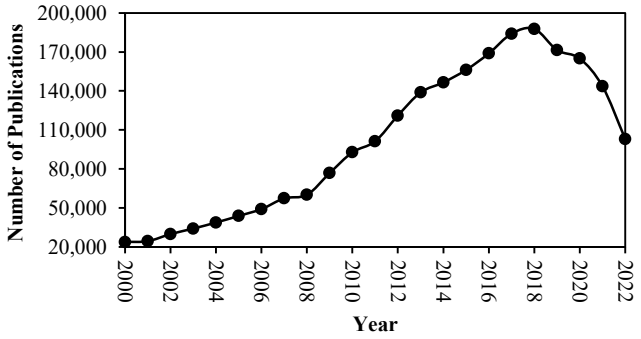

Figure 1.3 Number of published scientific documents related to decentralized water infrastructure (source: Google Scholar; keywords: "rainwater harvesting" and "green Infrastructure"; search date: 2/31/2023; search time: 0.05-0.25 s)

1.2.5 Social barriers in decentralized infrastructure adoption

Various studies have been recently conducted on social barriers to the implementation of RWH and GI, which are summarized in Table 1.2. According to this table, although social factors are usually difficult to quantify, they can be generally classified into three following categories:

(i) demographic factors (e.g., age, race, income, and education);

(ii) public engagement (i.e. people's awareness and attitudes toward environmental issues as well as their participation in decision-making and problem-solving processes); and

(iii) governance discord (i.e. inconsistent strategies within or among governance entities).

Table 1.2 Selected studies on social barriers in adoption of decentralized infrastructure

Study	Studied parameters			Type of infrastructure	Location
	Demographic factors	Public engagement	Governance discord		
Finewood et al. (2019)	–	–	Tensions and convergences among various management strategies	GIs in general	Pittsburgh, PA, USA
Gao et al. (2016)	Age, gender income, education, property specifications	Knowledge about practices, attitudes towards the environment, and cost of maintenance	–	Rain barrel	Salt Creek and Wabash watersheds, IN, USA
Maeda et al. (2018)	Race and homeownership status	Relevant knowledge and preferred dissemination platforms	–	Rain barrel, rain Gardens, pervious paving, and lawn depression	Chesapeake Bay watershed, MD, USA
Mason et al. (2019)	Age, education, and homeownership	Awareness and interest in practices as well as prior experience of floods	–	Rain barrels, rain gardens, and pervious paving	Knoxville, TN, USA
Meerow (2020)	–	–	Conflicting priorities and limited focus on multi-functionality of GIs during planning	GIs in general	New York, NY, USA
Miller and Montalto (2019)	–	Lack of public awareness	Lack of adaptivity in policies to align with local priorities and values	Green roofs, bioswales, parks & natural areas, community gardens, and permeable playgrounds	New York, NY, USA
Newell et al. (2013)	–	–	Lack of interdepartmental collaboration and private-public partnership	Green alleys	Seven cities in USA
Qi and Barclay (2022)	Age, gender, race, income, education	Participation in water conservation measures, intention to adopt GI, and platforms for knowledge dissemination	Organizational influence of higher hierarchy institutions and lack of institutional capacity for public outreach	GIs in general	Mecklenburg County, NC, USA

The literature suggests that homeownership status is an important parameter such that renters are less likely to implement decentralized infrastructure (Maeda et al. 2018). In addition, people with higher education levels, more positive attitudes toward the environment, higher knowledge about stormwater management, and prior experience with flooding are more likely to adopt RWH and GI practices (Gao et al. 2016; Mason et al. 2019; Qi and Barclay 2022). Considering the possible correlation between public knowledge and demographic factors, outreach activities may be needed for underserved communities including communities of color (Maeda et al. 2018). The discontinuation of about one-third of rain barrels in two watersheds in Indiana within

five years of their installation appears that their maintenance can be inconvenient and undesirable over time. Additionally, gardeners with the intention of water use reduction in their house yards could be the most likely potential adopters (Gao et al. 2016).

Effective communication and clear distribution of responsibilities among different stakeholders can facilitate RWH and GI practices, which necessitate the involvement of the general public and the partnership of decision makers (Keeley et al. 2013; O'Donnell et al. 2020; Porse 2013). In this regard, Shuster et al. (2008) emphasized that besides cost-benefit evaluations of decentralized infrastructure, public engagement strengthens the networks of government agencies and non-governmental organizations (NGOs), which can lead to faster adoption of decentralized infrastructure systems on larger scales. It is worth noting that communities do not necessarily have the same priorities as infrastructure managers (Finewood et al. 2019). For example, while stormwater management benefits remain the primary focus of decision-makers in New York City (as one of the leading cities in GI implementation by investing ~ 1 billion dollars), its residents valued other ecosystem services more (i.e., reduction of air pollution and urban heat) (Meerow 2020; Miller and Montalto 2019). In this city, more socially vulnerable neighborhoods are at higher air quality risks, and they can be prioritized for GI implementation from a public health perspective (Meerow 2020).

1.3 Research gaps, questions, and objectives

Climate change and urban expansion are both overwhelming traditional centralized water infrastructure (collecting water from the source and conveying it to distant areas). Previous studies confirm the vulnerability of coastal communities to compound flooding events (Table 1.1). However, due to the multiplicity and complexity of involved mechanisms, there is an urgent need to evaluate the compound impacts of seawater-groundwater-stormwater stressors on coastal

drainage infrastructure systems, especially after considering climate change effects (i.e., SLR, groundwater shoaling, and precipitation intensification).

In response to high loadings on centralized water infrastructure, decentralization has been utilized as an effective technique to delay or prevent stormwater from reaching piped systems. Despite the proven fact that decentralized water infrastructure (i.e., RWH and GI) can support local communities by reducing stormwater runoff volume and pollution, there is a knowledge gap about their capability in mitigation of watershed-scale compound flooding and adaptation of coastal communities to climate change.

While RWH and GI practices (especially rain barrels and rain gardens) offer real potential to reduce stormwater impacts, there is scant literature on the reasons for their low adoption rates by urban residents. More importantly, there is even less information about stakeholders' potential preferences for decentralized infrastructure promotion. Therefore, additional research is urgently needed to improve the comprehension of stakeholders' barriers and motivations in climate change adaptation strategies, especially in underserved coastal communities where they are most needed while limited funding sources are available.

Considering the above-mentioned research gaps, this study primarily aims to assess the compound impacts of emerging climate change phenomena on the performance of coastal drainage systems and subsequently devise appropriate adaptation strategies aligned with communities' needs. The proposed study hypothesizes that:

H1. Since GroundWater Table (GWT) in coastal areas is connected to sea-level variations, urban infrastructure far from the shoreline may be still threatened by subsurface flooding during high sea-level events (i.e., groundwater emergence and shoaling).

H2. Rising sea levels and groundwater tables may exert substantial burdens on coastal drainage

infrastructure through SeaWater Intrusion (SWI) and GroundWater Infiltration (GWI) into immersed outfalls and defects, respectively (which can occupy significant portions of the system capacity).

H3. Although the literature has been predominantly focused on extreme events (with low frequency of occurrence), more frequent events may also result in infrastructure flooding for compound impact analyses. For instance, while the combination of SLR and extreme coastal storms (with a 100-year return period) have been conventionally discussed as the worst-case scenario in the literature, the most critical stressors on infrastructure may happen during typical rainfall events (due to their possible interactions with SLR, tides, and rising groundwater).

H4. Resilient coastal water infrastructure for adapting to climate change requires a paradigm shift toward public engagement in science-based decisions for reducing the burden on centralized infrastructure (e.g., pipelines and pump stations) through decentralization techniques [e.g., RWH and GI].

Consequently, this study aims to answer the following questions through the development of a novel mechanistic framework:

Q1. How much (and how far from the shoreline) permanent and temporary sea-level variations can change GWT distribution in LECZs?

Q2. How does the vulnerability of drainage infrastructure systems change under compound mechanisms of seawater, groundwater, and stormwater stressors?

Q3. To what extent vulnerable coastal communities will be impacted by emerging climate change phenomena over the century?

Q4. How can decentralization enhance the resilience of vulnerable coastal communities against

compound flooding? How the low rates of decentralized infrastructure adoption can be promoted in such communities?

Linked to the above-mentioned hypotheses and questions, the objectives of the present research are

O1. improving the comprehension of hydrologic interconnections between sea level and coastal groundwater table and identifying the extent of subsurface flooding (linked to Q1);

O2. understanding the response of coastal drainage infrastructure systems (i.e., stormdrain and sanitary sewer systems) to compound impacts of seawater, groundwater, and stormwater stressors (linked to Q2);

O3. obtaining novel insights on the effects of climate change (i.e., SLR, groundwater shoaling, and more intense rainfalls) on stormdrain flooding and sanitary sewer overflows in coastal communities (linked to Q3);

O4. proposing adaptation strategies against climate change (i.e., resilience decentralized infrastructure for compound flood mitigation) by incorporating social data on the community's barriers, preferences, and motivations (linked to Q4).

1.4 Case Study

The current study focuses on Imperial Beach (California, USA), a coastal community in San Diego County that is also the southwestern-most city in the continental United States with ~30k population (mostly Hispanic or Latino demographics according to 2019 census estimates), ~2.5 km coastline, ~5.5 km^2 residential area, and 2−10 m elevation (Gallien 2016). As shown in Figure 1.4, IB's residential area is geographically surrounded by water bodies from three sides: The Pacific Ocean on the west, San Diego Bay on the north, and Tijuana Estuary on the south.

Therefore, IB has historically experienced marine flooding. Due to its unique setting, this low-lying coastal community is also vulnerable to subsurface flooding during high sea-level conditions. In addition, compound impacts of coastal stressors may impact its aging water infrastructure (i.e., stormdrain and sanitary sewer systems as described in sections 2.2.1 and 3.2.1, respectively). Moreover, IB is considered an underserved community since it has higher poverty and uninsured rates as well as lower homeownership and education rates compared to San Diego County, California, and the United States (demographic factors are extensively described in section 4.2.1). Therefore, IB is especially vulnerable to compound flooding, and in strong need of community-specific solutions to build resilience to climate change impacts.

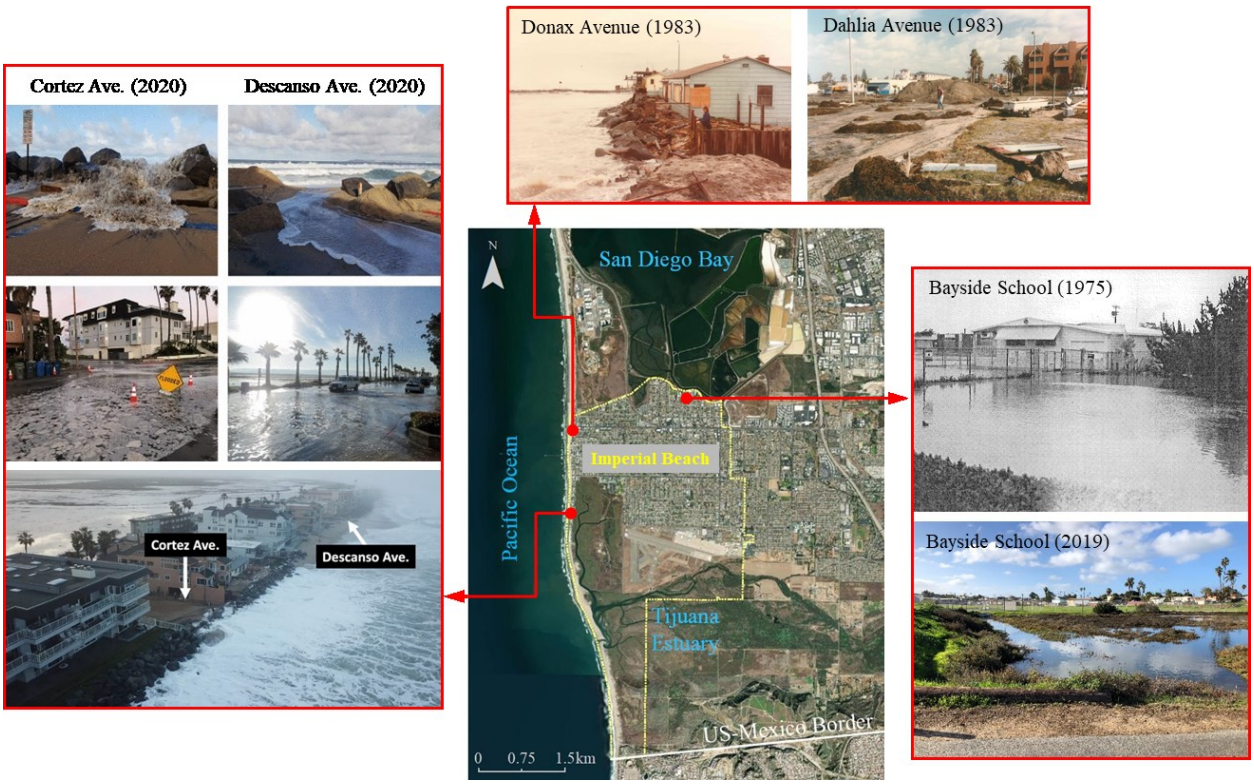

Figure 1.4 Examples of marine-based flooding in Imperial Beach: (left) ocean wave overtopping (Merrifield et al. 2021); (right) Bayside School flooding by high tides (courtesy of the City of IB); (top) debris cleanup efforts after a storm in 1983 (courtesy of the City of IB)

The research team has established a working relationship with the City of IB, whose managers and decision-makers have expressed strong interest in using the results of this research

to promote public safety against SLR and other climate change consequences. Little (2021a) and Little (2021b) present some media coverage of our partnership with the City of IB. It should be noted that although the focus of this research is on IB, the modeling approaches are generalizable to other coastal communities after considering their site-specific conditions.

1.5 Research Steps

The present study is part of a collaborative research project between San Diego State University (SDSU) and the University of California−San Diego (UCSD) receiving National Science Foundation's grants (Merrifield 2021; Tavakol-Davani and Welsh 2021). As a multidisciplinary project, it involves three disciplines: Water Resources Engineering (dissertation author's field), Oceanography, and Social Science. Table 1.3 indicates the three steps of this study such that Steps 1-3 correspond to Chapters 2-4 of the dissertation, respectively. The oceanographers and social scientists in the team deliver some of their research outputs to the dissertation author, which have been used as input data for modeling procedures (and vice versa).

As pointed out in Table 1.3, Chapter 2 of the dissertation (or Step 1 of the research) mainly aims to understand the vulnerability of coastal stormwater infrastructure to compound flooding under a changing climate. Besides analyzing the effects of sea-level changes on the coastal groundwater table, Chapter 3 (or Step 2) evaluates the impacts of current and future defect flows (from inflow and infiltration processes) on the performance of coastal wastewater infrastructure. The main goal of Chapter 4 (or Step 3) is to develop resilient adaptation measures by integrating engineering criteria (i.e., outputs of developed models by the dissertation author) with social data (i.e., responses to social surveys framed and conducted by the Social-Science part of the research team). In this step, the 1D stormwater model has been extended to 2D and incorporated science-based and community-adopted mitigation solutions. Finally, Chapter 5 summarizes the main

findings of this research and presents some topics for future studies. Figure 1.5 presents the present study scope.

Table 1.3 Conducted research tasks

Research step [I] (Dissertation chapter)	Research tasks				
	Spatial analysis and flood mapping	Groundwater table modeling	Stormdrain system modeling	Sanitary sewer system modeling	Community-based adaptation strategies
Step 1 (Chapter 2)	GIS	Befus et al. (2020)	PCSWMM (1D, unsteady)	–	–
Step 2 (Chapter 3)		MDOFLOW (3D, steady) [II]	–	PCSWMM (1D, steady)	–
Step 3 (Chapter 4)		–	PCSWMM (2D, unsteady) [III]	–	Analyzing a social survey on decentralization [IV]

[I] The research steps 1 and 2 correspond to the research objectives of O1-3, and the research step 3 corresponds to the research objectives of O2-4 (mentioned in section 1.3).

[II] The Oceanography part of our research team (i.e., Mark Merrifield and Austin Barnes) installed four groundwater monitoring wells in the study area in December 2021. The collected data was used for calibration of the developed groundwater model.

[III] The 1D stormwater model, developed in Step 1, has been extended to 2D and incorporated decentralized infrastructure (rain barrel and rain garden systems) in Step 3.

[IV] Social surveys have been developed and conducted by Megan Welsh (a social scientist at San Diego State University) and her students

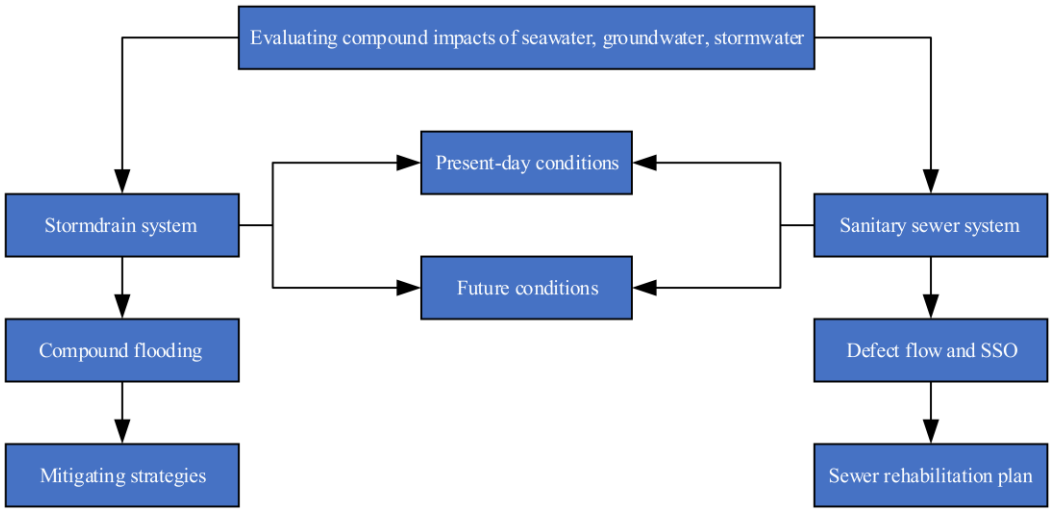

Figure 1.5 Present study scope

CHAPTER 2 VULNERABILITY OF COASTAL STORMDRAIN INFRASTRUCTURE SYSTEMS TO COMPOUND FLOODING UNDER A CHANGING CLIMATE

2.1 Objectives

In response to the urgent need for improving the comprehension of coastal community vulnerability to compound flooding (1.3), this chapter evaluates the compound impacts of seawater-groundwater-stormwater stressors on stormdrain infrastructure systems under emerging climate change phenomena (i.e., SLR, groundwater shoaling, and precipitation intensification).

Developing a novel and generalizable framework, this study focuses on a case study of Imperial Beach (IB), which is a coastal community in California surrounded by water bodies on three sides and vulnerable to compound flooding (Figure 1.4). Different sources of marine, subsurface, and surface inundations (Figure 1.1) are evaluated using a 'bathtub' approach, analyzing the state-wide groundwater model developed by Befus et al. (2020), and developing an integrated Hydrologic-Hydraulic (H&H) model using the Personal Computer Storm Water Management Model (PCSWMM, version 7.4.3240). ArcGIS is utilized for geospatial analysis as well as flood assessment and mapping. The principal objectives of this chapter are to:

- identify the extent and volume of seawater intrusion and groundwater infiltration into coastal stormdrain infrastructure by studying different scenarios for SLR and system defects;
- advance knowledge of the vulnerability of coastal drainage infrastructure to coupled oceanographic, hydrological, and meteorological stressors; and
- examine climate change impacts (i.e., SLR, groundwater rise, and more intense rainfall) on the performance of coastal stormdrain systems by estimating the extent and frequency of flood events.

2.2 Material and methods

2.2.1 Study area

As pointed out previously in section 1.4, the current study focuses on IB as a highly vulnerable community due to its unique setting (surrounded by bodies of water from three sides) and aged water infrastructure (susceptible to additional hydraulic loading from inflow and infiltration processes). Thus, IB's stormrain system (shown in Figure 2.1 and described in section 2.2.3.3) is subject to compound flooding, particularly when a rainfall event occurs while the stormdrain system is significantly occupied by SeaWater Intrusion (SWI) and/or GroundWater Infiltration (GWI).

2.2.2 Primary datasets

Table 2.1 describes the main datasets obtained and utilized in this study. Topographic data is acquired from a high-resolution Digital Elevation Model (DEM with 0.762 m × 0.762 m resolution) provided by the San Diego Association of Governments (SANDAG). The sea-level records are obtained from the National Oceanic and Atmospheric Administration (NOAA) for the San Diego Bay station (ID: 9410170), which is the closest tide station to the study area (located ~20 km north of IB with over a 100-year record). Following NOAA's regional scenarios, SLR = 0, 1, and 2 m are examined (Sweet et al. 2022). The scenario of SLR = 0 m refers to the present-day sea level at Mean Higher-High Water [MHHW = 1.658 m referenced to the North American Vertical Datum of 1988 (NAVD88)] while 1 and 2 m represent intermediate and high scenarios of SLR by 2100, associated with moderate and high greenhouse-gas emission scenarios over the century (Sweet et al. 2022). MHHW is obtained for the most recent 19 years (2002−2021) providing an estimation of high-water levels that are persistently and frequently reached in the

region (Hoover et al. 2017).

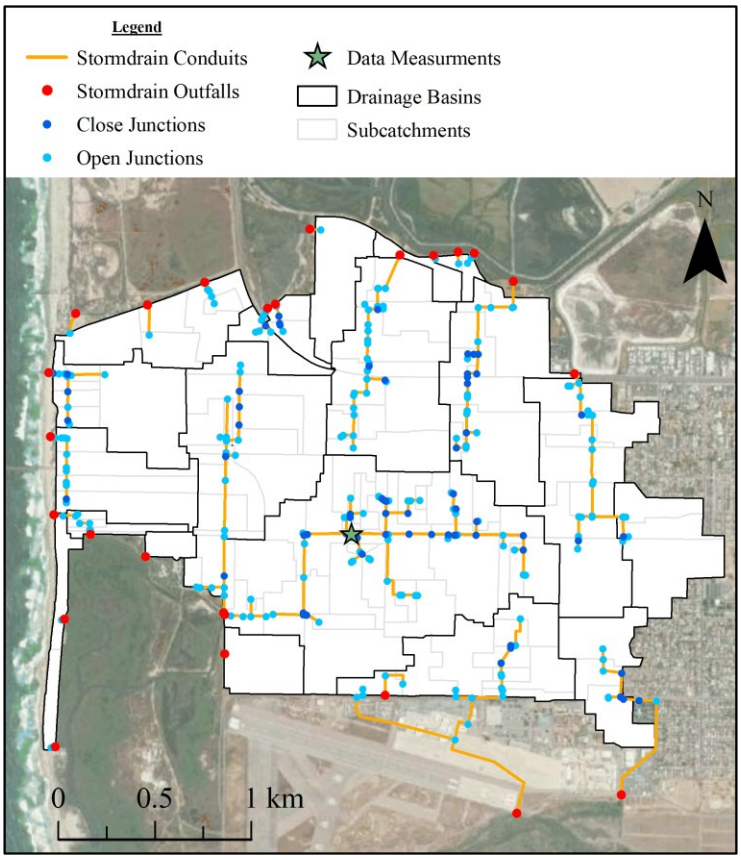

Figure 2.1 Specifications of the PCSWMM stormwater model

Table 2.1 Description of the main datasets used in the current study

Data		Source	Description
Digital Elevation Model (DEM)		SANDAG ArcGIS Server	Resolution: 0.762 m × 0.762 m
Sea level (SL)		NOAA–Tides and Currents	SL = 1.658-3.658 m for SLR = 0-2 m at MHHW
Groundwater table	Modeled spatial data	Befus et al. (2020)–MODFLOW model	Resolution: 10 m × 10 m; K = 0.1, 1, 10 m/d;
	Observed data point	USGS–National Water Information System	No active groundwater site inside IB
Stormdrain system data		City of Imperial Beach	Conducting multiple field visits to fill missing data
Rainfall data	Nested Storm	NOAA Atlas SD Hydro Tools	Converting NOAA's precipitation-frequency data to 24-hr nested storm using the SD Hydro Tools package
	Historical data	Project Clean Water	Considering 1983-1986 water years as the representative wet period

Groundwater flow is generally described by Darcy's Law, which can be combined with conservation of mass to obtain a partial-differential equation describing the distribution of hydraulic head as the target parameter (Langevin et al. 2017). In this research, GroundWater Table (GWT) data is acquired and analyzed from the MODFLOW model developed by Befus et al. (2020). These researchers assessed the steady-state and three-dimensional responses of GWT to

various SLR scenarios across the California coast (including IB) for three values of hydraulic conductivity (K = 0.1, 1, and 10 m/day). To validate the applicability of MODFLOW results for IB, the modeled GWT at Local Mean Sea Level (LMSL) are compared with temporal mean values of the observed GWT in nearby groundwater sites [available on the United States Geological Survey (USGS) website and visualized in Figure 2.2(a)]. The best agreement between modeled and observed time-averaged GWT (within 20%) is found for K = 1 m/d [Figure 2.2(b)]. Thus, to obtain the spatial distribution of GWT across IB, the present study has utilized the MODFLOW data for K = 1 m/day and the mentioned SLR scenarios in Table 2.1.

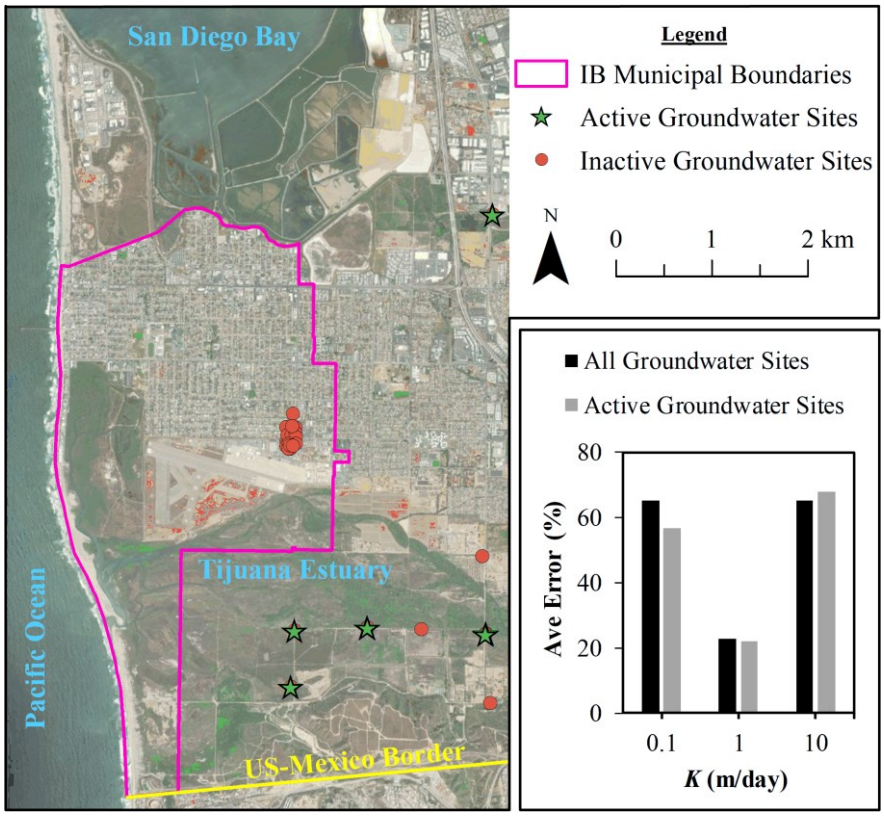

(a) (b)

Figure 2.2 Demonstration of (a) USGS groundwater sites around Imperial Beach (b) the difference between the observed and modeled groundwater table data

The primary input parameters for the stormwater model (the PCSWMM model described in section 2.2.3.3) include stormdrain system specifications, rainfall and evaporation data, soil

properties, and land-use characteristics. The spatial and geometric specifications of the stormdrain system elements (i.e., conduits, junctions, and outfalls) are available at the data warehouse of the City of IB. Gaps in the data have been filled through contacting the Environmental & Natural Resources Department in IB and conducting in-situ and virtual field visits by our research team and Google Street View. The hydrological package of SD Hydro Tools developed by The County of San Diego is utilized to generate 24-hr nested design storms (having 1-year, 2-year, and 100-year return periods) from NOAA's precipitation-frequency data. The design storms with 1-year and 2-year return periods represent heavy rainfall events while extreme rainfall events are represented by 100-year return period (occurring on average once in a century). In addition, 38 years of rainfall data with a 1-hour interval are obtained from Project Clean Water (2019) to perform a continuous simulation of the stormdrain system performance. From Figure 2.3, the time interval of 1983-1986 water years (with the maximum yearly, monthly, daily, and hourly values of 531, 198, 76, and 28 mm) is considered as the representative wet period and imported in the model. Other involved parameters in stormwater modeling (i.e., subcatchment roughness, imperviousness, and infiltration in addition to conduit roughness and energy loss) are set by referring to local sources covering the study area [e.g., The City of San Diego Stormwater Standards (2021) and County of San Diego Hydrology Manual (2003)]. These parameters are described in the section 2.2.3.3.

2.2.3 Methods

2.2.3.1 Marine and subsurface inundations

Figure 2.4 presents the workflow carried out in the present study steps. The first studied component is Marin Inundation (MI), which represents the passive flooding from seawater across

the coastline at MHHW level (as shown in Figure 2.5(a) and described in section 2.3.1). Other sea-related flooding sources, like storm surge and wave runup, are not included in MI due to the focus of this research on the inland drainage system.

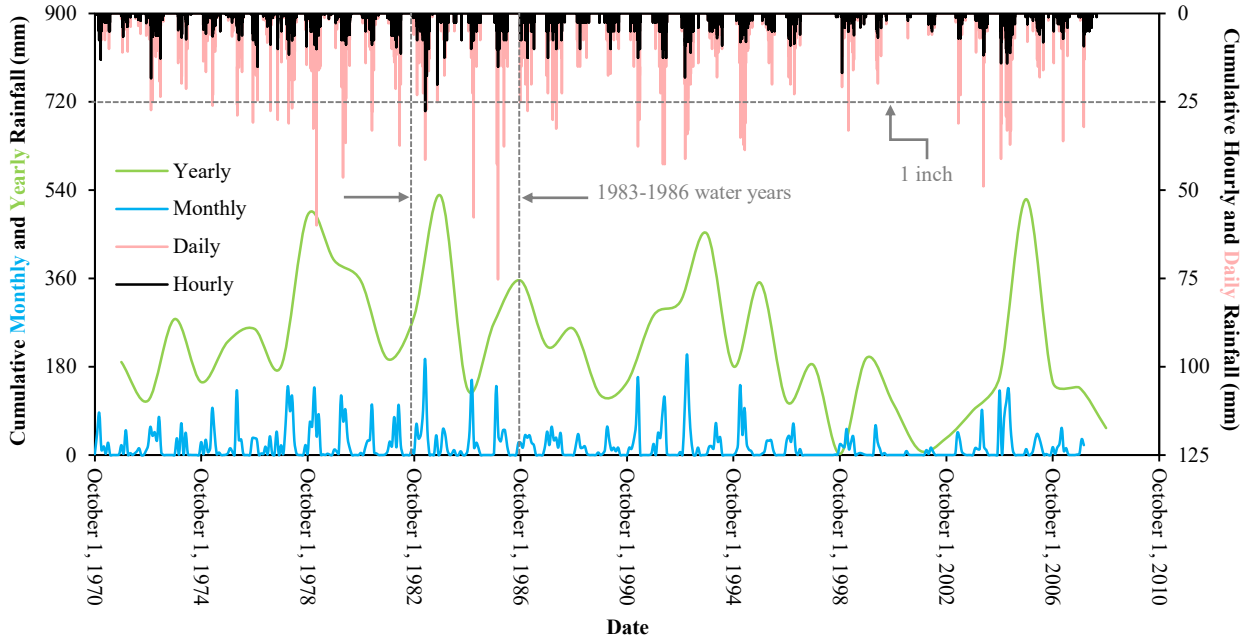

Figure 2.3 Long-term rainfall data including the 4-year representative wet period (specified with the vertical dashed lines)

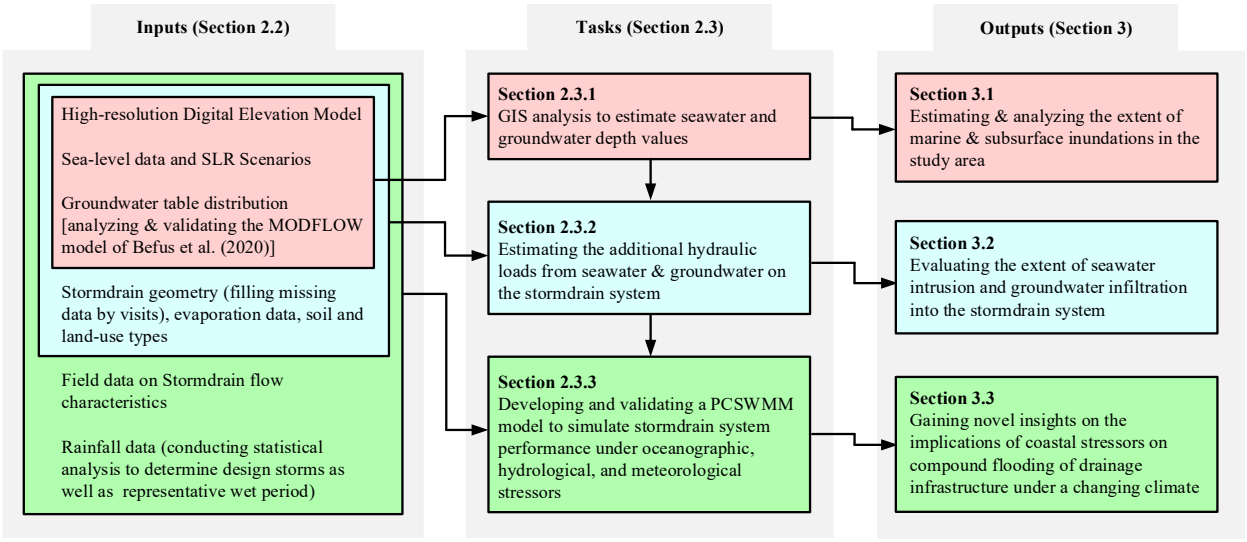

Figure 2.4 Schematic diagram of the workflow carried out in the present study

The vulnerable locations to MI are identified using a bathtub approach in ArcGIS, which

subtracts the sea-level elevation in a given scenario from the DEM to identify the areas that host elevations below that of the seawater surface (Habel et al. 2020). Due to topographic obstructions, the identified areas without a surficial connection to the marine source are excluded from MI although the subsurface inundation still threatens these areas by flooding from underneath (Rotzoll and Fletcher 2013). Through subtracting GWT elevation from the DEM, a similar method is applied to identify the areas potentially vulnerable to groundwater emergence and shoaling [as shown in Figure 2.5(b) and described in section 2.3.1].

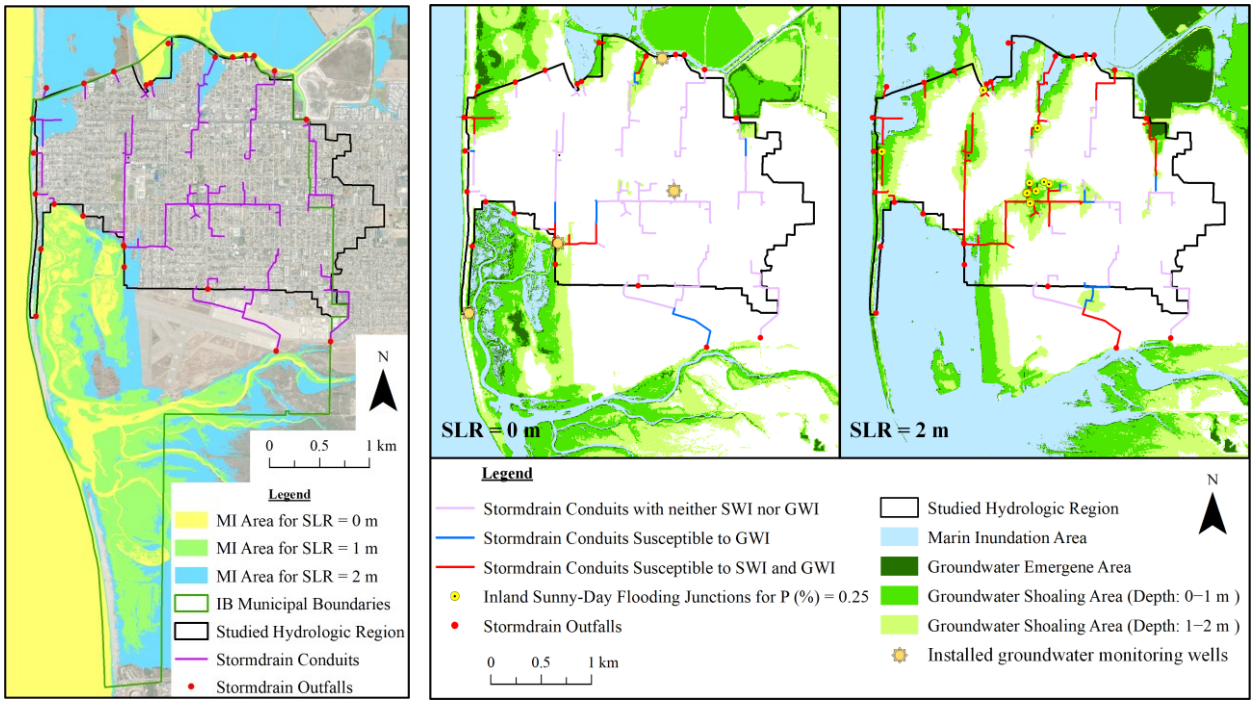

(a) (b)

Figure 2.5 Variations of (a) marine inundation and (b) groundwater emergence and shoaling for various SLR scenarios

2.2.3.2 Seawater intrusion and groundwater infiltration

Flow conveyed through the stormwater network ultimately discharges through the outfalls (represented by red-filled circles in Figure 2.5). By generating a reverse flow, SWI through the outfalls may limit the discharge capacity of the system at high sea-level conditions. This

oceanographic stressor is considered in the stormdrain model simply by setting a fixed water elevation in the outfalls corresponding to the sea-level elevation for a given scenario. Generally, stormdrain system elements are susceptible to SWI if their elevations are lower than sea level.

As drainage pipes age, high-level groundwater may infiltrate into the system through the defects on the pipe walls and result in an increased hydraulic loading [see Figure 2.6(a)]. Thus, in the case of having a defective system, stormdrain system elements are susceptible to GWI if their elevations are lower than local GWT.

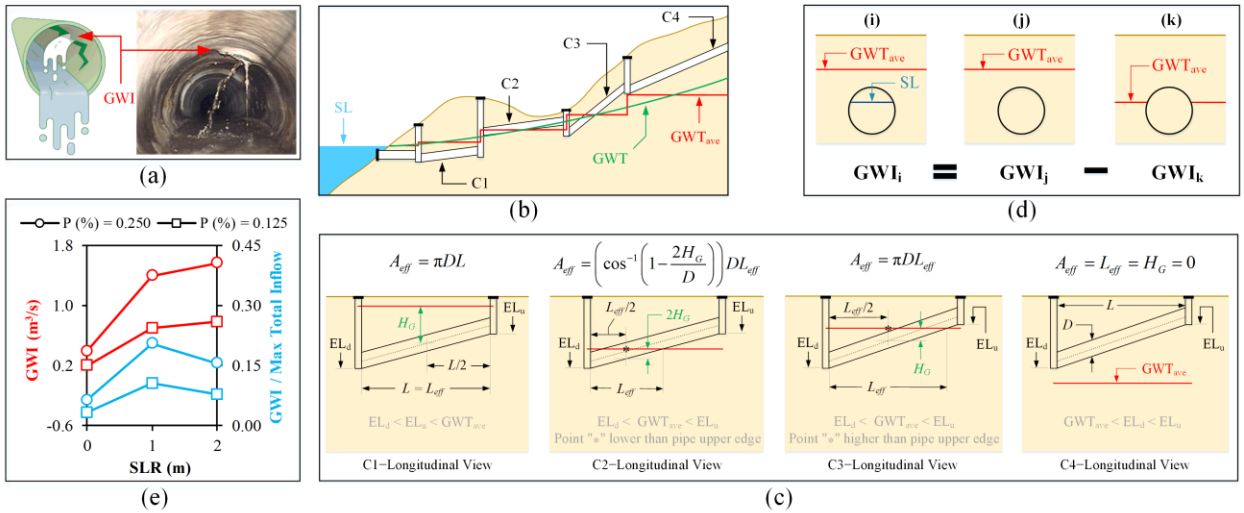

Figure 2.6 Visualization of (a) GWI, (b) GWT and GWT_{ave} longitudinal profiles, (c) different GWT_{ave} situations respect to conduits, (d) GWI determination in the presence of SWI, and (e) estimations of GWI into the system (normalized by maximum total inflow during a 24-hr rainfall with 1-yr return period)

This study considers groundwater head (H_G) and system porosity (P) to estimate GWI rate into the stormdrain system. Considering the small variations of GWT (< 5 cm changes over ~95% of conduits), its average value above each conduit (GWT_{ave}) was used for GWI determination [see Figure 2.6(b)]. Having a uniform value for the whole system, P is defined as the ratio of defect-to-conduit surface area in percent (results independency from defect position and size). Due to the lack of stormdrain monitoring data, three scenarios of P = 0.000, 0.125, and 0.250% are defined in this study to evaluate the effects of system defects on its performance. Understanding the

differences between stormwater and sewer networks, these scenarios are defined based on the CCTV sewer inspection dataset conducted in IB in 2014 (courtesy of the City of IB). To simplify the GWI calculation, non-circular conduits (consisting of < 5% of total conduits) are approximated by equivalent circles $D = 4R$, where D and R are the equivalent circle diameter and the hydraulic radius of non-circular conduits, respectively.

The following assumptions are made to simplify the problem making it suitable for city-scale long-term simulations: (I) the surrounding soil is homogeneous and isotropic; (II) all system defects are in a regular circular form (in the order of cm) and uniformly distributed on the conduits (the results are independent of defect position and size); and (III) possible groundwater flow effects in terms of washing the surrounding soil can be neglected. Consequently, a modified form of the head-discharge equation for a circular orifice (Guo and Zhu 2017) is used to determine the amount of GWI into the system,

$$\mathrm{GWI} = Q_d N \quad \xrightarrow[N = \dfrac{PA_{eff}}{100 A_d}]{Q_d = \varepsilon\, C_d\, d^2 \sqrt{gH_G}} \quad \mathrm{GWI} = \frac{PA_{eff}}{25\pi}\, \varepsilon\, C_d \sqrt{gH_G} \tag{2-1}$$

where Q_d = infiltration rate through a single defect; N = number of defects; ε = void ratio of the surrounding soil (= 0.2); C_d = discharge coefficient of a circular orifice (= 0.6); d = circular defect diameter; g = gravity acceleration; and A_{eff} = effective area for receiving GWI (= conduit surface area under GWT. As shown in Figure 2.6(c), H_G and A_{eff} are estimated for each conduit based on its situation with respect to $\mathrm{GWT_{ave}}$ elevation. In addition, in the case of SWI into a conduit, the amount of GWI is determined through the presented superposition in Figure 2.6(d). The calculated amount of GWI for each conduit is subsequently assigned as a constant flow rate to its upstream junction in the PCSWMM model.

2.2.3.3 Stormwater modeling

To simulate the stormdrain system performance, an integrated hydrology-hydraulic model is developed using PCSWMM (version 7.4.3240) with SWMM5 engine. To estimate surface runoff produced by rainfall over urban subcatchments, a nonlinear reservoir model is used along with Manning equation [Equations (2-2) and (2-3)]. Flow routing within conduits is governed by the conservation of mass and momentum [Equations (2-4) and (2-5) known as 1D Saint-Venant equations) (Rossman 2015). Using the Finite Difference Method, the complete form of these equations is solved (referring to an unsteady and non-uniform flow in the system).

$$\frac{\partial d}{\partial t} = i - e - f - q$$

$$\begin{cases} \frac{\partial d}{\partial t} = \text{change in depth over time; } i = \text{rate of rainfall, snowmelt, and runon;} \\ e = \text{evaporation rate; } f = \text{infiltration rate; } q = \text{runoff rate per unit surface area.} \end{cases} \quad (2\text{-}2)$$

$$q = \frac{Q}{A} = \frac{1}{n} R^{2/3} S_f^{1/2}$$

$$\begin{cases} Q = \text{runoff's volumetric flow rate; } A = \text{flow area } \left(= W \times \left(d - d_s\right)\right); \\ n = \text{Manning's roughness coefficient; } d_S = \text{depression storage;} \\ W = \text{subcatchment width; } R = \text{hydraulic radius } \left(= d - d_s\right); \\ S_f = \text{friction slope } \left(= \text{bed slope, } S_0, \text{ in uniform flow}\right). \end{cases} \quad (2\text{-}3)$$

As shown in Figure 2.1, the study area, consisting of 20 major drainage basins, is divided into 122 fine-resolution subcatchments to provide a precise rainfall-to-runoff modeling in the study area. In addition, the stormdrain system is described in a substantially high resolution by having 263 conduits in the model (linked to 200 open and 63 close junctions). Referring to the The City of San Diego Stormwater Standards (2021), the Green-Ampt method is selected for infiltration modeling while Manning roughness coefficients for subcatchments and conduits are determined in the ranges of 0.024−0.200 and 0.013-0.030, respectively. The energy loss coefficients at the

entrance and exit conduits range from 0.1−1.0 based on their relative diameters to the neighboring junctions (Frost 2006).

$$\frac{\partial A}{\partial t}+\frac{\partial Q}{\partial x}=0 \tag{2-4}$$

$$\frac{\partial Q}{\partial t}+\frac{\partial\left(Q^2/A\right)}{\partial x}+gA\frac{\partial H}{\partial x}+gAS_f=0;\ \text{or}$$

$$S_f=\left\{\begin{matrix}S_0\\ S_0-(V/g)(\partial V/\partial x)-(\partial Y/\partial x)\\ S_0-(V/g)(\partial V/\partial x)-(\partial Y/\partial x)-(1/g)(\partial V/\partial t)\end{matrix}\right\}\text{for a}\left\{\begin{matrix}\text{steady \& uniform flow}\\ \text{steady \& non-uniform flow}\\ \text{unsteady \& non-uniform flow}\end{matrix}\right. \tag{2-5}$$

$$\left\{\begin{matrix}Q=\text{Volumetric flowrate}\ (=A\times V);\ A=\text{flow area},\ V=\text{flow velocity},\\ H=\text{hydraulic head}\ (=z+Y),\ z=\text{elevation, Y = flow depth},\\ g=\text{gravity acceleration},\ S_f=\text{friction slope},\ S_0=\text{bed slope}\end{matrix}\right.$$

To calibrate and verify the model, wet-weather field monitoring data (courtesy of John Wood Group PLC) is obtained with a 1-min interval at the specified location in Figure 2.7 (in the vicinity of IB's Public Library), where the system is free of SWI and GWI in current conditions [see Figure 2.5(b)]. Satisfying the recommended ranges by the County of San Diego Hydrology Manual (2003) for different land uses, the subcatchment imperviousness is set as the target parameter for calibration (ranging 25−80%). According to Figure 2.7, there is an outstanding agreement between the modeled and measured data for both calibration and verification periods. The modeled flow characteristics (i.e., stormdrain inflow and depth) match well with the measurements in terms of both the timing and magnitude of peak flow (< 20% difference).

Twenty scenarios are studied in this research (Table 2.2) to comprehensively evaluate the effects of SLR, system porosity, and rainfall properties on the performance of coastal stormdrain systems. According to Fischer et al. (2014), a ~25% increase in heavy rainfalls could be expected in southern California by 2100. In Table 2.2, the nested storm with a 2-year return period corresponds to that increase in the intensity of the nested storm with a 1-year return period; thus,

this magnitude of rainfall could be expected to happen every year (instead of every other year) in the region by the end of the century. However, no significant change in the annual mean precipitation is expected in the region (Fischer et al. 2014).

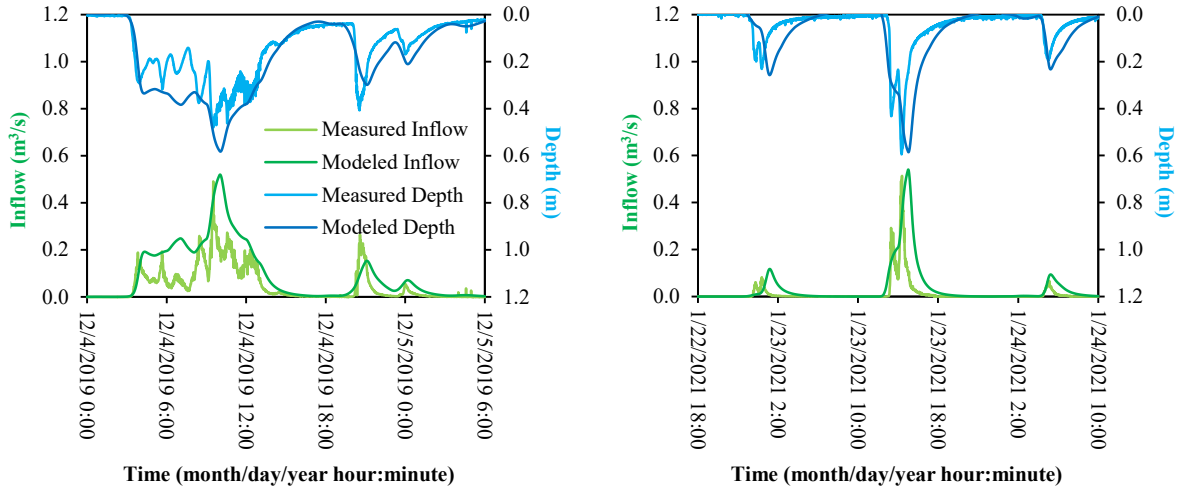

Figure 2.7 Comparison of the measured and modeled data for (a) calibration and (b) verification periods

Table 2.2 Studied scenarios in the present research

Rainfall		SLR (m)	*P* (%)		
			0	0.125	0.250
24-hr Nested Storm	1-Year Return Period	0	S0-P0.000-R1	S0-P0.125-R1	S0-P0.250-R1
		1	S1-P0.000-R1	S1-P0.125-R1	S1-P0.250-R1
		2	S2-P0.000-R1	S2-P0.125-R1	S2-P0.250-R1
	2-Year Return Period[1]	2	S2-P0.000-R2	S2-P0.125-R2	S2-P0.250-R2
	100-Year Return Period	0	S0-P0.000-R100	–	S0-P0.250-R100
		2	S2-P0.000-R100	–	S2-P0.250-R100
4-Year Historical Data		0	S0-P0.000-Historical	–	S0-P0.250-Historical
		2	S2-P0.000-Historical	–	S2-P0.250-Historical

[1] The nested storm with a 2-year return period corresponds to the 25% increase in the intensity of the nested storm with 1-year return period [happening every year in the region at the end of century according to Fischer et al. (2014)].

2.3 Results and discussion

2.3.1 Extent of marine and subsurface inundations

To improve the understanding of the vulnerability of coastal water infrastructure and resources to SLR, the first step is to assess the inundation potential. SLR-driven marine and subsurface inundation extents are shown in Figure 2.5, and Table 2.3 summarizes the estimates of

the impacted urbanized areas under no, moderate, and high SLR scenarios. The baseline year for the present-day condition (SLR = 0 m) scenarios is 2021. From Figure 2.2(a) and Figure 2.5(a), Tijuana Estuary and its natural ecosystem will be extensively and directly impacted by marine inundation as sea level rises. However, marine inundation is predicted to have minimal impacts on the urbanized populated region where the present study focuses on. For SLR = 0, 1, 2 m scenarios, 0.00%, 0.44%, and 6.74% of the urbanized area is under marine inundation, respectively (Table 2.3). The urban area inundation is limited to the San Diego Bay shoreline and the ocean facing coast (particularly along the thin strip between the ocean and estuary).

Table 2.3 Percentages of the IB populated region (total area = 5,784,987 m^2) and the stormdrain system (total length = 15,961 m) impacted by marine and groundwater flooding sources

SLR (m)	Marine Inundation Area (%)	Groundwater Emergence Area (%)	Groundwater Shoaling with less than 1 m Depth (%)	Groundwater Shoaling with less than 2 m Depth (%)	Length of Stormdrain Conduits susceptible to both SWI and GWI (%)	Length of Stormdrain Conduits susceptible to GWI (%)
0	0.00	0.02	2.18	8.50	11.09	20.10
1	0.44	1.51	7.17	16.98	38.26	41.11
2	6.74	0.62	9.53	23.01	60.00	66.73

From Figure 2.5(b) and Table 2.3, groundwater emergence and shoaling pose a more widespread threat than marine inundation for all SLR scenarios. In the current sea-level conditions, groundwater shoaling (with a depth < 2 m) threaten subsurface urban infrastructure in 8.5% of the populated region (including areas far from the coastline). The SLR-induced groundwater rise will increase this number to 16.98% and 23.01% for 1 and 2 m SLR. Therefore, for the high SLR scenario, it is expected that around 30% of the city will be permanently threatened by marine inundation and shallow GWT at the end of the century.

It is worth noting that both marine and subsurface inundations can be more widespread during dynamic ocean conditions (i.e., storm surge and wave action), which are excluded in the present study because of its focus on the long-term performance of the inland drainage system. In terms of spatial distribution, it is expected that the regions closer to the sea will be heavily impacted

during dynamic sea-level events (Laster Grip et al. 2021). From the studies of Gallien (2016) and Merrifield et al. (2021) on IB, the ocean shoreline will be particularly vulnerable to wave-driven impacts. Anderson et al. (2018) showed that the flooded area (mapped in three Hawaiian islands) can be increased up to 50% by adding wave inundation to the passive flooding. In addition, a king tide can temporarily raise inland GWT while its fluctuations attenuate at a distance in the order of 1 km from the shoreline (Rotzoll and Fletcher 2013).

2.3.2 Extent of seawater intrusion and groundwater infiltration

A substantial portion of the IB's stormdrain conduits is at risk of SWI and GWI through outfalls and system defects, respectively [Figure 2.5(b)]. From Table 2.3, about 11 and 60% of the conduits (with an invert elevation lower than sea level at MHHW) may experience some amount of SWI at the current and high sea-level conditions, respectively. In addition, the stormdrain conduits located in the emergent-to-shallow groundwater regions [Figure 2.5(b)] are the most sensitive to GWI (enlarging by SLR-induced groundwater rise). At the high SLR scenario, ~67% of the stormdrain length will be susceptible to GWI. This number is more than twice the above-mentioned percentage for the city area experiencing shallow GWT with a depth of less than 2m (which is the typical depth for stormdrain systems). This difference is because a water drainage system with gravity-driven flow is typically located in low-lying regions of an urbanized area, where the risk of emergent-to-shallow groundwater is the highest. Therefore, water drainage systems are one of the most vulnerable coastal infrastructures to SLR impacts.

The estimations of GWI for different scenarios are plotted by the red-line graphs in Figure 2.6(e). As expected, this parameter increases by rising sea level and spreading system defects. While it grows about four times by a 2 m SLR, GWI and *P* change with the same factor for a given

sea level (due to assuming a uniform distribution of defects on the system). To have a better sense of the extent of this additional stressor, GWI is also normalized by the maximum total inflow during a 24-hr rainfall with a 1-year return period. As shown by the blue-line data in Figure 2.6(e), GWI can consist of ~20% of the maximum total inflow at SLR = 1 m. However, GWI may form a smaller part of the total inflow at higher SLR because of an increase in SWI contribution. It should be noted that the SLR-induced groundwater lift in LECZs can cause some additional issues like exposing the public to sewage effluent contamination and degrading groundwater quality through saltwater intrusion into coastal aquifers (as shown in Figure 1.1) and failure of immersed cesspool systems (Befus et al. 2020; Habel et al. 2020; Habel et al. 2017). These topics merit more research beyond the present study scope.

2.3.3 Compound flooding

The main effects of SLR, rainfall intensity, and stormdrain system porosity on its performance are presented in Figure 2.8(a). As these parameters increase (which is expected to happen due to climate change effects and lack of maintenance in underserved areas), a higher percentage of inland junctions will flood (shown by the blue-line graphs in the top-left chart). The red-line graphs in other charts show that the stormdrain compound flooding is projected to increase in total area, depth, volume, and time over the century.

It is worth noting that the junctions located in marine inundation areas are excluded from the stormdrain flooding analysis. This point may explain why the number of flooding junctions (shown by the red-line graphs in the top-left chart) is not a monotonic increasing function of SLR at $P = 0$. Unlike their total values, the average values of the flood properties (shown by the blue-line graphs in other charts) do not have a monotonic increasing trend with the rainfall return period.

This is because although total flooding values increase during a 2-year rainfall event (more stormwater inflow), the increase in the number of flooding junctions may be larger; as a result, the average value may decrease (i.e., average value = total value / number of flooding junctions).

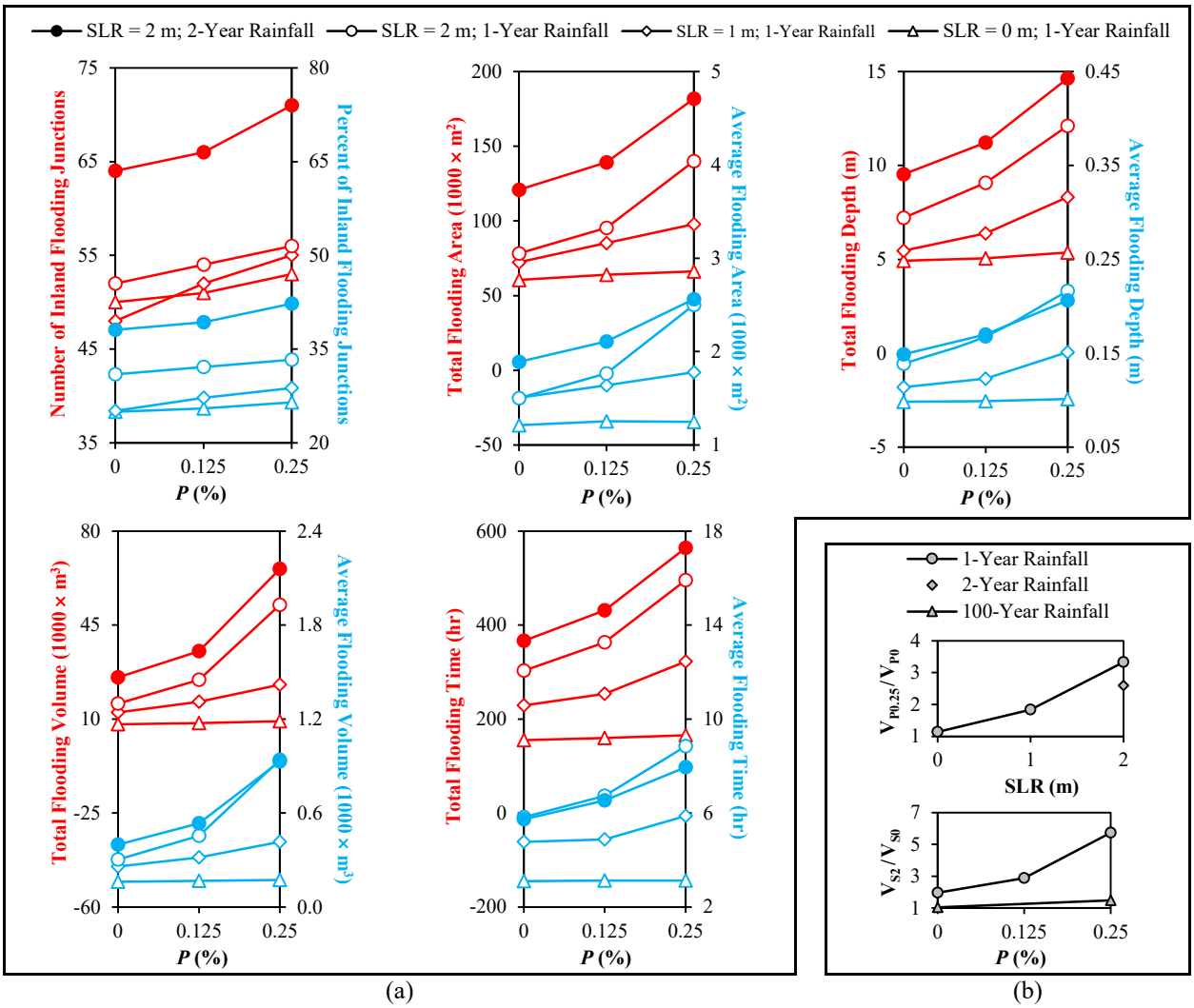

Figure 2.8 Visualization of (a) main and (b) interaction effects on compound flooding ($V_{P0.25}$, V_{P0}, V_{S2}, and V_{S0} respectively refer to total flooding volume at P (%) = 0.25 & 0.00 and SLR = 2 & 0 m)

Interaction between different parameters implies that the effect produced by changing one parameter depends on the level of other parameters (Sangsefidi et al. 2017). Figure 2.8(b) indicates the interactive effects of the three studied parameters on the total flooding volume (the vertical axis titles of the graphs are described in the figure caption). As shown, a more defective system

will be impacted by SLR to a greater extent such that under a 1-year rainfall event, the flooding volume will grow up to 6 times by a 2 m rise in seal level when P = 0.25%. However, this ratio may decrease to less than a third by avoiding GWI into the system (P = 0). Moreover, since the stormwater contribution to compound flooding increases by an increase in rainfall return period, the flooding extent is less sensitive to SWI and GWI under more extreme rainfall events.

Figure 2.9 shows today's observations of frequently flooded locations (courtesy of the City of IB), and Figure 2.10 presents the flooding extent maps obtained from the developed stormwater model for five selective scenarios in current and future conditions (defined in Table 2.2). As a ground truth, Figure 2.9 reveals that even for the current sea-level conditions, there are still serious problems across the city for draining stormwater from low-intensity rainfalls. This point also can be found from the presented flooding maps for S0-P0.000-R1 and S0-P0.250-R1 scenarios in Figure 2.10, on which the nine frequently flooded locations are pinpointed. Considering the small extents of SWI and GWI at SLR = 0 m [Figure 2.5(b)], the main driver of these floods should be rainfall-induced stormwater. From the comparisons of the two mentioned scenarios in Figure 2.10, it can be found that the effects of system porosity are not significant in the current sea-level conditions (i.e., low GWT values in the region).

By sea-level rising over the century, SWI may have a significant contribution in the stormdrain inflow and flooding (S2-P0.000-R1 scenario). However, comparison of the S2-P0.000-R1 and S2-P0.250-R1 scenarios indicates that the SLR impacts are considerably more severe for higher P values because GWI leads to a further increase in the hydraulic loadings on the system in these challenging circumstances. As a result, the flooding hotspots during more-frequent design storms (i.e., 1-year return period) generally correspond to the shallow GWT regions depicted in Figure 2.5(b).

No.	Location
❶	Date Ave at Seacoast Dr (W−E view)
❷	Intersection of Palm Ave and 2nd St (NE−SW view)
❸	Seacoast Dr at Carnation Ave (S−N view)
❹	Calla Ave at 5th St (S−N view)
❺	7th St at Delaware St (S−N view)
❻	8th St between IB Blvd and Elkwood Ave (E−W view)
❼	Ebony Ave at 11th St (W−E view)
❽	Intersection of 12th St and Holly Ave (SW−NE view)
❾	Oneonta Ave between 11th St and 12th St (W−E view)

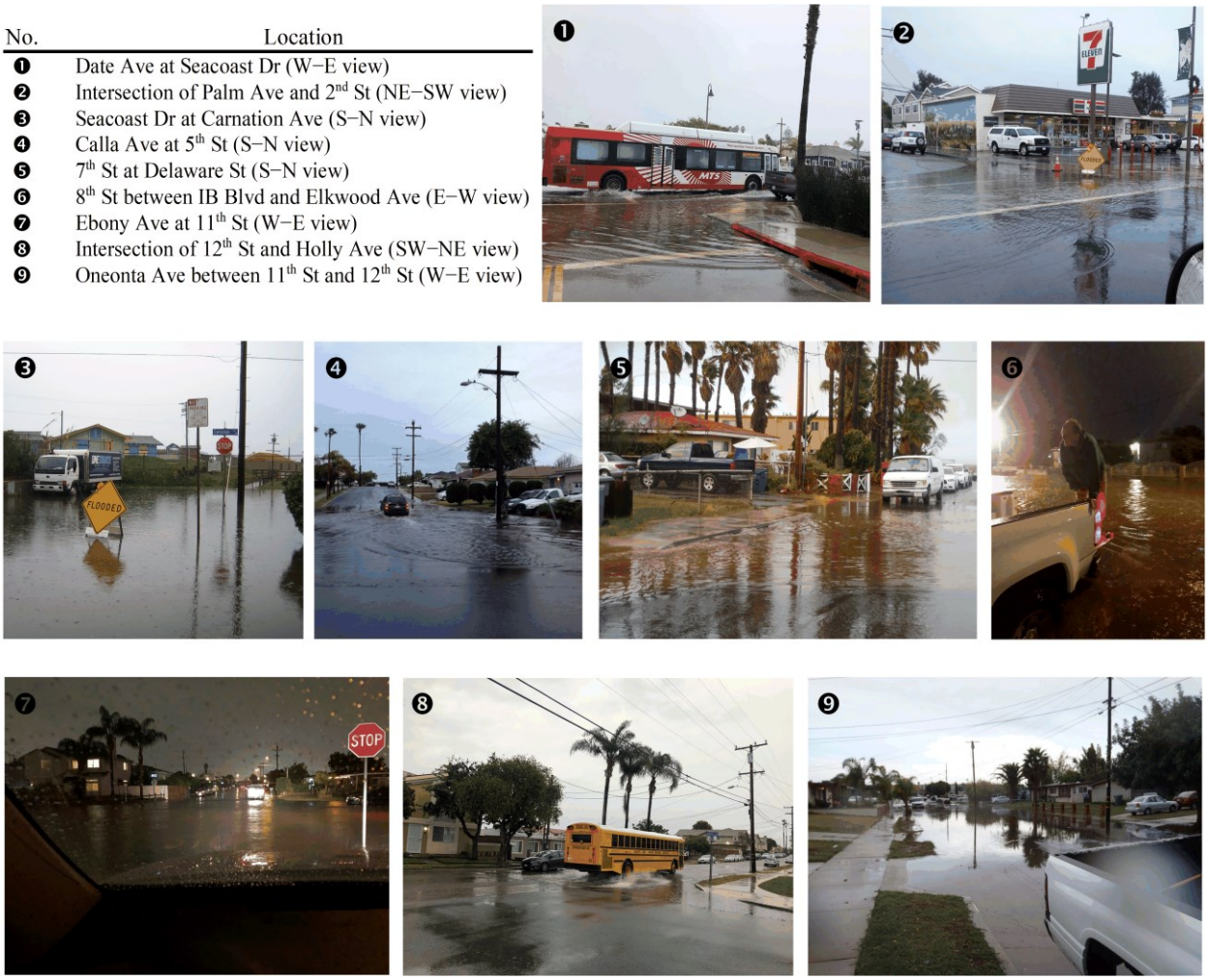

Figure 2.9 Observations of the frequently flooded locations across The City of IB

Comparing the S0-P0.000-R1 and S2-P0.250-R1 scenarios (Figure 2.10), the most important insight is that adverse impacts of SLR are not limited to marine inundation and a potential landward shift in the shoreline. SLR also can impact regions kilometers from the coastline through contributions to compound flooding events. The expected 25% increase in the heavy rainfall intensities by climate change effects over the century (annual occurrence of the current 2-year rainfall in 2100) may cause additional stress on the system and enlarge the compound flooding extend even more (S2-P0.250-R2 scenario).

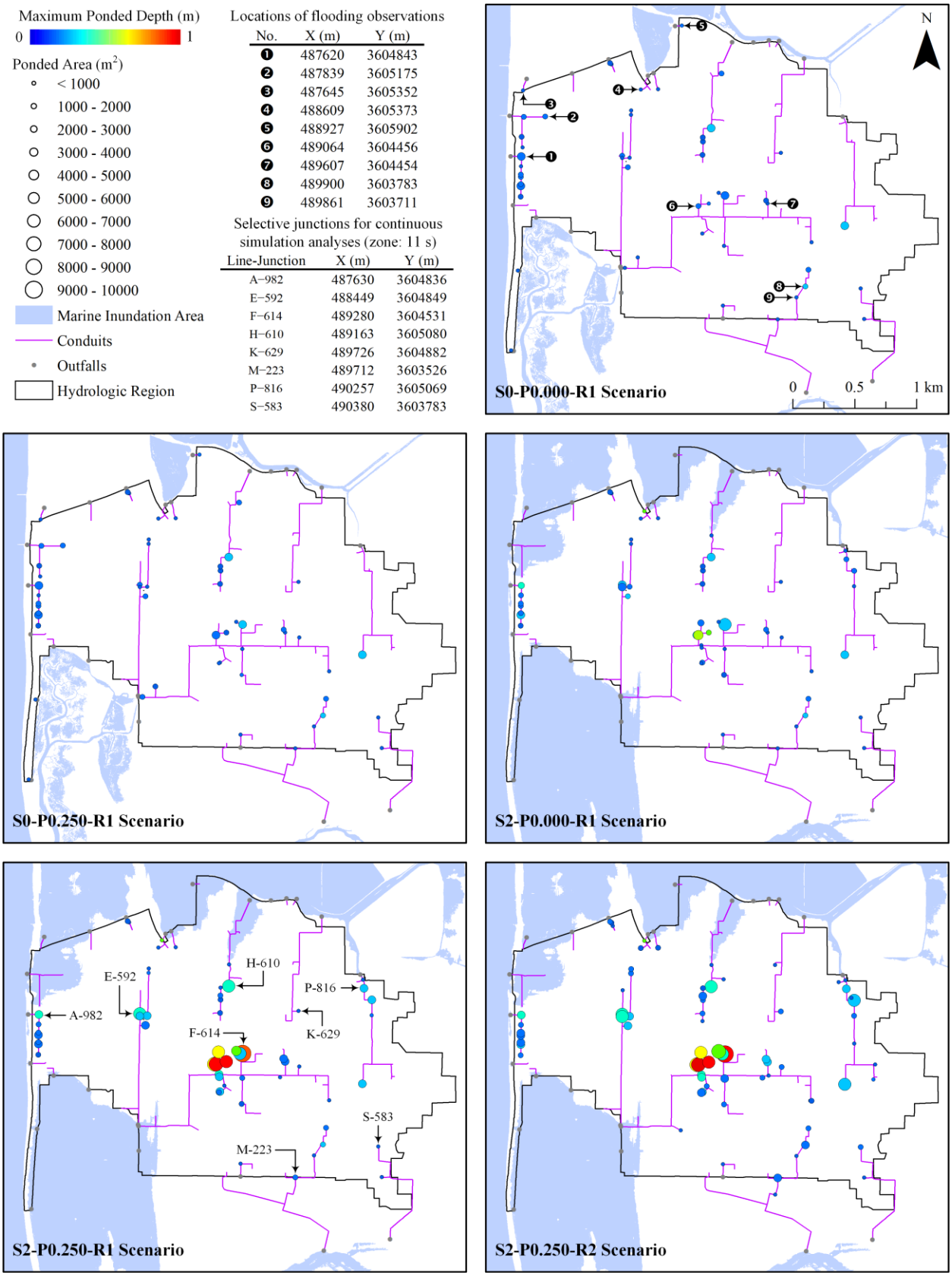

Figure 2.10 Compound flooding maps for five selected scenarios (defined in Table 2.2)

Based on the performed continuous simulations for the 4-year representative wet period, the long-term performance of the stormdrain system (as opposed to a single design storm) is analyzed by focusing on the selective junctions specified on the legend and bottom-left map in Figure 2.10. As shown, the selected junction on each stormdrain line has a critical flooding condition compared to other junctions on that specific line. In addition, these junctions are selected from eight major stormdrain lines to inform us about various conditions of the system. Referring to Figure 2.5(b), some selective junctions may be invulnerable to SWI and GWI while other ones can be susceptible to either SWI, GWI, or both. Figure 2.11(a) presents the frequency (and number) of flood events with a separation time of 6 hours. As shown, some parts of the system (i.e., K-629 and S-583 junctions) may experience similar flooding events in different scenarios because they receive neither SWI nor GWI [previously depicted in Figure 2.5(b)]. However, for those parts susceptible to either SWI or GWI, the flood events are expected to happen more frequently depending on the amount of these additional stressors. For example, since junction #E-592 is at the risk of both SWI and GWI at SLR = 2 m, a higher number of flooding events is expected for this area compared to the current conditions [jumps in the data for S2-P0.000-Continuous and S2-P0.250-Continuous scenarios in Figure 2.11(a)]. More challenging, some parts of the system may be always flooding at the end of the century (i.e., A-982, F-614, and H-610 junctions with a flood event frequency of 1) attributed to the high amount of SWI and GWI. Figure 2.5(b) shows the 11 sunny-day flooding junctions across the study area for SLR = 2 m and P = 0.25%, which are generally located in low-lying areas with emergent-to-shallow groundwater.

Figure 2.11(b) demonstrates the flood frequency-volume plots for some of the selective stormdrain junctions. As expected, larger floods happen less frequently in the region, and vice versa. Due to the contribution of SWI and GWI into stormdrain inflow, a flood with a given

frequency will have a larger extent, or conversely, a given flood is expected to happen more frequently in the future. The effects of the SLR-induced stressors are more significant in more-frequent floods, especially in the sunny-day flooding areas. However, the difference between the data for S0-P0.000-Continuous and S2-P0.250-Continuous scenarios diminishes at lower values of flood frequency, and they eventually converge to each other for very extreme floods. In these circumstances, the contributions of seawater and groundwater sources in compound flooding are insignificant compared to that of the stormwater source. As a result, the flooding extent is highly dependent on the typical drainage characteristics of subcatchments (rather than SWI and GWI).

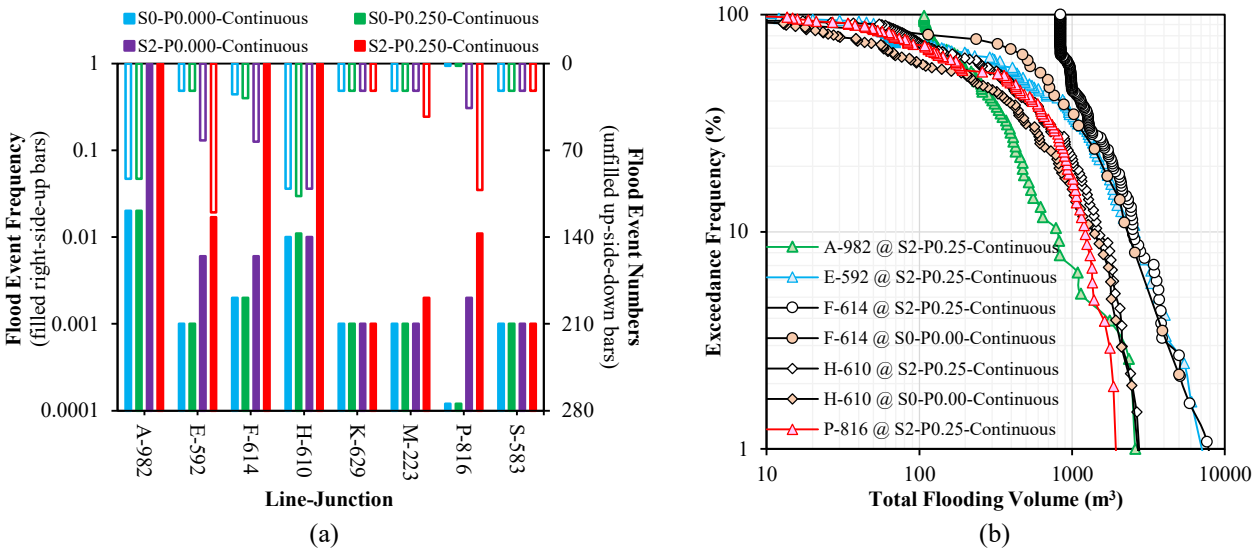

Figure 2.11 Continuous simulation results for the specified junctions in Figure 2.10: (a) flood event frequency and numbers (b) flood frequency-volume plot

2.4 Summary

This chapter (Step 1 of the research) has clearly proven the significance of considering the compound effects of coastal stressors on water drainage infrastructure, by which flood events will be more destructive and frequent. While marine inundation is a concern only near the coast, compound flooding can impact places far from the shoreline. To improve our understanding of compound flooding and adaptation strategies, the flowing topics are studied in Chapters 3 and 4

(Steps 2 and 3 of the research):

- Due to a lack of data, the Oceanography part of the research team has installed four groundwater monitoring wells inside Imperial Beach. In Chapter 3, this data has been analyzed for a better understanding of groundwater table connections with sea level and to develop a high-resolution, 3D, and city-wide groundwater model.
- Including decentralized infrastructure systems and more site-specific conditions, a 2D stormwater model is developed in Chapter 4. It also presents an interdisciplinary framework to determine how decentralized infrastructure systems can be adopted by the community and contribute to flood mitigation and SLR adaptation.

CHAPTER 3 CLIMATE CHANGE IMPACTS ON COASTAL GROUNDWATER AND SANITARY SEWER INFRASTRUCTURE SYSTEMS

3.1 Objectives

The capacity of a sanitary sewer system, as a valuable urban asset, is typically designed based on wastewater generation from homes and businesses. However, after decades of operation, groundwater infiltration through sewer defects, including Rainfall-Driven Inflow and Infiltration (RDII), can increase hydraulic loading on the system. To establish efficient adaptation strategies, therefore, there is a strong necessity for an improved understanding of the coastal stressors on sanitary sewer systems and new assessments of their interactions.

This chapter aims to determine climate change impacts on coastal aquifer behavior in general, and on wastewater infrastructure performance in particular, by incorporating the RDII as well as other sources of inflows due to Sea Level Rise (SLR) and groundwater shoaling. To achieve these goals, the present study focuses on Imperial Beach (IB) as an urban laboratory in Southern California, for which a 3D and high-resolution groundwater model has been developed using Visual MODFLOW Flex version 8.0 and incorporating site-specific conditions. Due to the lack of groundwater data in this underserved community, the Oceanography part of the research team has installed four monitoring wells inside IB. The groundwater table measurements were then utilized by the dissertation's author to calibrate the developed groundwater model. In addition, the performance of IB's sanitary sewer system is simulated using the Personal Computer Storm Water Management Model (PCSWMM, version 7.5.3406). ArcGIS is also used for geospatial analysis and flood mapping. The principal objectives of this study are to

- provide new insights on interactions of coastal groundwater with surface-water bodies; and
- identify the vulnerability of sewer systems to subsurface flooding in a changing climate.

3.2 Material and methods

3.2.1 Study area

This study focuses on Imperial Beach (IB) located near the US-Mexico border, which is highly vulnerable to subsurface flooding during high sea-level conditions (previously described in section 1.4). Due to its unique setting, additional stressors may impact the aged wastewater infrastructure of this underserved community through inflow and infiltration processes.

Figure 3.1 illustrates the domains of groundwater and sewer system models developed in the current step of the research. For observing unconfined aquifer levels (required for the groundwater model calibration), four groundwater monitoring wells were drilled and installed in December 2021 around IB's frequently flooded areas (GMW 1-4 in Figure 3.1). As presented in Figure 3.2 and Table 3.1, the sewage flow is collected across three tributary areas (sewer zones I−III with slight upward slopes from the surrounding water bodies) through ~66 km gravity and ~8 km force mains (ranging 0.102−0.610 m in diameter) connected to 11 pump stations. The flow is eventually discharged into the City of San Diego sewer system through three connection points (POC 1-3).

While the useful life of Vitrified Clay (VC) pipes is roughly 50−60 years, about 84% of IB's sewer length consists of VC pipes, of which more than 90% were installed before the 1970's (Table 3.2). A closed-circuit television (CCTV) sewer inspection in 2014−2015 confirms that about one third of sewer lines currently have a significant degree of structural damage (visualized in Figure 3.3), and this ratio is expected to increase as the system ages over the century with lack of proper system maintenance in an underserved community. Defective sewer elements are susceptible to increased hydraulic load due to GWI and/or RDII.

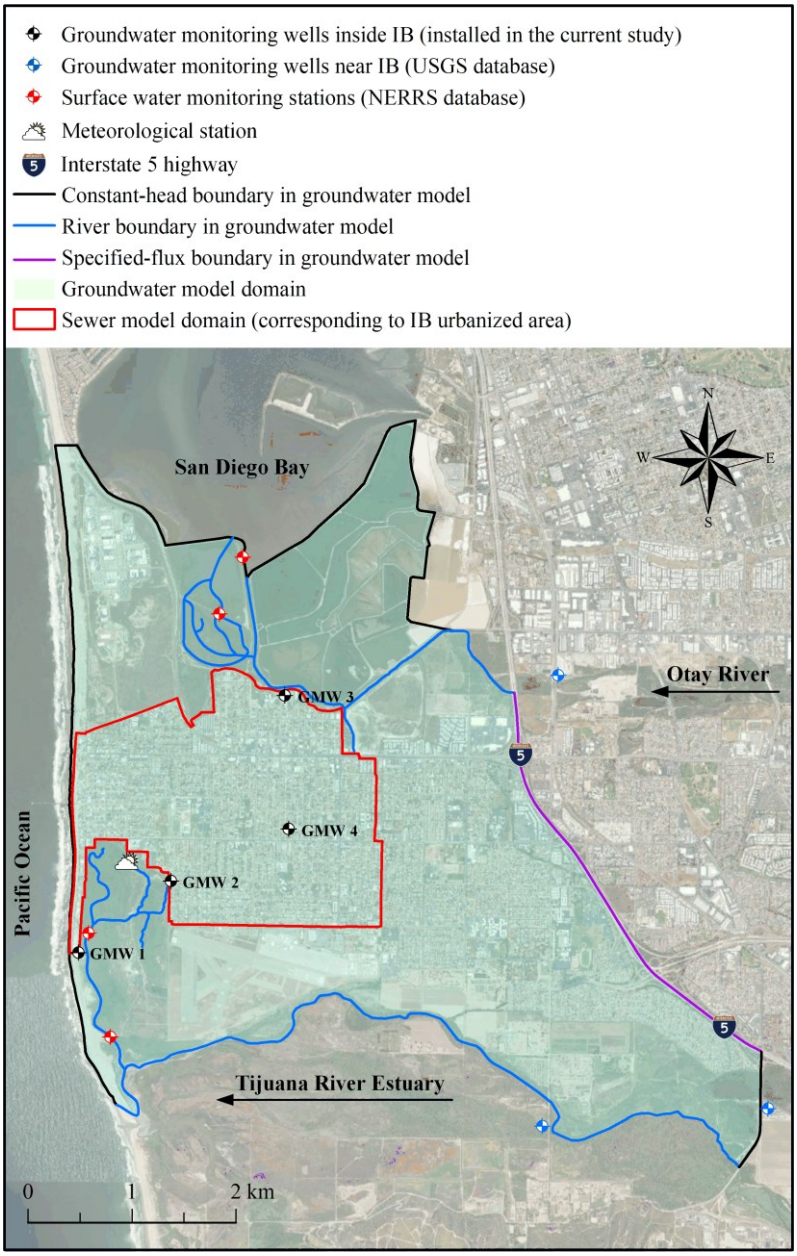

Figure 3.1 Domains of the groundwater and sewer models

Table 3.1 Sewer lengths (in percentage) with different sizes (total length = 74,289 m)

Diameter (m)	Gravity mains	Force mains	Total
0.102	0.2%	0.0%	0.2%
0.152	19.1%	0.4%	19.5%
0.203	61.0%	0.5%	61.5%
0.254	3.5%	2.4%	5.9%
0.305	3.0%	7.2%	10.3%
0.381	1.4%	0.0%	1.4%
0.406	0.1%	0.0%	0.1%
0.457	0.1%	0.3%	0.5%
0.533	0.4%	0.0%	0.4%
0.610	0.1%	0.0%	0.0%
Total	89.2%	10.8%	100.0%

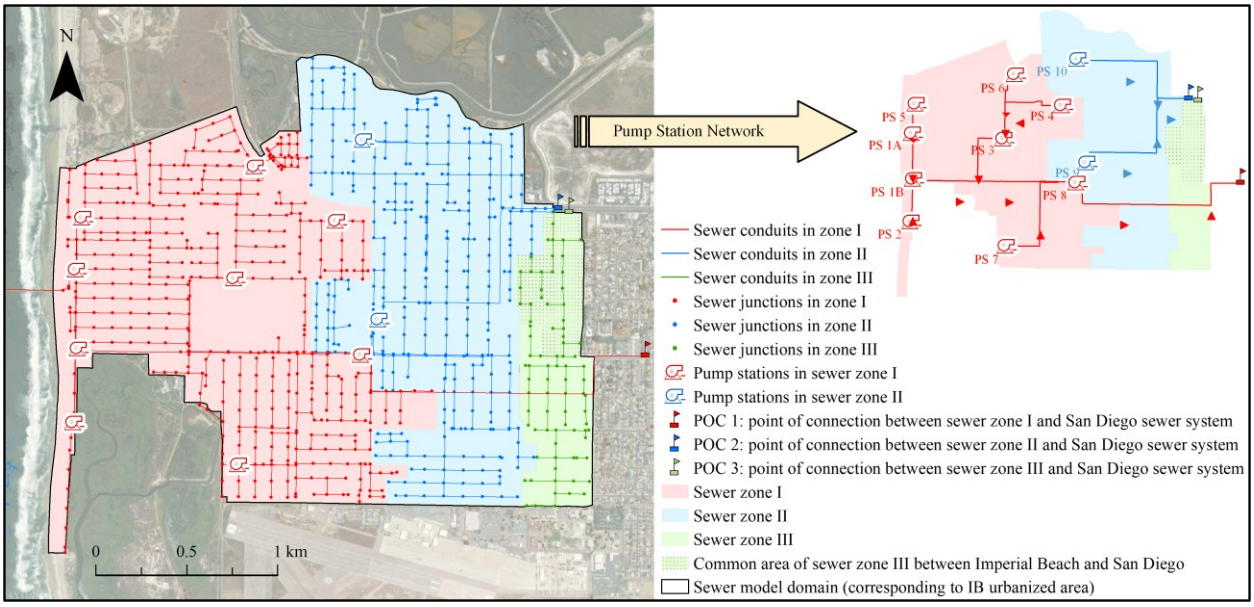

Figure 3.2 Specifications of the sanitary sewer model

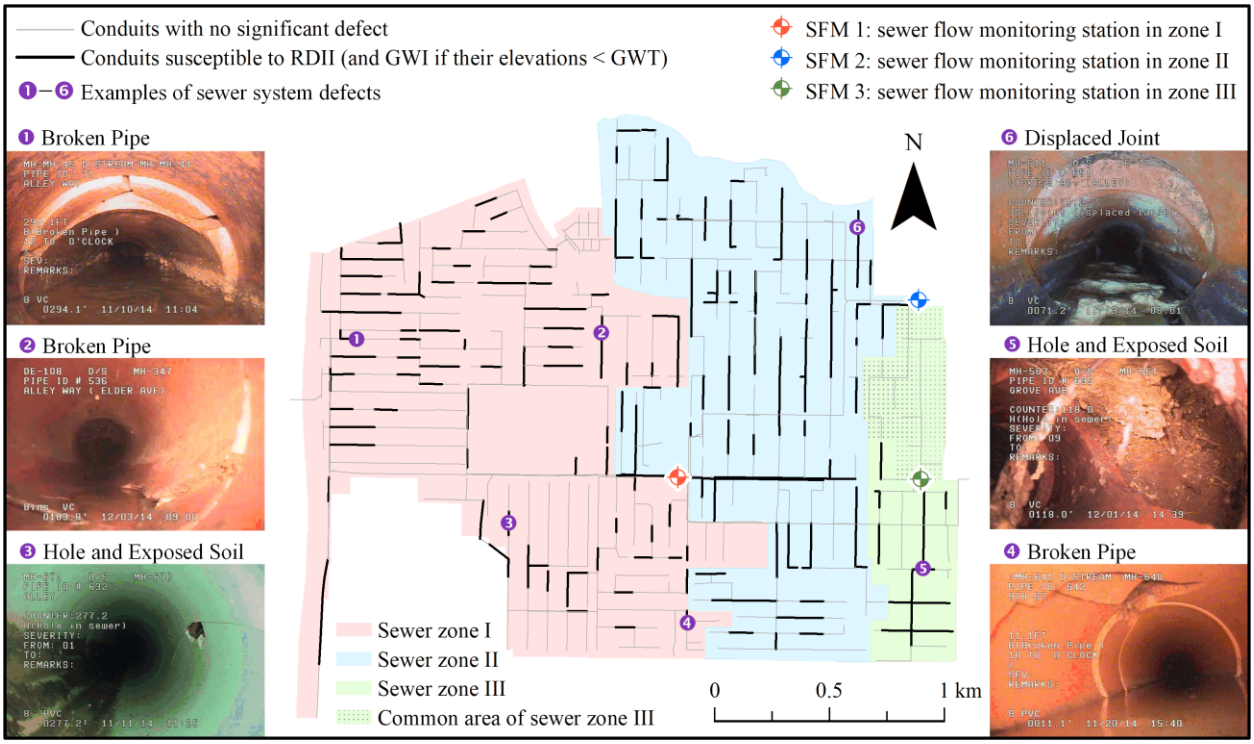

Figure 3.3 Visualization of sewer flow monitoring stations along with defective conduits (photos from CCTV sewer inspections are in courtesy of the City of IB).

3.2.2 Primary datasets

Table 3.3 presents the main datasets utilized in the present study. A Digital Elevation

Model (DEM with 0.762 m × 0.762 m resolution) and a parcel layer are acquired from the data warehouse of the San Diego Association of Governments (SANDAG). The sea-level records in the San Diego Bay (station ID: 9410170) are obtained from the National Oceanic and Atmospheric Administration (NOAA). Following NOAA's regional scenarios, SLR = 0, 1, 2, and 3 m are examined (Sweet et al. 2022). While SLR = 0 m refers to the present-day Mean Sea Level [MSL = 0.811 m referenced to the North American Vertical Datum of 1988 (NAVD88)], the studied scenarios of SLR = 1, 2, and 3 m are associated with intermediate, high, and extreme greenhouse-gas emission scenarios over the century (Sweet et al. 2022). For developing the groundwater model using Visual MODFLOW Flex, monitoring data on river levels and groundwater tables around IB are acquired from nearby sites from the United States Geological Survey (USGS) and the National Estuarine Research Reserve System (NERRS) websites (station locations are depicted in Figure 3.1). The IB monitoring wells are described in section 3.2.3.1.

Table 3.2 Sewer lengths (in percentage) with different material constructed in each decade (total length = 74,289 m)

Decade Constructed	Sewer material [1]				Total
	VC	PVC	CI	DI	
1940s	10.7%	0.0%	0.1%	0.0%	10.8%
1950s	55.8%	2.5%	1.0%	0.0%	59.3%
1960s	10.2%	0.4%	0.0%	0.0%	10.6%
1970s	7.0%	1.7%	0.0%	0.0%	8.7%
1990s	0.0%	3.8%	0.0%	0.0%	3.9%
2000s	0.5%	4.6%	0.0%	0.1%	5.1%
2010s	0.1%	1.5%	0.0%	0.0%	1.6%
Total	84.3%	14.6%	1.1%	0.1%	100.0%

[1] VC, PVC, CI, and DI respectively refer to vitrified clay, polyvinyl chloride, cast iron, and ductile iron.

Table 3.3 Main datasets used in the present study

Data		Source	Description
Digital Elevation Model		SANDAG ArcGIS Server	Resolution: 0.762 m × 0.762 m
Land-use parcel layer			Used for the estimation of wastewater production across the city
Surface-water level	MSL & SLR scenarios	NOAA–Tides and Currents	MSL = 0.811−3.811 m for SLR = 0−3 m
	River level	NERRS	TJRBRWQ, TJROSWQ, TJRPRWQ, TJRSBWQ stations
Groundwater table	Inside IB	N/A	Installing 4 monitoring wells in IB in the current study
	Near IB	USGS	No active groundwater site inside IB
Sanitary sewer system	Geometric & spatial data	City of Imperial Beach	Available at the data warehouse of the City of IB
	CCTV inspection		Conducted in Dec. 2014 – Jan. 2015 by Tran Consulting Eng.
	Monitoring sewage flow		Conducted in Dec. 2016 by V&A Consulting Engineers
Rainfall data	Monitoring rainfall data	NERRS	TJRTLMET station records over the period of sewage monitoring
	24-hour storm	NOAA Atlas	Referring to 24-hour NOAA precipitation-frequency data

The main input parameters for the sanitary sewer model (PCSWMM described below in section 3.2.3.4) are sewer system specifications, land-use information, rainfall data, and monitoring sewage flow. The geometric and spatial specifications of the sewer system elements (e.g., junctions, conduits, and pump stations) are obtained from the City of IB by request, whose gaps are filled through field and virtual visits performed by our team. Defective conduits are identified and classified based on CCTV sewer inspections conducted in IB during December 2014 – January 2015 (courtesy of the City of IB). A GIS parcel layer −available in the SANDAG data warehouse− is utilized for the estimation of wastewater loads from each land-use unit. Utilizing NOAA's precipitation-frequency data, a 24-hour rainfall with a 25-year return period is selected to represent a reasonably significant storm condition that is likely to occur within the next couple of decades. Other parameters involved in calibration of the groundwater and sewer models (e.g., hydraulic conductivity, groundwater recharge, conduit roughness, monitoring rainfall and sewage flow) are obtained or set by referring to local sources (described in sections 3.2.3.2 and 3.2.3.4).

3.2.3 Methods

Figure 3.4 presents the workflow carried out in the present study. The methodologies used to conduct the mentioned tasks are described in this section.

3.2.3.1 Groundwater monitoring[1]

The four groundwater monitoring wells were drilled using an 0.203-m hollow stem auger down to a depth of 6.096 m or 20 ft (drill cuttings were collected every 1.524-m for soil analysis). The well casing is 0.051 m in diameter, and the bottom 3.048 m of each well is screened with

[1] The material of section 3.2.3.1 (describing the methods of groundwater monitoring3.2.3.1) are drafted by Austin Barnes and edited by the dissertation author.

0.0005 m perforations. The wells were permitted and finished according to San Diego County regulations: the bottom 3.658 m was filled with #3 filter pack sand, above that 1.524 m of the annular seal bentonite, and finally 0.914 m of surface concrete to seal the well.

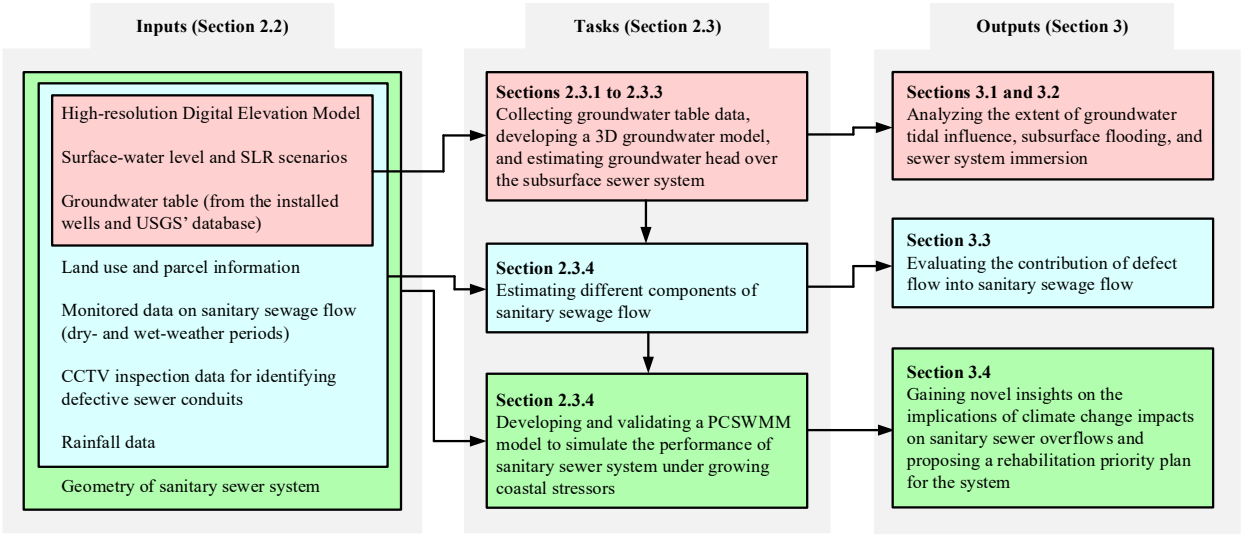

Figure 3.4 Schematic diagram of the present study workflow

Each well was equipped with a 0.0254 m diameter RBR Solo pressure sensor with sampling at 1 Hz frequency, suspended between 0.914−1.828 m above the well bottom. Atmospheric pressure measurements taken every 6 minutes at NOAA meteorological station 9410170 in San Diego Bay were interpolated to 1 second and then subtracted from the RBR pressure measurements. The remaining pressure is assumed to be hydrostatic pressure. The salinity structure of each well was determined using a conductivity-temperature-depth survey every two months, which was relatively fixed over the observation period. Thus, the average densities were used to convert hydrostatic pressure to groundwater depth. Reference depths (from the well heads to the water tables) and well head elevations were measured using a Solinst water-level meter and GPS, respectively.

The continuous records from December 8th, 2021 to June 5th, 2022 are analyzed to

determine time-averaged ground water table (GWT) and tidal influence in each monitoring well. The latter is described by two parameters of phase lag (T_{lag} = time delays between sea level and GWT signals) and tidal efficiency (A = ratio of amplitude variation in a well compared to ocean-tide amplitude) (Su et al. 2022). The pure tidal signal for each GMW (determined by Python package UTide) is cross-correlated with the pure tidal signal from the tide gauge using Python package SciPy. Then, the tidal phase lag with the highest correlation is selected as the lag time between the ocean and the GWT. Linear regressions on the pure tidal signals of GMWs versus the tide gauge are performed, and the slopes of the linear regressions are reported as A at each GMW.

3.2.3.2 Groundwater modeling

Incorporating site-specific conditions, a three-dimensional and steady-state groundwater flow model is developed for the coastal unconfined aquifer using the open-source MODFLOW-2005 engine (distributed by USGS) implemented in the graphical interface of Visual MODFLOW Flex [developed by Waterloo Hydrogeologic (2021)]. Based on a finite difference numerical scheme, MODFLOW has been widely used for groundwater flow modeling by previous researchers such as Su et al. (2022) and Befus et al. (2020).

The equilibrium water-table responses to SLR can be described by the following differential equation, which is a combination of Darcy's Law with conservation of mass (Harbaugh 2005):

$$\nabla.\left(\mathbf{K}\ \nabla h\right) = W \tag{3-1}$$

where h = groundwater hydraulic head; $\mathbf{K}$ = diagonal tensor of hydraulic conductivity; and W = volumetric flux per unit volume representing sources and sinks. Figure 3.1 illustrates the groundwater model domain and its side boundary conditions. While the domain is extended to

major surface-water bodies and groundwater divides, it is discretized into ~1 million cells in a one-layer model with a high-resolution of 7 m × 7 m to represent topography details. The model bottom was set to the elevation -50 m NAVD88 (covering the quaternary deposits placed above the San Diego formations with a low hydraulic conductivity) with a no-flow boundary condition (assuming a horizontal groundwater flow at the bottom) (Befus et al. 2020; Stuart 2008). A drain−recharge boundary condition is applied to the model top to serve as either a groundwater discharge or recharge feature for levels at or below the ground surface, respectively. Considering a high and low conductance drain for natural and urbanized areas (5−500 m^2/d), the spatial recharge rates are prescribed by the annual effective recharge (4−12 mm/yr), from which evapotranspiration fluxes are already removed (Reitz et al. 2017). According to the sensitivity analysis of Sangsefidi et al. (2023) on the study area, **K** = 1 m/d is set in the model by assuming a homogeneous and isotropic aquifer. For the model calibration, the modeled GWT at MSL are compared with temporal mean values of the observed GWT from the installed wells (section 3.3.13.3.1).

3.2.3.3 Flood mapping

The locations impacted by marine inundation (MI) are determined using a bathtub approach, in which the sea-level elevation in a given SLR scenario is subtracted from the DEM raster data to identify the areas with elevations lower than MSL (Habel et al. 2020). The identified locations without a surficial connection to the seawater source are excluded from MI. However, these areas are still threatened by subsurface flooding (Rotzoll and Fletcher 2013). By subtracting GroundWater Table (GWT) values from the DEM, a similar method is applied to identify the areas potentially vulnerable to groundwater emergence and shoaling. In addition, considering the small variations of GWT over conduits (< 3 cm changes in GWT for 98% of conduits), its average value above each conduit (GWT_{ave}) was determined by ArcGIS and utilized for estimation of

groundwater head (H_G) over subsurface sewer infrastructure.

3.2.3.4 Sanitary sewer system modeling

The performance of the sewer system is evaluated through developing and calibrating a PCSWMM model that is supplemented by flow monitoring data and CCTV inspection data. Using the SWMM version 5.1 engine, this model is widely used for simulating wastewater, stormwater, and combined infrastructure systems (Sangsefidi et al. 2023; Tavakol-Davani et al. 2016).

Recalling from Figure 3.2, the separate sewer system is modeled in a substantially high resolution by having 920 conduits distributed across the three sewer zones. Using a combination of gravity and pumping systems, sewage flows from sewer zones I and II to POC 1 and 2, respectively. However, only a gravity system transfers the flow from zone III to POC 3. At the three locations shown in Figure 3.3, flow monitors were installed by the City of IB in sewer manholes for two weeks beginning on December 15th, 2016. As essential data sources for calibrating the PCSWMM model, the flow monitors were able to measure the sewage flow leaving the three sewer zones in both dry and wet weather conditions (Figure 3.5).

According to Equation (3-2), the sanitary sewage flow (SSF) consists of WasteWater Inflow (WWI) and defect flow (= GWI + RDII) (Rezaee and Tabesh 2022). To estimate WWI and assign its corresponding loads to the city-wide sewer system, a multi-step GIS analysis is conducted. After creating a land-use GIS layer based on available parcel information (Figure 3.6), daily average WWI rates are determined for different land-use categories according to the City of San Diego Sewer Design Guide (2015) presented in Table 3.4. Then, individual WWI loads from the existing 4648 urban parcels are attributed to their nearby sewer junctions using GIS analyses and subsequently imported into PCSWMM as junction baselines.

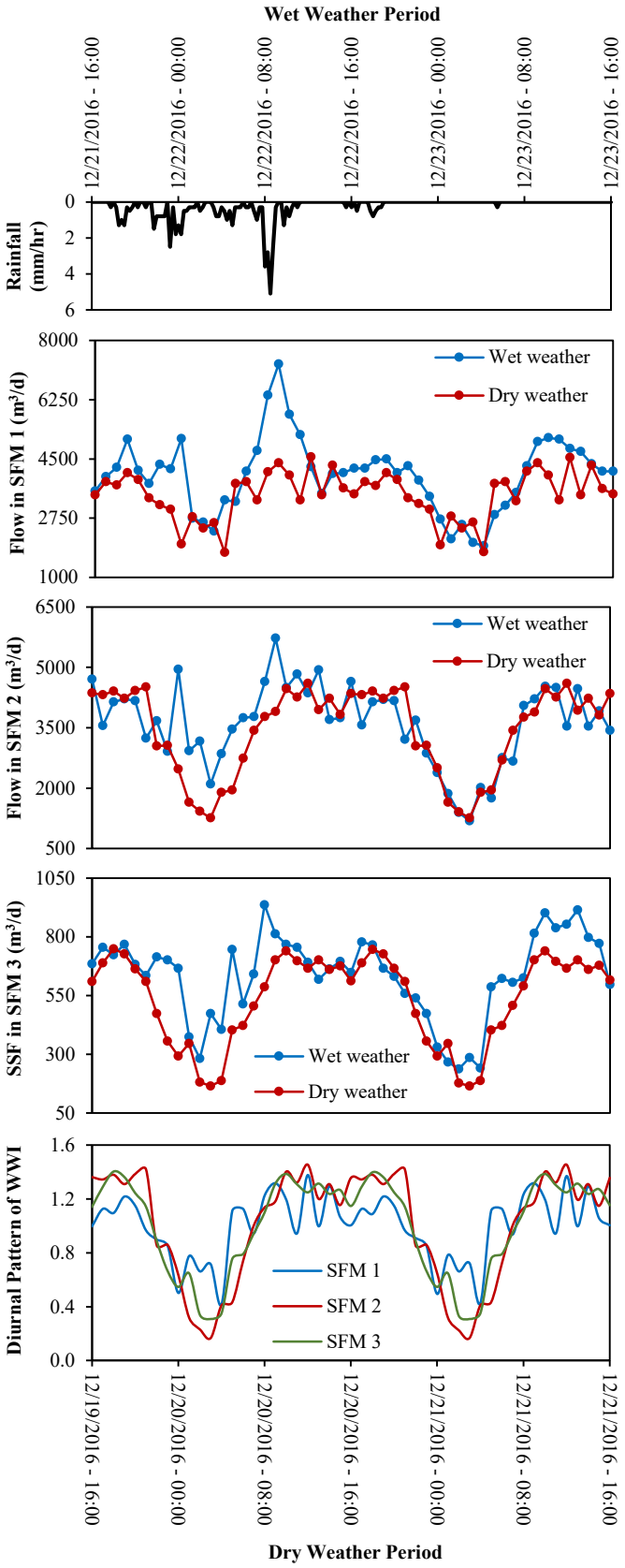

Figure 3.5 Monitored Sanitary Sewage Flow (SSF) during dry- and wet-weather periods

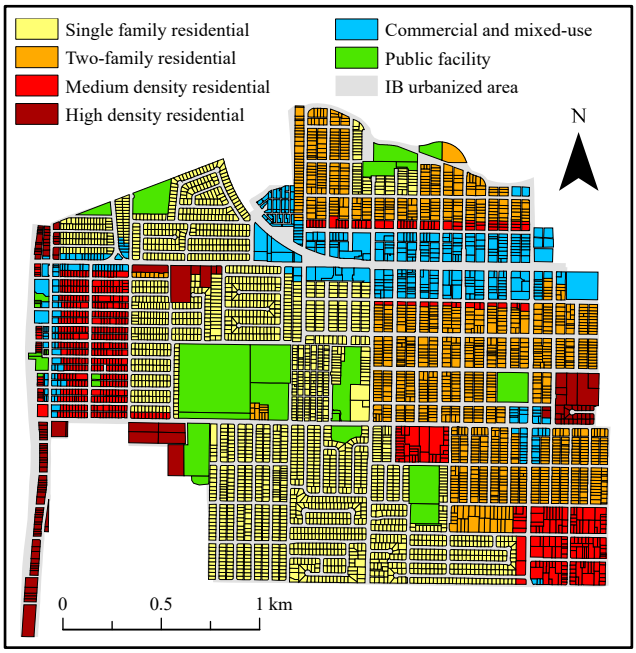

Figure 3.6 Land-use parcels in IB

Table 3.4 Wastewater inflow rates for different land uses

Land-use category	WWI rate (m^3/d)
Single family residential	0.570 (per parcel)
Two-family residential	0.494 (per 280 m^2 or 1 DU)
Medium density residential	0.456 (per 185 m^2 or 1 DU)
High density residential	0.418 (per 140 m^2 or 1 DU)
Commercial and mixed-use	7.733 (per 4047 m^2 or 1 acre)
Public Facility	9.503 (per 4047 m^2 or 1 acre)

According to the diurnal pattern presented in Figure 3.5, WWI loads during peak hours are also estimated by multiplying daily average WWI loads by a factor of 1.4.

$$\text{SSF} = \begin{Bmatrix} \text{WWI} \\ \text{WWI + GWI} \\ \text{WWI + GWI + RDII} \end{Bmatrix} \text{ for a } \begin{Bmatrix} \text{non-defective system} \\ \text{defective system in dry weather} \\ \text{defective system in wet weather} \end{Bmatrix} \quad (3\text{-}2)$$

The defect flow primarily includes GWI and RDII. In the case of having a defective system located under the GWT, groundwater constantly infiltrates into the system through its immersed defects. This study considers GWT elevation and system porosity (P = ratio of defect-to-conduit surface area in percent) as the two main parameters affecting GWI. According to Equation (3-2), GWI values for the three sewer zones are estimated by subtracting their daily-averaged dry-

weather SSF (Figure 3.5) from the estimated WWI (presented in Table 3.5 and previously described in this section). Then, by assuming that system defects are in an idealized circular form and uniformly distributed on defective conduits, the parameter P is adjusted in each of three sewer zones such that the calculated GWI from Equation (3-3) matches the estimated value from the monitoring data (during dry-weather conditions: GWI = SSF - WWI). This equation is a modified form of the head-discharge equation for a circular orifice, which assumes that the surrounding soil is homogeneous and isotropic, and not significantly washed out into the pipes (Guo and Zhu 2017). In this equation, ε = void ratio of the surrounding soil [= 0.2 according to the Web Soil Survey of The United States Department of Agriculture (2019)]; C_d = discharge coefficient of a circular orifice [= 0.6 according to Swamee and Swamee (2010)]; g = gravity acceleration; H_G = groundwater head over conduits; and A_{eff} = effective conduit area receiving GWI (Figure 3.7). It is worth noting that by assuming insignificant changes happening in the sewer system deficiency over the time, the calibrated P values for the existing system is considered for future scenarios too (ranging from 0.0015 to 0.0027). However, GWI variations with SLR are considered through involving A_{eff} and H_G parameters (which can be estimated based on the modeled GWT by MODFLOW). The calculated GWI for each defective and immersed conduit is allocated to its upstream junction as an additional baseline in the PCSWMM model.

$$\mathrm{GWI} = \frac{P A_{eff}}{2160000\pi} \varepsilon \, C_d \sqrt{g H_G} \tag{3-3}$$

Unlike GWI, RDII only occurs during rainfall events, and it can be obtained by subtracting dry-weather SSF from wet-weather SSF. As shown in Figure 3.5, the rainfall event during the sewer flow monitoring period occurred on December 21−22, 2016 with a total depth of 40.9 mm (determined based on the area under the rainfall hyetograph). As presented in Table 3.5, the resulting RDII from this rainfall event is estimated as the difference between SSF values from the

wet- and dry-weather monitoring periods. For estimation of RDII from a different rainfall event, it is assumed that the total depth of a rainfall event and its resulting RDII are proportional. For example, the total depth of a rainfall event with a 25-year return period is 69.6 mm, which is 70% larger than that of the monitored storm (69.6 ÷ 40.9 = 1.70). Thus, the monitored RDII values for each sewer zone (reported in Table 3.5) are multiplied by 1.7 to estimate the RDII for a 25-year storm. The resulting RDII values are assigned to upstream junctions of defective conduits as a wet-weather baseline in PCSWMM. It should be noted that due to climate change, approximately a 25% increase in heavy precipitation intensity is expected for southern California by 2100 (Fischer et al. 2014). A similar method is applied to consider potential additional RDII loads from the precipitation intensification for scenarios corresponding to SLR = 1-3 m.

Table 3.5 Comparison of monitored and modeled sanitary sewage flows

Station	Monitored SSF (m^3/d)			Modeled SSF (m^3/d)			Difference (%)
	Dry weather (WWI + GWI)	Wet weather (WWI + GWI + RDII)	RDII (wet weather – dry weather)	WWI	Dry weather	Wet weather	Dry/Wet weather
SFM 1	3448.1	4027.7	579.5	2953.0	3447.2	4027.1	0.0%
SFM 2	3427.7	3773.3	345.6	2603.2	3427.7	3772.6	
SFM 3	534.1	625.4	91.2	523.3	534.1	625.3	
Total	7410.0	8426.3	1016.4	6079.5	7409.0	8425.0	

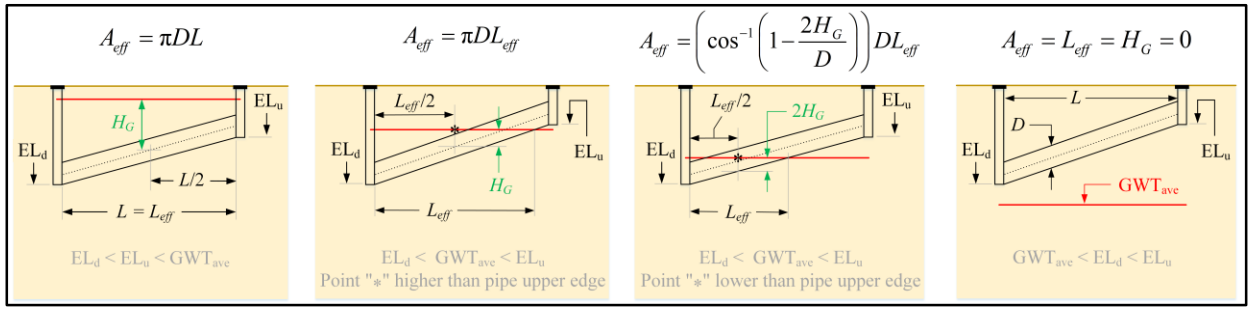

Figure 3.7 Different situations of conduits with respect to GWT_{ave}

After assigning three components of SSF to corresponding junctions in PCSWMM, flow routing within conduits is simulated by solving conservation of mass and momentum [i.e., 1D Saint-Venant equations; Equations (2-4) and (2-5)] using the Finite Difference Method (Rossman 2015). While Hazen-Williams coefficients of 150, 120, and 90 are respectively assigned to PVC,

DI, and CI sewer force mains, Manning's roughness coefficients for VC and PVC gravity mains are considered 0.014 and 0.011 [Engineering ToolBox (2004a) and (2004b)]. In addition, entry and exit loss coefficients of conduits range from 0.1−0.6 based on their relative sizes (Frost 2006). To evaluate the effects of SLR, system porosity, and rainfall properties on the performance of sanitary sewer systems, 17 scenarios are defined as presented in Table 3.6.

Table 3.6 Studied scenarios in the present study

Sanitary sewer system	Wastewater	Weather [I]	SLR (m)			
			0	1	2	3
Defective	Daily mean	Dry	WWm_SLR0_Dry	WWm_SLR1_Dry	WWm_SLR2_Dry	WWm_SLR3_Dry
		Wet [II]	WWm_SLR0_Wet	WWm_SLR1_Wet	WWm_SLR2_Wet	WWm_SLR3_Wet
	Daily peak [III]	Dry	WWp_SLR0_Dry	WWp_SLR1_Dry	WWp_SLR2_Dry	WWp_SLR3_Dry
		Wet	WWp_SLR0_Wet	WWp_SLR1_Wet	WWp_SLR2_Wet	WWp_SLR3_Wet
Non-defective	Daily mean	Dry/Wet	WWm			

[I] Wet weather condition refers to a 24-hour rainfall with a 25-year return period.
[II] To consider climate change effects on rainfall intensity, a 25% increase in RDII is applied for the scenarios corresponding to SLR = 1-3 m.
[III] Daily peak wastewater is approximately 40% larger than the daily mean value (diurnal pattern presented in Figure 3.5).

3.3 Results and discussion

3.3.1 Groundwater table variations in monitoring wells[1]

Figure 3.8 presents the time series of groundwater depth and head for the four monitoring wells across IB. From Figure 3.8(a), the GWT near the coast is the shallowest and most heavily influenced by ocean tides (GMW 1 shown in Figure 3.1). However, the observed GWT in other wells (GMW 2−4) are deeper, farther from the nearest coastline, and nearly stationary in comparison to GMW 1. Having semi-diurnal tidal fluctuations (i.e., two low and two high tides per day), the average GWT is approximately 0.2−0.4 m above MSL [Figure 3.8(b)]. Except for GMW 1 located in the small peninsula between the Pacific Ocean and the Tijuana Estuary, GWT fluctuations in the other wells across the city are less than 0.1 m, which is not impactful for urban infrastructure planning.

[1] The material of section 3.3.1 (describing the results of groundwater monitoring) are drafted by Austin Barnes and edited by the dissertation author.

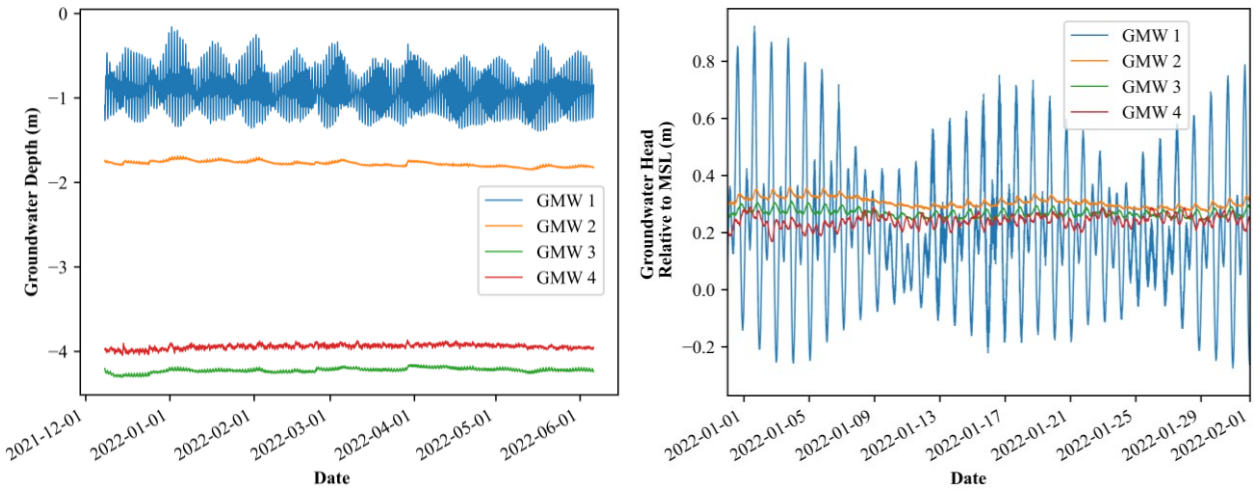

(a) (b)

Figure 3.8 Time series of (a) groundwater depth; (b) groundwater head for the monitoring wells (provided by Austin Barnes)

Tidal influence can be further quantified by the parameter of tidal efficiency (A), a measure of how damped the ocean tide amplitude is at a particular well, and the parameter of tidal phase lag (T_{lag}), a measure of the delay between the tidal forcing and GWT response. Table 3.7 shows a significant tidal influence at GMW 1 and a relative damping at all other wells. From this table, the parameter A at GMW 1 is about 0.4, which is 1-2 orders of magnitude greater than that of GMW 2−4. In addition, T_{lag} < 15 min at GMW 1, while this parameter is more than 3 and 5 hours at GMW 2 and 3, respectively. The tidal signal at GMW 4 is highly damped and distorted from the tidal forcing, and a phase lag cannot be determined because multiple plausible peaks in cross-correlation exist. From these possible peaks in cross-correlation, a range of tidal efficiency is reported for GMW 4 in Table 3.7. The high A and small T_{lag} values at GMW 1 are expected due to its proximity to the ocean and the relatively coarse sandy soil in the narrow area near the coastline. However, the tidal influences at GMW 2 and 3 are much smaller than our initial expectation considering their proximities to the Tijuana Estuary (30 m) and San Diego Bay (75 m), respectively. The significant damping of the tidal signal at these two wells near tidally-influenced water bodies suggests that the fine clay sediment underlying most of IB attenuates tidal

fluctuations of GWT across the city [Web Soil Survey of The United States Department of Agriculture (2019)]. These findings are consistent with GWT observations from Honolulu, Hawaii, where significant damping of tidal influence was observed in a relict river channel composed of fine-grained sediment (Habel et al. 2017). Since GMW 4 in the center of IB is located on a similar soil type with a larger distance from the surrounding water bodies, a small tidal influence occurs.

Table 3.7 Tidal influence parameters in the monitoring groundwater wells (provided by Austin Barnes)

Parameter	GMW 1	GMW 2	GMW 3	GMW 4
A (−)	0.393	0.007	0.008	0.004−0.007
T_{lag} (hr)	0.236	3.246	5.193	−

Because GMW 2−4 represent the soil type for the majority of IB, their minimal responses to the tidally-influenced water bodies suggest that a steady-state GWT approximation is appropriate for the management and planning of the sewer infrastructure systems. Thus, a steady-state groundwater model is developed for simulating spatial variations of GWT under different SLR scenarios. The modeled GWT at MSL are compared with temporal mean values of the observed GWT from the installed wells in Figure 3.9. From this figure, there is a strong agreement between the modeled and observed data, which validates the applicability of the groundwater model in predicting the spatial distribution of GWT across IB.

3.3.2 Marine and subsurface flooding

The assessment of potential marine and subsurface inundations is the first step for understanding the sewer system vulnerability to climate change. From Figure 3.1 and Figure 3.10, while Tijuana Estuary will be permanently impacted by marine inundation at higher SLR values, there will be minimal impacts on IB's urbanized area from this source of surface flooding. The presented results in Table 3.8 reveal that less than 2% of the populated region will be inundated at

the high SLR scenario (i.e., 2-m rise in the present-day sea level). It is worth noting that the areas near water bodies may be heavily impacted during temporary surface-water events. For example, the studies of Gallien (2016) and Merrifield et al. (2021) revealed that the IB's shoreline is notably vulnerable to dynamic wave-driven impacts. However, the dynamic conditions of the surrounding water bodies are not included in the present study due to their small effects on GWT and the sewer system's response across the city (discussed in the previous section).

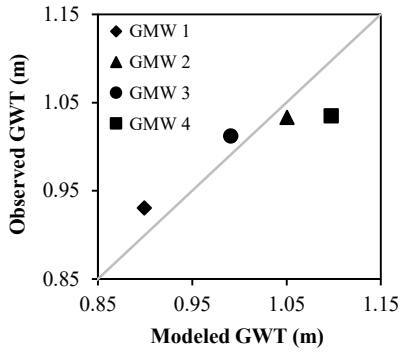

Figure 3.9 Comparison of the modeled and observed values of groundwater table

Table 3.8 Percentages of the IB urbanized area (total area = 5,515,463 m^2) impacted by marine and subsurface flooding

Source	SLR (m)			
	0	1	2	3
Marine inundation	0.0%	0.1%	1.8%	9.1%
Groundwater emergence	0.0%	0.2%	3.9%	9.8%
Groundwater shoaling with < 1 m depth	0.3%	4.2%	11.1%	20.2%
Groundwater shoaling with < 2 m depth	5.0%	11.7%	23.7%	36.0%
Groundwater shoaling with < 4 m depth	27.2%	41.9%	61.7%	75.3%
Groundwater shoaling with < 6 m depth	67.1%	80.7%	90.6%	94.7%

Compared to marine inundation, subsurface flooding (i.e., groundwater emergence and shoaling) has a more widespread spatial extent including areas far from the coastline (Figure 3.10 and Table 3.8 as the groundwater model outputs). Even in the current conditions, the GroundWater Depth (GWD) is less than 2 and 4 m in 5% and 24% of city areas, respectively. As a growing challenge for subterranean urban infrastructure systems, the SLR-driven groundwater lift will increase these numbers to 24% and 62% at SLR = 2 m. In addition, in the case of the extreme

scenario of SLR = 3 m, almost the entire city (95% of the urbanized area) will experience a GWD < 6 m at the end of the century.

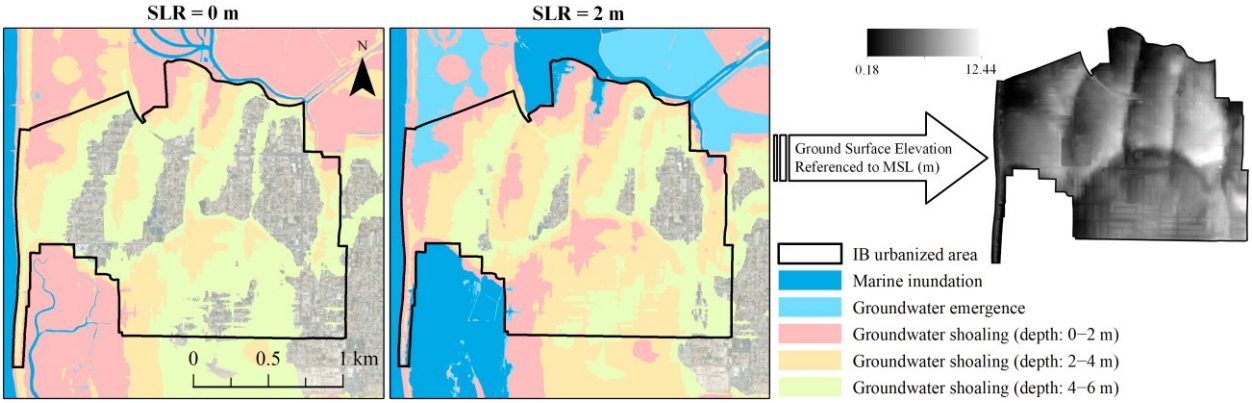

Figure 3.10 Marine inundation and subsurface flooding in current and future conditions

Having a general west-to-east direction, IB's sewer system is transmitting sewage flow away from the water bodies, and is not at the risk of direct seawater intrusion (Figure 3.2). However, due to the shallow GWT in IB, a substantial portion of the city's sewer pipelines may be at risk of GWI through their defects (adding a base flow to the system with a relatively steady rate). The presented results in Figure 3.11 and Table 3.9 demonstrate that about 12% and 36% of the sewer pipeline lengths may be under GWT and susceptible to GWI at SLR = 0 and 2 m, respectively. Comparison of Figure 3.10 and Figure 3.11 reveals that the sewer pipelines below the GWT are typically located in low-lying regions of the city where the potential for a shallow GWT is the highest.

3.3.3 Defect flows in the sanitary sewer system

The calculation of defect flow magnitudes is initiated by WWI estimations. Once WWI is determined, the sewer infrastructure's response to GWI (adding a base flow to the system with a relatively steady rate) can be represented by deviations of dry-weather SSF from WWI. Then, differences between SSF in dry- and wet-weather conditions become the basis of RDII calculations

(Figure 3.5). The diurnal patterns of WWI also can be used for the estimation of daily peak values. According to Table 3.5, the modeled SSF values (from the calibrated model) outstandingly agree with the monitored data (from SFM 1-3) in both dry and wet weather conditions.

Table 3.9 Percentages of sewer pipes under groundwater table [= 100 × L_{eff} / (total length of 74,289 m)]

Range (m)	SLR (m)			
	0	1	2	3
$H_G > 5$	0.0%	0.0%	0.0%	0.1%
$H_G > 4$	0.0%	0.0%	0.2%	1.5%
$H_G > 3$	0.0%	0.2%	2.6%	7.4%
$H_G > 2$	0.2%	2.8%	9.4%	17.3%
$H_G > 1$	4.2%	11.6%	21.5%	34.4%
$H_G > 0$	12.3%	22.6%	35.8%	48.7%

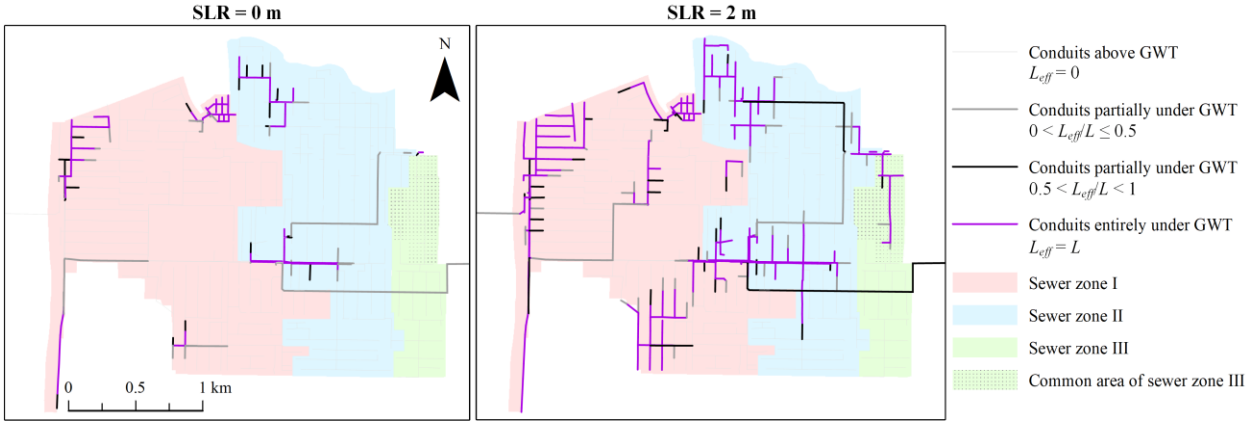

Figure 3.11 Sewer pipelines under groundwater table in current and future sea levels

The water consumption in the study area during the monitoring period was approximately 8330 m^3/d based on the urban water use data from Pacific Institute (2018). According to Water Environment Federation (2010) and Mayer (2016), WWI is generally in the range of 70−75 percent of the supplied water (i.e., ranging from 5830 m^3/d to 6250 m^3/d for the study area). From Table 3.5, since the modeled WWI (with a total of 6079.5 m^3/d) perfectly fits in the expected range, the significant deviations of the monitored SSF from the modeled WWI can be attributed to defect flows (1330.5 and 2346.8 m^3/d respectively for dry- and wet-weather monitoring periods).

The estimations of GWI for different SLR scenarios are presented in Figure 3.12. As

expected, GWI increases with rising sea level (red graph), and it grows about 4 times with 2 m of SLR (blue graph). In fact, the SLR-driven groundwater lift increases both A_{eff} and H_G parameters enlarging GWI [Equation (3-3) and Figure 3.7]. The mentioned results are obtained with the assumption that only defective conduits in the existing system (Figure 3.3) are contributing in GWI in both current and future conditions. Nonetheless, higher GWI values are generally expected by extending structural damages to non-detective parts of the system over the time. By considering the calibrated P values (section 3.2.3.4) for the whole system, it was found that GWI can increase almost three-fold in all SLR scenarios.

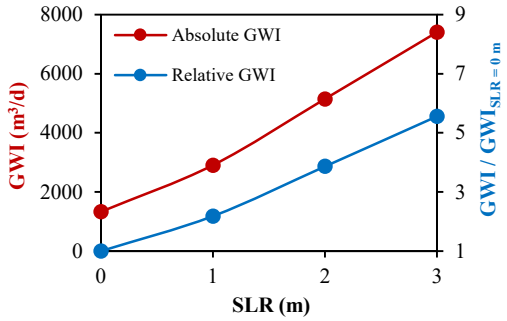

Figure 3.12 Estimations of GroundWater Infiltration (GWI) into the sewer system

To improve the understanding of the extent of defect flows, Figure 3.13 demonstrates the variations of SSF with SLR in both dry and wet-weather condition. From Figure 3.13(a), GWI increases hydraulic loads on the sewer system by 21% and 84% under current conditions and the high sea level scenario, SLR = 0 and 2 m, respectively. These numbers can be increased up to 49% and 120% during a 25-year rainfall event. The ratio of peak to mean SSF is presented in Figure 3.13(b) for different oceanographic and meteorological conditions. In the current sea-level and dry-weather conditions, there might be a 33% uplift in SSF during peak hours. However, due to higher contributions of GWI and RDII into SSF, this ratio may reduce almost to half in the high sea-level and wet-weather conditions.

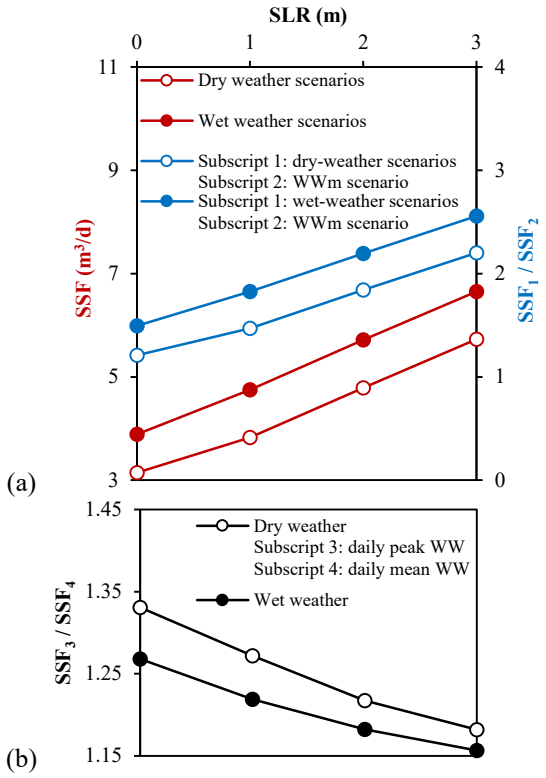

Figure 3.13 Estimations of Sanitary Sewage Flow (SSF) by considering: (a) daily mean wastewater inflow; (b) daily peak wastewater inflow

Besides increasing the potential for Sanitary Sewer Overflow (SSO), which is known as an environmental catastrophe and discussed in the next section, the defect flows at least place a burden on wastewater collection systems and treatment facilities if all these elevated loads can be handled by the infrastructure. Based on our results, with 300 mm of total annual rainfall, the defect flows in IB's sewer system can be up to 0.5, 1.1, 1.9, and 2.7 million m^3/yr for SLR = 0, 1, 2, 3 m, respectively. In addition, unit costs related to the collection system and treatment plant are estimated at \$0.61 and \$0.81 per cubic meter of SSF [sewer service studies for The City of Imperial Beach (2021)]. Therefore, for SLR = 0, 1, 2, and 3 m scenarios, the defect flows may respectively cost the city an additional approximate amount of 0.7, 1.5, 2.7, and 3.9 million dollars each year (not to include their possible contributions in SSO and mitigation costs).

3.3.4 Potential of Sanitary sewer overflows

The potential for overflows in the sewer system is evaluated based on hydraulic conditions in its junctions (i.e., free, surcharged, or under-pressure flow). As shown in the legend of Figure 3.14, in a free junction, water surface elevation [or Hydraulic Grade Line (HGL)] is lower than the crown of connecting conduits. However, a surcharged condition may occur by increasing SSF when connecting conduits get full of water. Due to further increases in SSF, sewer junctions eventually become pressurized and vulnerable to SSO if Energy Grade Line (EGL = HGL + velocity head) exceeds the ground surface elevation.

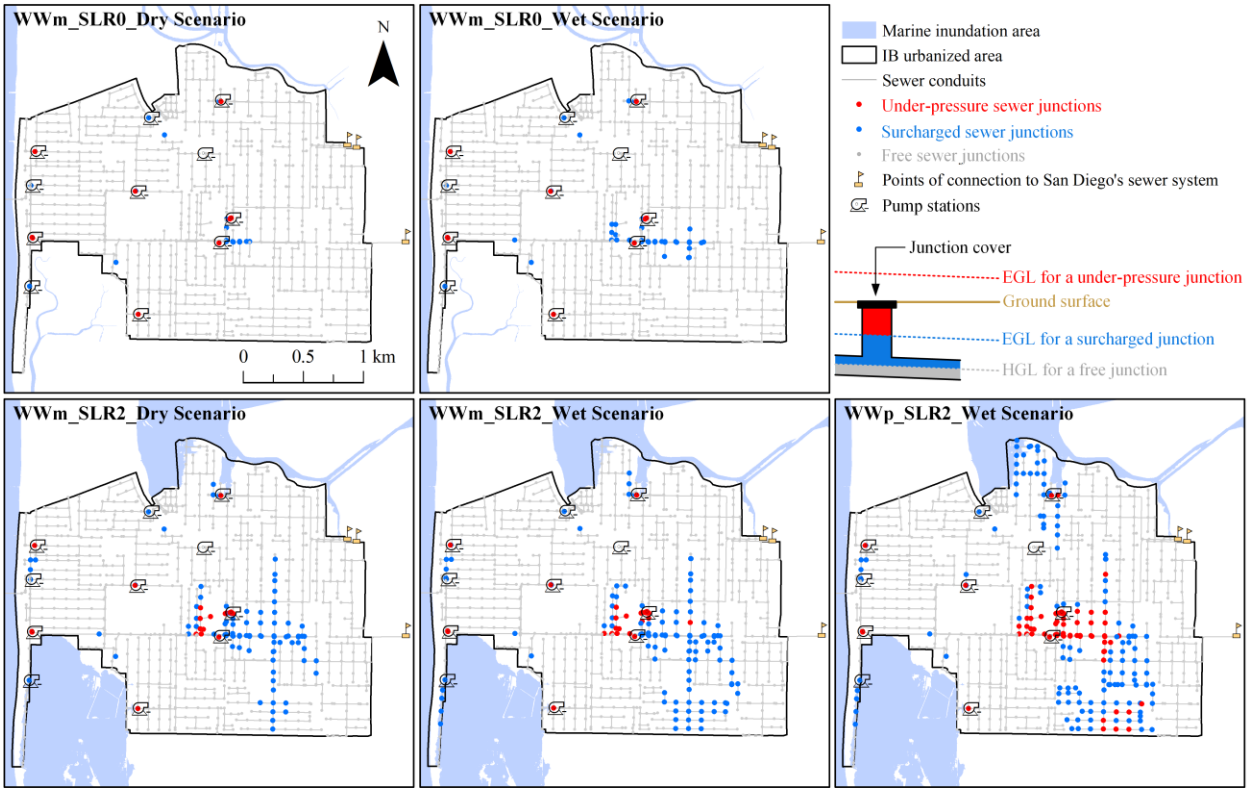

Figure 3.14 Mapping of SSO potential for five selected scenarios (defined in Table 3.6)

The SSO potential of IB's sewer system is mapped in Figure 3.14 for five scenarios in current and future conditions (defined in Table 3.6). As shown, even for the current sea-level conditions, there are some potentials for SSO occurrences across the city, especially in the

pressurized junctions. This point can be confirmed by 34 SSO events reported by the city since 2000 (internal reports of The City of IB shared with our team), which caused more than 74 m^3 of sewage spill in total. It is worth noting the real-world performance of the sewer system might be poorer in comparison to the presented results. For example, local blockages (e.g., debris, grease deposition, and root intrusion) in a sewer system can temporarily increase EGL in free or surcharged junctions and cause SSO.

From Figure 3.14, SLR not only will shift the shoreline landward but also increase the SSO potential substantially through enlarging GWI contribution to SSF in a defective system. With 2 m of SLR, the number of pressurized junctions across the city is expected to increase from 13 to 22 and 30 in dry and wet-weather conditions, respectively. This number can be increased up to 73 during peak flow hours. With rising sea level over the century, the area most impacted by SSO in the city will be kilometers away from the coastline (frequently impacted by dynamic sea-level events). In fact, the SSO hotspots will be more concentrated on the shallow-groundwater regions where the groundwater head over the defective sewer pipelines is the highest (depicted in Figure 3.10 and Figure 3.11). More challengingly, SSO events can be considerably more widespread and severe due to larger amounts of WWI and RDII during peak flow hours and wet-weather periods, respectively (leading to further increases in the hydraulic loadings on the system). These findings confirm the importance of considering compound impacts of coastal stressors on urban infrastructure systems.

Based on the CCTV assessment of defective conduits and the obtained results from the present study, a holistic approach is presented and implemented for prioritizing sewer system repairs (Figure 3.15). As a comprehensive index, Sanitary Sewer Vulnerability Index (SSVI) involves different structural, hydrological, and hydraulic conditions in the rehabilitation priority

plan. From Figure 3.15, each defective conduit is given a severity rating of low, moderate or high. In addition, higher degrees of vulnerability are assigned to defective conduits immersed by groundwater at lower values of SLR (which are more prone to GWI and additional structural deterioration). Moreover, structural deficiencies are rated based on their proximities to junctions with higher SSO potential. As a result, each defective conduit in IB's sewer system is given a low, moderate, high, or urgent priority, which demands the most immediate action for rehabilitation.

Index	Degree of sewer structural damages			Sewer inundation by groundwater at different greenhouse-gas emission scenarios				Flow condition in downstream junction		
	Slight	Moderate	Severe	Low (SLR = 0 m)	Moderate (SLR = 1 m)	High (SLR = 2 m)	Extreme (SLR = 3 m)	Free	Surcharged	Pressurized
Sanitary sewer deficiency index (A)	2	4	8							
Groundwater head index (B)				8	4	2	1			
SSO potential index (C)								2	4	8

(a)

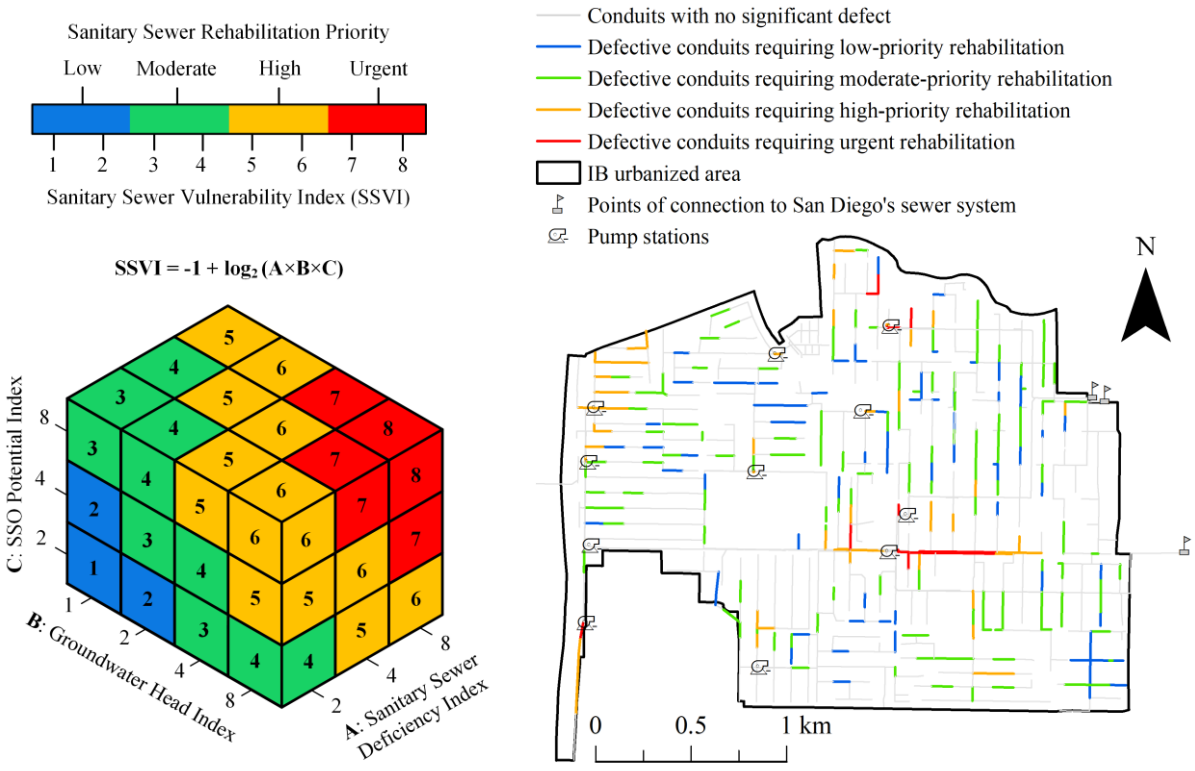

(b) (c)

Figure 3.15 Rehabilitation priority plan: (a) definition of involved indices; (b) visualization of vulnerability matrix; (c) Implementation on IB's sewer system

From the rehabilitation priority map shown in Figure 3.15(c), the higher priority repairs

(SSVI ≥ 5) are mostly located in the low-lying areas (Figure 3.10), which are more susceptible to experiencing defect flows (Figure 3.11) and SSO events (Figure 3.14). In addition, while The City of IB is currently paying most attention to the coast in its SLR planning projects, Figure 3.15(c) reveals that the urgent-priority rehabilitation of the water infrastructure is mostly needed further inland (~2 km from the coastline). This point emphasizes the importance of considering the interactions of oceanographic, hydrological, and meteorological processes in planning of urban infrastructure systems and developing efficient adaptation strategies against climate change.

3.4 Summary

To improve the understanding of emerging climate change impacts on coastal water infrastructure, the current and future roles of defect flow in the performance of IB's sanitary sewer system have been studied in this chapter. The results show significant increases in hydraulic loads on the system (leading to higher costs of operation and maintenance) due to defect flow (i.e., GWI and RDII). More importantly, defect flow also can heighten the risk of sanitary sewer overflow, as an environmental catastrophe, especially by rising sea levels and intensifying rainfall events. Considering the compound impacts of oceanographic-hydrological-meteorological stressors, the most impacted area will be in the middle of the city (kilometers away from the coastline). From the previous chapter, the highest impacts of stormdrain flooding also will be experienced in this region. Thus, specific attention is paid to this area in the next chapter, which focuses on climate change adaptation using decentralized water infrastructure.

CHAPTER 4 COUPLING ENGINEERED AND SOCIAL STUDIES TO DEVELOP RESILIENT WATER INFRASTRUCTURE AGAINST COASTAL CLIMATE CHANGE

4.1 Objectives

This chapter constitutes the plan for the utilization of this project, which is promoting coastal community resiliency against climate change through mitigating flood impacts (as well as improving the water budget) in a watershed scale and a distributed manner. From the literature review (sections 1.2.4 and 1.2.5), there are low rates of decentralized infrastructure adoption by urban residents regardless of their high potential in addressing stormwater quantity and quality issues. Thus, the success of decentralized infrastructure heavily relies on understanding the barriers and motivations that communities face in implementing and operating such systems.

Focusing on the coastal city of Imperial Beach, this study aims to develop resilient adaptation measures by integrating hydrologic-hydraulic criteria (i.e., outputs of the stormdrain model developed by the dissertation author) with responses to social surveys (i.e., framed and conducted by the Social-Science part of the team under the supervision of Dr. Megan Welsh). As one of the first known attempts to gather the perspectives of the residents of an underserved coastal community on barriers and motivations to adopt decentralized infrastructure (see Table 1.2), the social survey is critical for this research to advance public knowledge and mitigation practices in vulnerable communities. This chapter also extends the one-dimensional stormwater model (developed in Step 1 or Chapter 2) to simulate rainwater capture through decentralized infrastructure as well as flow propagation in two dimensions over the land surface under coastal climate change (i.e., SLR, groundwater rise, and more intense rainfall. For decentralization, this study focuses on two popular practices of RainWater Harvesting (RWH) and Green Infrastructure (GI), specifically Rain Barrel (RB) and Rian Garden (RG) shown in Figure 4.1 and Figure 4.2.

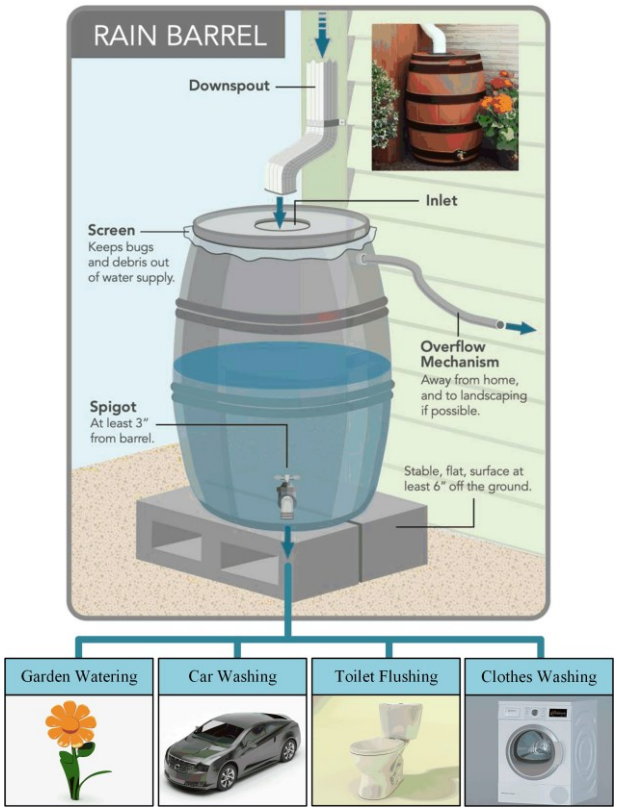

Figure 4.1 Schematic view of a Rain Barrel (RB) [adapted from Lincoln Stormwater Program (2022)]

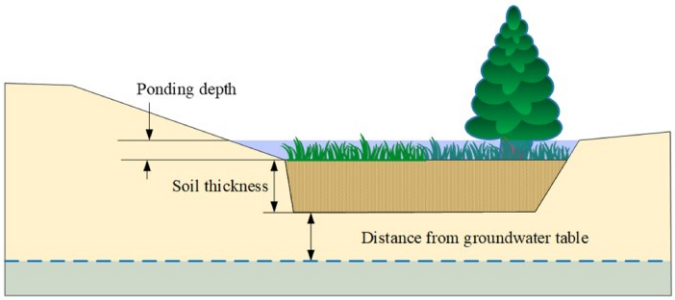

Figure 4.2 Schematic view of a Rain Garden

The principal objectives of the present research are

- analyzing social survey responses and the public's perceptions to estimate the extent to which decentralized water infrastructure might be accepted by the target underserved coastal community;
- evaluating the capability of decentralized water infrastructure in reducing precipitation-based runoff (and subsequently mitigating the extent of overland flooding) under different

climate change scenarios and adaptation measures.

4.2 Material and methods

4.2.1 Study area

As pointed out previously in section 1.4, the current study focuses on Imperial Beach (IB), San Diego County, California, USA. This low-lying coastal community is surrounded geographically by water bodies from three sides (The Pacific Ocean, San Diego Bay, and Tijuana Estuary), and it has historically experienced marine flooding due to its unique setting (Figure 1.4). In the previous chapters (i.e., Figure 2.10, Figure 3.3, and Figure 3.14), it was shown that the aged and defective water drainage infrastructure of IB is especially vulnerable to compound impacts of seawater-groundwater-stormwater stressors when a heavy rainfall coincides with a high sea-level event. In these challenging circumstances, IB's stormdarin system (shown in Figure 4.3) is prone to compound flooding since significant portions of the stormdrain system capacity have been already occupied by SeaWater Intrusion (SWI) and GroundWater Infiltration (GWI) through immersed outfalls and defects, respectively.

IB is considered an underserved and underrepresented community based on its resident demographics, which makes it highly vulnerable to compound flooding and in strong need of community-specific solutions to build resilience against climate change impacts. California Department of Water Resources defines a disadvantaged community as a community with an annual median household income of less than 60% of the statewide average value (Haaland and Ortiz 2022). The corresponding numbers for IB and the state of California are respectively reported as $68,917 and $119,149 by the most current (2021) income statistics obtained from the United States Census Bureau (2022a).

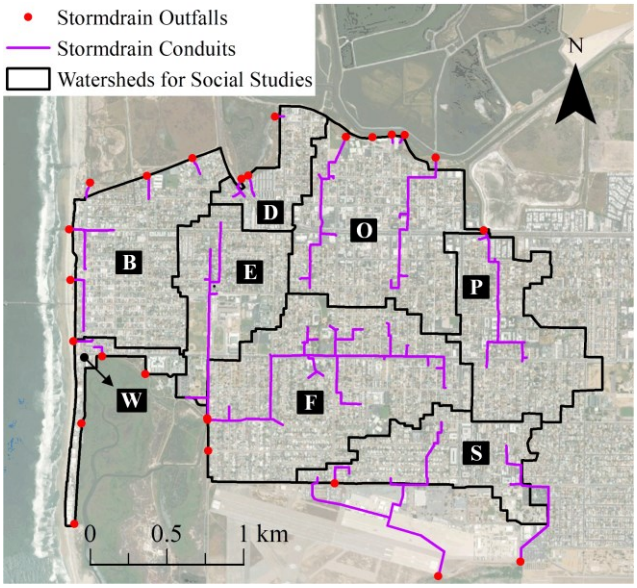

Figure 4.3 Visualization of IB's stormdrain system along with the eight watersheds used for residency identification in the social survey

According to the demographic data presented in Table 4.1, IB has an estimated 26,059 population, of which 51.9%, 7.8%, and 5.4% are respectively from minority groups of Hispanic or Latino, Asian, and Black or African American. The owner-occupied housing unit rate in IB is 31.8%, which is substantially lower than that for San Diego County (54.1%), California (55.5%), and the US (64.6%). In addition, as low as twenty-three percent of IB residents have a bachelor's degree or higher, compared to 40.3% of San Diego County residents. Moreover, the poverty and uninsured rates are 13.4% and 13.6% in IB while the corresponding numbers for San Diego County are 10.7% and 8.2%, respectively (United States Census Bureau 2022b).

4.2.2 Primary datasets for stormdrain modeling

The datasets utilized for stormdrain modeling (ground elevation, sea level, stormdrain system characteristics, and rainfall specifications) have been mainly described in section 2.2.2 and Table 2.1. Additionally, GWI estimations have been updated in the PCSWMM model by applying the methodology mentioned in Chapter 2 (section 2.2.3.2) and using high-resolution estimations

of GWT from the developed groundwater model in Chapter 3 (section 3.2.3.2). As a new input for stormdrain modeling, a GIS layer of urban buildings is obtained from the data warehouse of the City of Imperial Beach (Figure 4.4), which was validated through visual comparison with available aerial imagery. This layer has been used for (i) the determination of rooftop footprints needed for the estimation of the number of RBs for each building and (ii) the prevention of water flow in overland areas by defining an obstruction layer.

Table 4.1 Comparison of demographic factors [obtained from United States Census Bureau (2022b)]

Demographic factor	Value			
	Imperial Beach	San Diego County	California	United States
Population	26,059	3,274,954	39,142,991	332,031,554
Land area (Km^2)	11	10,904	403,672	9,150,534
Persons under 18 years (%)	22.7	21.3	22.4	22.2
Persons 65 years and over (%)	10.0	14.9	15.2	16.8
Owner-occupied housing unit rate (%)	31.8	54.1	55.5	64.6
Bachelor's degree or higher, persons age 25 years+ (%)	23.4	40.3	35.3	33.7
Persons in poverty (%)	13.4	10.7	12.3	11.6
Persons without health insurance, under age 65 years (%)	13.6	8.2	8.1	9.8

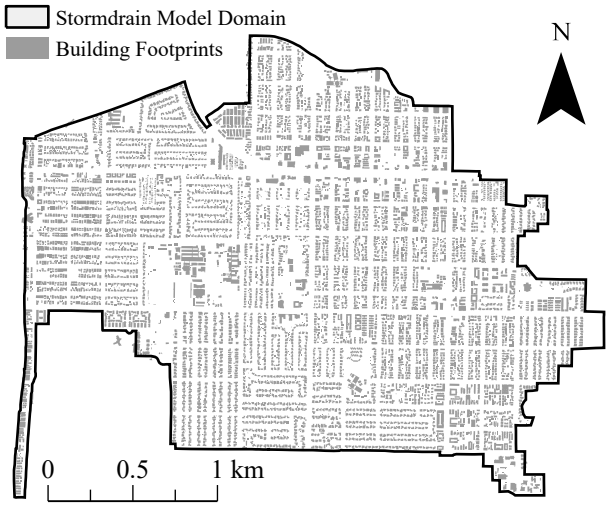

Figure 4.4 Visualization of building footprints in IB

Local sources [e.g., the County of San Diego Hydrology Manual (2003) and The City of San Diego Stormwater Standards (2021) are used to set primary parameters for the model (e.g., subcatchment roughness, imperviousness, infiltration, and evaporation as well as conduit roughness and energy loss), which have been previously described in section 2.2.3.3. Other

parameters for simulation of overland flooding (e.g., surface roughness) and decentralized water infrastructure (e.g., RB sizing and drainage) are described in sections 4.2.3.1 and 4.2.3.2.

4.2.3 Methods

Figure 4.5 presents the workflow carried out in the present study, which mainly aims to develop resilient adaptation solutions by integrating hydrologic-hydraulic criteria (top part of the figure) with the community's perception of stormwater management measures (bottom part of the figure).

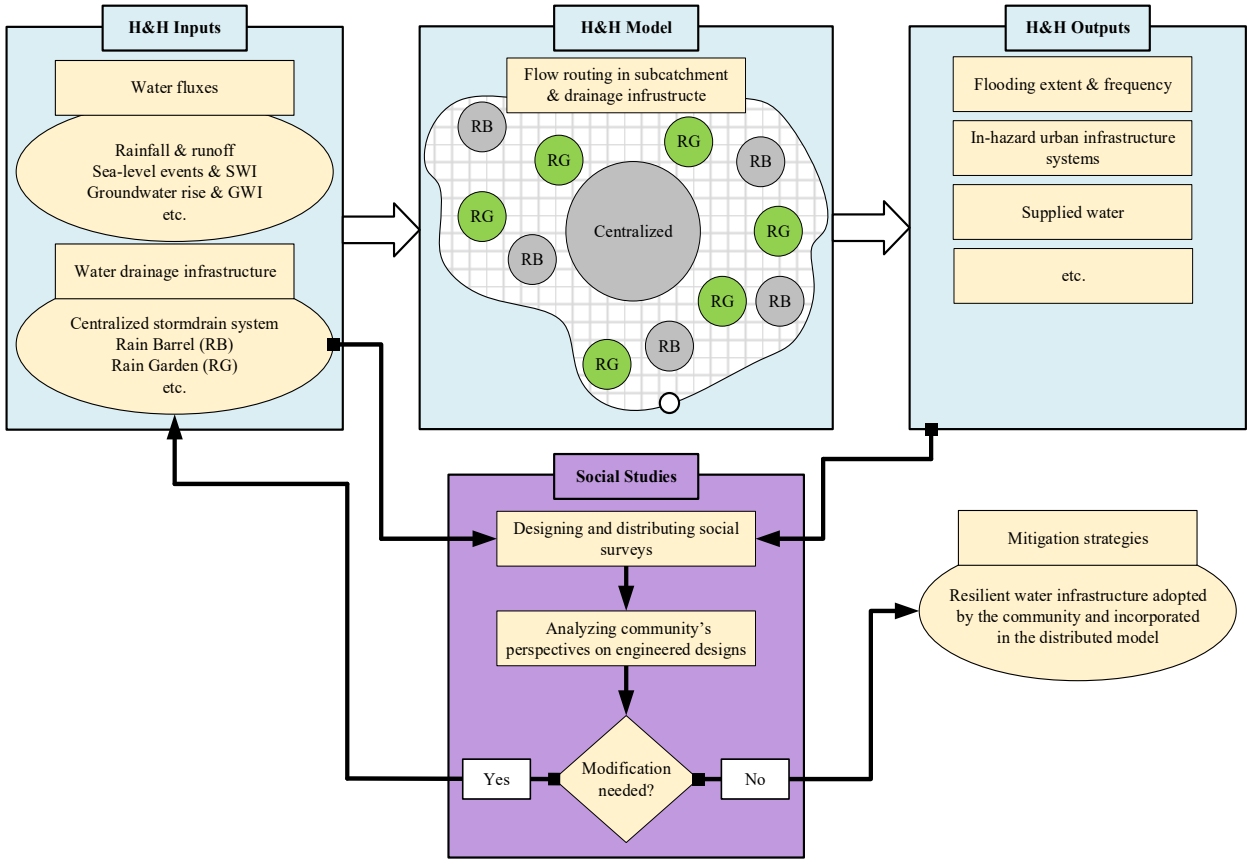

Figure 4.5 Framework of coupled engineering and social studies

Based on the framework, decentralized infrastructure systems are implemented in the watershed-scale stormdrain model (the PCSWMM model developed in Chapter 2) to evaluate their

capabilities in flood mitigation. The findings are communicated with the Social-Science part of the research team to be reflected in the social survey. Estimating the extent to which the engineered designs might be accepted by the target community, the stormdrain model configurations are then refined to properly address stakeholders' preferences in adaptation strategies and predict their capabilities in mitigation of overland flooding. The utilized methodologies for engineering and social studies are described in the flowing sections.

4.2.3.1 Overland flood modeling

In order to perform the hydrologic-hydraulic modeling, the developed and calibrated PCSWMM model in Chapter 2 is used as the base model. In this chapter, the base model is extended to simulate (i) rainwater capture through decentralized infrastructure and (ii) flow propagation in two dimensions of the land surface under a changing climate.

The general characteristics of the model have been presented in section 2.2.3.3 (see Figure 2.1), which includes 122 fine-resolution subcatchments, 263 conduits/junctions, and 25 outfalls. The rainfall-runoff transmission over urban subcatchments (hydrological modeling) is performed using a nonlinear reservoir model coupled with Manning's equation [Equations (2-2) and (2-3)]. Flow routing into the system (hydraulic modeling) is simulated by solving the complete form of Saint-Venant equations (referring to an unsteady and non-uniform flow) in one dimension along conduits [Equations (2-4) and (2-5)] (Rossman 2015).

Despite their computational efficiency, 1D urban flooding models are unable to simulate the flow propagation in overland areas. For simulating overland flow propagation, PCSWMM solves the conservation of mass and momentum (Saint-Venant equations) in two dimensions (or multiple directions) of the land surface and one dimension along the underlying drainage

infrastructure. Figure 4.6 visualizes how PCSWMM relates a minor system (1D water conveyance in conduits) to a major system (2D water conveyance on the surface).

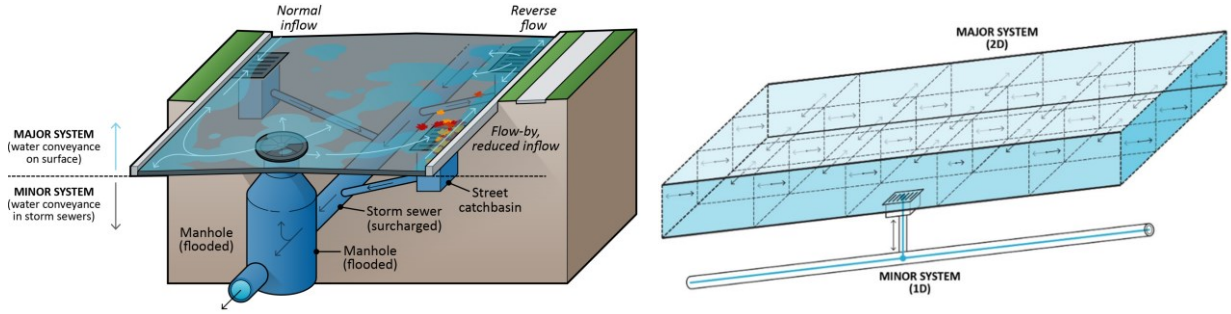

Figure 4.6 Relating minor (1D) and major (2D) systems in PCSWMM (Computational Hydraulics International 2023). The figure on the top also depicts the 2D model's ability in terms of simulating split-flow conditions across right of way

As the first step for the 2D model development, a bounding layer is defined to specify the extent of the overland system. As a starting point, the bounding layer was considered equal to the IB's urbanized area (the stormdrain model domain as shown in Figure 4.4) and discretized with a rough mesh. Considering the high computational cost of 2D simulation, it was then limited to the areas prone to flooding in the most pessimistic scenario (SLR = 2 m, P = 0.25, and 25 percent more intense rainfall with no decentralized system) by increasing the model resolution. For high-resolution modeling of distributed overland flow, the ground surface (i.e., the finalized bounding layer) is discretized generally by hexagonal grid cells with the size of 4 m, which is significantly finger than the 10-m resolution of previous studies (Rangari et al. 2018; Sidek et al. 2021). This size is optimized based on the required resolution and computational resources (i.e., a personal computer with 128 GB RAM and 36 logical processors of an Intel Core i9-10980XE CPU @ 3.00GHz). Each grid cell will contain basic hydrological and hydraulic inputs such as elevation (taken from the DEM layer) and Manning's roughness coefficient (ranging from 0.025 to 0.033) (Computational Hydraulics International 2023).

Figure 4.7 illustrate how the overland system is discretized into the 2D mesh and connected

to the 1D underlying drainage system visualizes in the PCSWMM model. As shown, a 2D node layer is generated based on DEM layer data for representing the floodplain topography. The final mesh layer consists of more than 20 thousand 2D cells (and junctions). Each junction from the 1D system is connected to its closest 2D junction through a side orifice using the "Connect 1D to 2D" tool in PCSWMM. This connection allows a free transfer of flow from the underlying 1D system to the 2D overland areas. By defining an obstruction layer based on IB's building footprints (Figure 4.4), the size and shape of 2D cells are modified to account for structures & barriers that impede the water flow motion (Figure 4.7).

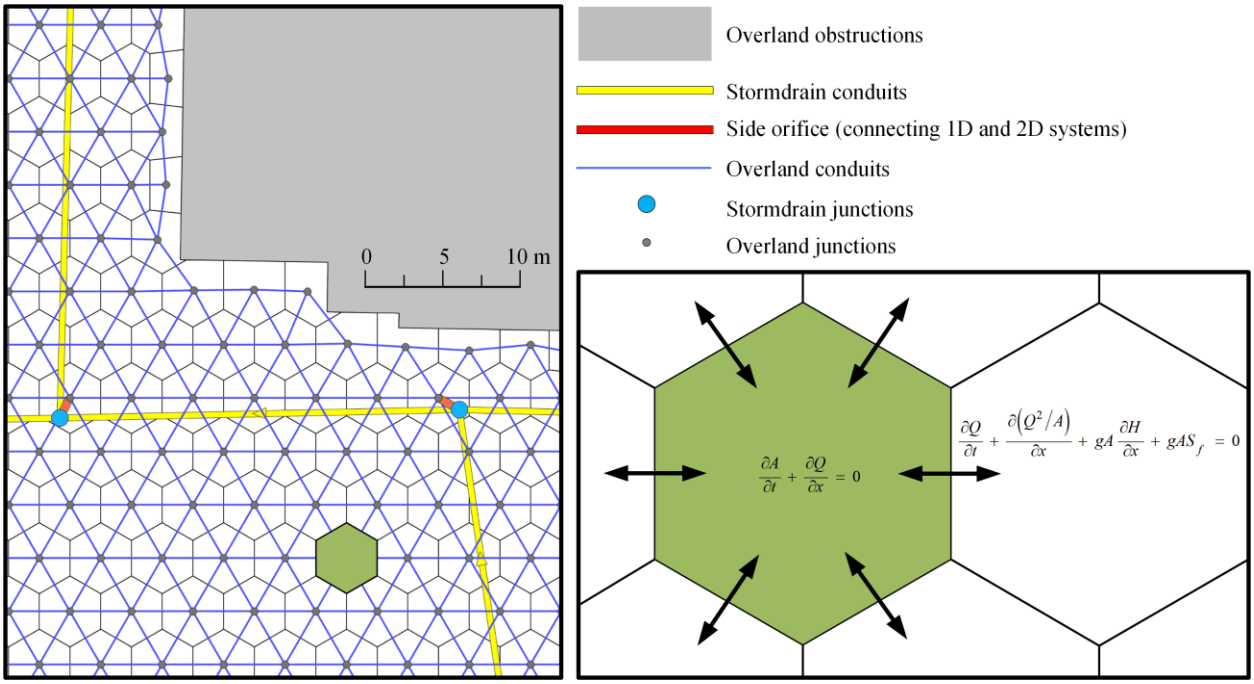

Figure 4.7 Connections between 2D overland mesh and 1D drainage system

Boundary conditions are applied using the "Create Boundary Outfalls" tool in PCSWMM, which uses a downstream polyline layer to create outfalls on the 2D domain boundary and connect them to existing 2D nodes through new 2D conduits. In the intersection of the bounding layer and marine inundation area, the boundary condition is set to a fixed value corresponding to the sea-level elevation at MHHW for a given scenario. For other areas, the bounding layer was large

enough for water not to cross (or touch) the boundary. Finally, GIS analysis is performed on the stormdrain model outputs (e.g., flood depth and area) to provide floodplain maps and identify in-danger areas for different climate change scenarios and adaptation strategies.

4.2.3.2 Decentralized infrastructure modeling

The PCSWMM model, explained in the previous section, is extended to simulate the watershed-scale performance of RB and RG systems (Figure 4.1 and Figure 4.2) in reducing hydraulic loadings on vulnerable centralized infrastructure (Figure 2.10 and Figure 3.14). An RB system also can adjust the water budget by providing new sources for both indoor and outdoor end uses. The SWMM engine is a widely used framework for developing and sizing decentralized infrastructure (Elliott and Trowsdale 2007; Tavakol-Davani et al. 2016; Walsh et al. 2014).

A schematic diagram illustrating RB flow routing in PCSWMM is presented in Figure 4.8. As one of the baseline scenarios, the County of San Diego Rain Barrel Tutorial (2022) recommends a 600-gallon (or 2.271 m^3) volume of RB for each 1000-ft^2 (92.9 m^2) rooftop area receiving 1-inch rainfall. In section 4.3.2, the feasibility of this recommendation is confirmed, and the adoption rates of the decentralized infrastructure is estimated based on social study outputs. Health-related risks (e.g., the attraction of mosquitoes) may increase with RWH storage time exceeding 48 hours (County of San Diego Standard Urban Stormwater Mitigation Plan 2012). In PCSWMM, the underdrain flow of an RB system is modeled as a submerged orifice and governed by Equation (4-1), which is matched to meet the drain time requirement. In this equation, U_d (in/h) represents underdrain flow, and its product with RB area yields the flow rate of demands (Tavakol-Davani et al. 2016). The drain coefficient is considered $C = 0.5$, which allows typical 60-gallon (or 227-liter) and 2000-gallon (7571-liter) barrels to be drained over 24-hour and 48-hour periods, respectively

(Walsh et al. 2014). Since the survey results in section 4.3.1 show that garden watering will be the most favorite benefit of decentralization in IB, a 24-hour drain delay was established for models to prevent irrigation during (or right after) precipitation events.

$$U_d = C\left(H_d - h_d\right)^n$$
$$\begin{cases} n = \text{drain exponent} = 0.5 \text{ representing the flow through an orifice}); \\ h_d = \text{drain offset} = 0 \text{ established at the bottom of barrels (in)}; \\ H_d = \text{water hieght from the barrel drain offset (in)}; \end{cases} \quad (4\text{-}1)$$

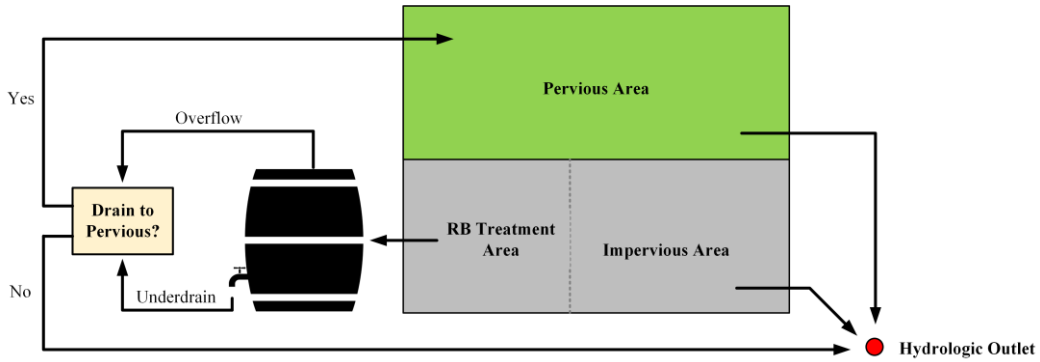

Figure 4.8 Schematic view of flow routing in a hydrologic unit with an RB system

The Geometric and Geological parameters of the RG system are set by referring to local sources of The City of San Diego Whitebook (2018) and The City of San Diego Stormwater Standards (2021). These parameters are described in Table 4.2. It is worth nosan diting that the RG system implementation was limited to areas with a distance more than 0.601 m (or 2 ft) from groundwater table. Table 4.3 presents the studied scenarios for evaluating the performance of the stormdrain system with and without decentralization.

Table 4.2 Selected values for RG system parameters

RG Parameters	Value
Ponding depth (m)	0.305
Soil thickness Land area (m)	0.457
Distance from groundwater table (m)	0.610
Porosity	0.4
Filed capacity	0.2
Wilting point	0.1
Conductivity (m/day)	3.048
Conductivity slope	5
Suction head (m)	0.038

Table 4.3 Studied scenarios in the present research

SLR (m)	*P* (%)	Rainfall period	Decentralization		
			Without RB or RB	With RB	With RB and RG
0	0.00	1-year	S0-P0.00-R1	S0-P0.00-R1-RB	S0-P0.00-R1-RB-RG
	0.00	5-year	S0-P0.00-R5	S0-P0.00-R5-RB	S0-P0.00-R5-RB-RG
	0.00	continuous	S0-P0.00-Rc	S0-P0.00-Rc-RB	–
	0.25	1-year	S0-P0.25-R1	S0-P0.25-R1-RB	S0-P0.25-R1-RB-RG
2	0.00	1-year*[1]	S2-P0.00-R1*	S2-P0.00-R1*-RB	S2-P0.00-R1*-RB-RG
	0.25	1-year*	S2-P0.25-R1*	S2-P0.25-R1*-RB	S2-P0.25-R1*-RB-RG

[1] The return period of 1-year* corresponds to the 25% increase in rainfall intensity due to climate change [happening every year at the end of century; Fischer et al. (2014)].

4.2.3.3 Social survey[1]

The purpose of social surveys (developed and conducted by other team members under the supervision of Dr. Megan Welsh) is to gather IB residents' and business owners' perceptions of flooding and decentralized water infrastructure. With an approved Institutional Review Board protocol (IRB no. HS-2022-0064), a total of 110 valid responses to the social survey are collected from IB's stakeholders (i.e., residents and business owners). The target number of survey responses (n) is determined based on the research feasibility and previous social studies by other researchers [n = 28, 90, 297, 396 in the studies of Meerow (2020), Gao et al. (2016), Maeda et al. (2018), and Mason et al. (2019), respectively]. During these human subject activities to understand (i) perceptions of flooding and related stormwater pollution issues in IB, (ii) awareness of decentralized water infrastructure [including Rain Barrel (RB) and Rian Garden (RG) as shown in Figure 4.1 and Figure 4.2], (iii) potential incentives for improving RB and RG adoption by the community, and (iv) barriers to the implementation and maintenance of decentralized water infrastructure.

The designed survey is composed of twenty questions (Q1−20 in APPENDIX) including 3 yes-or-no questions, 4 multiple-choice questions, 3 multiple-response questions, 6 numeric scale

[1] The material of section 4.2.2 (describing development, distribution, and collection of social surveys) is provided by Dr. Welsh (and/or other students working under her supervision) and edited/extended by the dissertation author.

questions, and 4 open-ended questions on the community's concerns, ideas, and preferences on decentralization and flood prevention. In addition, it includes brief and illustrative information on rainwater harvesting and green infrastructure practices, i.e., to help participants have a better understanding of survey questions and familiarize themselves terminology of RB and RG. A 2-min tutorial video on stormwater management practices has been included in the online version of the survey [provided by the United States Environmental Protection Agency (2022)]. Using screening questions at the beginning of the survey, the participants are limited to IB residents or business owners aged 18 and more.

The survey questions are developed based on past literature on assessing social barriers to the adoption of decentralized infrastructure (mentioned in section 1.2.5 and Table 1.2), public perceptions of stormwater management practices (Coleman et al. 2018; Giacalone et al. 2010; Persaud et al. 2016; Thomas et al. 2014), and water conservation attitudes and incentives (Meder and Kouma 2010; Willis et al. 2011; Zamani Sabzi et al. 2019). Mindfully adjusted to the socio-demographic context of IB, the questions are progressing from asking about demographic factors, awareness of decentralized water infrastructure, acceptability of financial incentive programs, and motivating benefits of RB and RG for community-based management of stormwater.

The survey has been offered in English and Spanish versions, and respondents are recruited using a mix of online and in-person outreach activities. The approximate duration of the survey questionnaires was 15 min. Online survey data are collected using the Qualtrics platform (Qualtrics 2022). Three in-person engagement events have been conducted by setting up a table with information about the project and opportunities to take the survey either by paper or electronically via a tablet. In partnership with the City of IB, these outreach events have been held in the IB's public library and farmers market in July-November 2022 (Figure 4.9). As noted previously, the

City of IB is a key partner in this work, and it has publicly expressed its commitment to utilizing our research to inform its climate change resiliency efforts.

Only the research team members have had access to the data (who have already completed the Collaborative Institutional Training Initiative (CITI) Program courses on human-subject research ethics). Following General Data Protection Regulation (GDPR) guidelines on privacy, online data is collected anonymously, and identifiable data (such as IP addresses) is eliminated from the collected responses. According to 0 APPENDIX, the only demographic questions in the survey are Q1, Q3, and Q6, which include (i) identification as an IB homeowner, renter, and/or business owner, (ii) identification of which drainage basin the respondent lives or does business in (dividing the city of IB into eight aggregated watersheds as shown in Figure 4.3); and (iii) a guesstimate of the respondent's monthly water bill. The minimal captured demographic data may not be traced back to respondents since these three data points are not individually identifiable in a city with over 26,000 populations.

Figure 4.9 Example of in-person engagement events conducted by the Social-Science part of the research team and supervised by Dr. Megan Welsh (camera-facing pictured from left-to-right: Giovanna Zampa, Jaeda Cook-Wallace, and Asuka Koga sharing the survey to IB's residents; location: IB's Farmers Market; date: October 15th, 2022; photo taken by Dr. Davani)

Basic statistics of the survey responses are processed in SPSS 29 (IBM 2023) and presented in the next section. More descriptive and inferential statistics are calculated in Microsoft Excel. In

addition to analyzing the main effects of each parameter on decentralized infrastructure adoption, this study also identifies and quantifies interactions between different parameters (implying that a parameter's effect depends on the level of other parameters) (Sangsefidi et al. 2017). Moreover, to gain insight into residents' perspectives on the benefits and limitations of decentralization, responses to the three open-ended questions of Q8, Q10, and Q19 are coded using an inductive approach (deriving the codes from the dataset).

4.3 Results and discussion

4.3.1 Analysis of survey responses

Considering the high capabilities of decentralized water infrastructure in reducing stormwater runoff and pollution as well as their low rates of adoption by local communities, this section analyzes the responses of IB's residents to the social survey to explore factors influencing the adoption of RWH and GI (especially RB and RG). The statistics of responses to numeric and open-ended questions of the survey are presented in Table 4.4 and Table 4.5.

Although the homeownership rate in IB is less than one-third (31.8% from Table 4.1, more than two-thirds of the survey respondents are homeowners (68.9% of responses to Q1 of the survey), which represents their higher public participation compared to home renters. As expected from Q2 of the survey, the majority of respondents (80.2%) were aware of IB's the city's ongoing stormwater issues such as stormwater pollution. Over the past 3 decades, the city has experienced sewage pollution within the Tijuana River Watershed, which is a large binational watershed lying across Mexico - California border. The watershed encompasses the densely urbanized City of Tijuana (Mexico), and it ultimately drains untreated sewage into the Tijuana River Estuary in the City of IB (California Water Boards 2020).

Table 4.4 Statistics of responses to conducted survey by the Social-Science part of the research team

Q1. Which of the following do you identify with?	Percentage	Count
Homeowner	68.2%	73
Renter	26.2%	28
Homeowner and business owner	3.7%	4
Renter and business owner	1.9%	2
Total	100.0%	107

Q2. Are you familiar with the city's ongoing storm water issues such as stormwater pollution?	Percentage	Count
Yes	80.2%	85
No	19.8%	21
Total	100.0%	106

Q3. Which part of IB does your residence or business reside at? Please choose all that apply if you have multiple residences or businesses within the City of IB. [I]	Percentage	Count
B	30.0%	33
D	8.2%	9
E	10.9%	12
F	22.7%	25
O	10.0%	11
P	6.4%	7
S	1.8%	2
W	10.0%	11
Total	100.0%	110

[I] A residency identification map (similar to Figure 4.3) has been attached to Q3 of the survey.

Q4. Are you familiar with any of the following terms? [Select all that apply: (a) Not familiar at all, (b) slightly familiar, (c) moderately familiar, or (d) very familiar]	Percentage [II]				Count			
	(a)	(b)	(c)	(d)	(a)	(b)	(c)	(d)
Rain Water Harvesting (RWH)	24.5%	23.6%	30.2%	21.7%	26	25	32	23
Green Infrastructure (GI)	32.1%	26.4%	22.6%	18.9%	34	28	24	20

[II] The denominator to calculate the percentage is 106, which is the overall number of responses to this question.

Q5. Are you familiar with any of the following terms? [Select all that apply: (a) Not familiar at all, (b) moderately familiar, (c) familiar but not currently using, or (d) I already have one and currently using]	Percentage [III]				Count			
	(a)	(b)	(c)	(d)	(a)	(b)	(c)	(d)
Rain Barrel (RB) [IV]	15.5%	13.6%	60.2%	13.6%	16	14	62	14
Rain Garden (RG)	46.6%	17.5%	35.0%	1.0%	48	18	36	1

[III] The denominators to calculate the percentage for RB and RG are respectively 106 and 103, which are the overall number of responses.

[IV] Brief and illustrative information on RB and RG was included in this question to help participants understand it better.

Q6. Please guesstimate your monthly water bill in U.S dollars	Average	Count
	$107.44	96

Q7. Would you be interested in receiving an incentive (such as a rebate on your water bill) for participating in rain barrel practices?	Percentage	Count
Yes	76.0%	79
No	24.0%	25
Total	100.0%	104

Q8. Please tell us why you chose your prior response. [V]

[V] There are 83 qualitative responses to this question, which are coded and presented in Table 4.5.

Q9. Would you be interested in receiving an incentive (like a rebate on your water bill) for participating in rain garden practices??	Percentage	Count
Yes	54.5%	55
No	45.5%	46
Total	100.0%	101

Q10. Please tell us why you chose your prior response. [VI]

[VI] There are 82 qualitative responses to this question, which are coded and presented in Table 4.5.

Q11. How much of a financial incentive would you need to install a rain barrel in your residence and/or business in U.S. dollars?	Average	Count
	$115.10	80

Q12. How much of a financial incentive would you need to install a rain garden in your residence and/or business in U.S. dollars?	Average	Count
	$137.49	56

Q13. If you were to start using a rain barrel, which of the following would you use the harvested water for? [Select all that apply]	Percentage [VII]			Count		
	Yes	Maybe	No	Yes	Maybe	No
Watering plants and/or lawn	95.9%	3.1%	1.0%	94	3	1
Laundry	14.1%	23.9%	62.0%	13	22	57
Toilet flushing	34.4%	31.2%	34.4%	32	29	32

[VII] The denominators to calculate the percentage for 3 above benefits are respectively 98, 92, and 93, which are the overall number of responses.

[XI] There are 51 qualitative responses to this question.

Table 4.4 Continued…

Q14. If you were to start using a rain garden, which of the following potential benefits interest you?? [Select all that apply]	Percentage [VIII]			Count		
	Yes	Maybe	No	Yes	Maybe	No
Reducing water pollution	83.9%	8.0%	8.0%	73	7	7
Preventing flooding	77.0%	12.6%	10.3%	67	11	9
Beautiful low-maintenance landscape	77.6%	11.8%	10.6%	66	10	9
Helping your community save millions of dollars in pollution clean-up and stormwater projects	87.8%	7.8%	4.4%	79	7	4

[VIII] The denominators to calculate the percentage for 4 above benefits are respectively 87, 87, 85, and 90 (the overall number of responses).

Q15. At your residence or business, how many times per week do you water your lawn and/or plants?	Percentage	Count
Everyday	7.0%	6
Two or more times per week	47.7%	41
Once per week	25.6%	22
Every other week	7.0%	6
Never	12.8%	11
Total	100.0%	86

Q16. At your residence or business, how many times per week do you do laundry?	Percentage	Count
Everyday	16.3%	14
Two or more times per week	43.0%	37
Once per week	33.7%	29
Every other week	7.0%	6
Never	0.0%	0
Total	100.0%	86

Q17. Do any of the following interest you? [select all that apply]	Percentage [IX]			Count		
	Yes	Maybe	No	Yes	Maybe	No
Learning how to make my own rain barrel	46.8%	14.9%	38.3%	44	14	36
Receiving a rain barrel for free	71.9%	9.4%	18.8%	69	9	18
Information on building your own rain garden	63.0%	15.2%	21.7%	58	14	20
Educational resources on RWH practices	64.2%	13.7%	22.1%	61	13	21

[IX] The denominators to calculate the percentage for 4 above benefits are respectively 94, 96, 92, and 95 (the overall number of responses).

Q18. After reviewing the previous questions, on a scale of 1-5 (1 being extremely unlikely and 5 being extremely likely), how likely are you to install a rain barrel or rain garden into your house or building?	Average	Count
	3.52	97

Q19. Do you have any concerns about integrating rain water harvesting interventions into your residence and/or business? [X]

[X] There are 62 qualitative responses to this question, which are coded and presented in Table 4.5.

Q20. Is there anything else you would like to share with us about your views on flooding and prevention in IB? [XI]

[XI] There are 51 qualitative responses to this question.

Table 4.5 Coded responses to the open-ended questions of the survey conducted by the Social-Science part of the research team under the supervision of Dr. Megan Welsh

Q8. Please tell us why you chose your prior response? [Referring to Q7 in Table 4.4)			
Prior response	Coded response to the current question	Percentage	Count
Yes	Environmental sustainability (e.g., water conservation, supporting environment)	48.1%	25
	Financial sustainability (e.g., saving money)	34.6%	18
	General statements	17.3%	9
No	Lack of authority (e.g., requiring permission from an owners or homeowner association)	22.6%	7
	Infrastructure infeasibility (e.g., site-specific restrictions)	22.6%	7
	General statement	16.1%	5
	Not having enough rain	12.9%	4
	Not needing an incentive	9.7%	3
	Disease transmission (e.g., attracting mosquitos and other insects)	9.7%	3
	Needing education	3.2%	1
	Start-up and maintenance difficulty	3.2%	1

Q10. Please tell us why you chose your prior response? [Referring to Q9 in Table 4.4)			
Prior response	Coded response to the current question	Percentage	Count
Yes	Financial sustainability (e.g., saving money)	52.9%	18
	Environmental sustainability (e.g., water conservation, supporting environment)	38.2%	13
	General statements	8.9%	3
No	Start-up and maintenance difficulty	31.3%	15
	Infrastructure infeasibility (e.g., site-specific restrictions)	25.0%	12
	Needing education	16.7%	8
	Lack of authority (e.g., requiring permission from an owners or homeowner association)	14.6%	7
	General statement	6.2%	3
	Not needing an incentive	4.2%	2
	Not having enough rain	2.1%	1

Table 4.5 Continued…

Q19. Do you have any concerns about integrating rain water harvesting interventions into your residence and/or business?		
Coded response to the current question	Percentage	Count
Infrastructure infeasibility (e.g., site-specific restrictions, installation and plumbing efforts)	35.5%	22
Lack of authority (e.g., requiring permission from an owners or homeowner association)	17.7%	11
Disease transmission (e.g., attracting mosquitos and other insects)	12.9%	8
Cost	11.3%	7
Needing education	6.5%	4
Not having enough rain	6.5%	4
Start-up and maintenance difficulty	6.5%	4
Bad appearance	3.2%	2

The interactive analysis of responses to Q1 and 2 (shown in Figure 4.10) indicates that 89% of homeowners and 62% of renters were familiar with IB's water issues (this number is 100% for business owners regardless of their homeownership status). This result implies that ownership can enhance people's attention to their community issues in order to protect their properties. Another reason for the low participation rate of IB's renters can be their specific limitations in implementing RB and RG (leading to their self-exclusion from the survey).

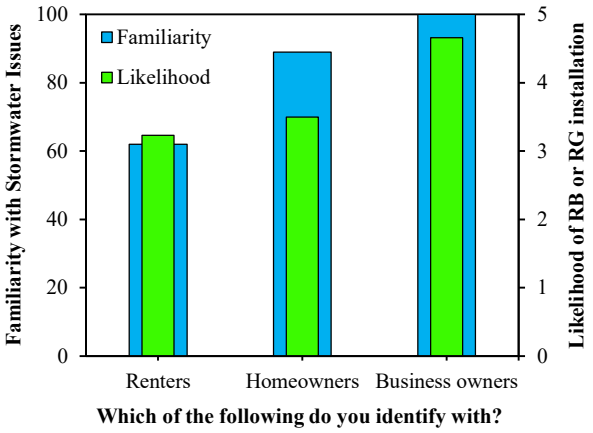

Figure 4.10 Variations of (a) familiarity with the city's stormwater issues and (b) likelihood of adoption with ownership status

Dividing the city of IB into eight aggregated watersheds, responses to Q3 are analyzed for identifying the residency of survey participants, and their spatial distribution is presented in Figure 4.11. From Figure 4.11(a), the highest survey participation across the city was respectively in watershed B (33 responses) and watershed F (25 responses). Since the counts are collected over unequal areas (or populations), the number of survey responses is normalized by the area of

watersheds using Equation (4-2), which factors out the size of the domain from survey participation. From Figure 4.11(b), the highest rates of relative participation respectively belong to watershed W (34.3%), watershed B (19.9%), and watershed D (16.0%), which have historically experienced marine-based flooding as shown in Figure 1.4. The studies of Gallien (2016) and Merrifield et al. (2021) revealed that even in current conditions, the thin peninsular strip in watershed W is notably vulnerable to wave-driven impacts (leading to the highest participation rate in this watershed). By the same reasoning, the low participation rate can be justified for watershed S where flood impacts are minimal (discussed in the next section). It is worth noting that public awareness of flooding issues needs to be improved particularly in watershed F, which will be at a high risk of compound flooding in the future (discussed in the next section).

$$r_i = \frac{I_i}{\sum_{m=1}^{8} I_m} \tag{4-2}$$

$$\begin{cases} r = \text{normalized participation rate (in percent);} \\ I_i = 100 n_i / A_i;\ i = \text{watershed representative index;} \\ A = \text{watershed area;}\ n = \text{number of survey responses in a watershed.} \end{cases}$$

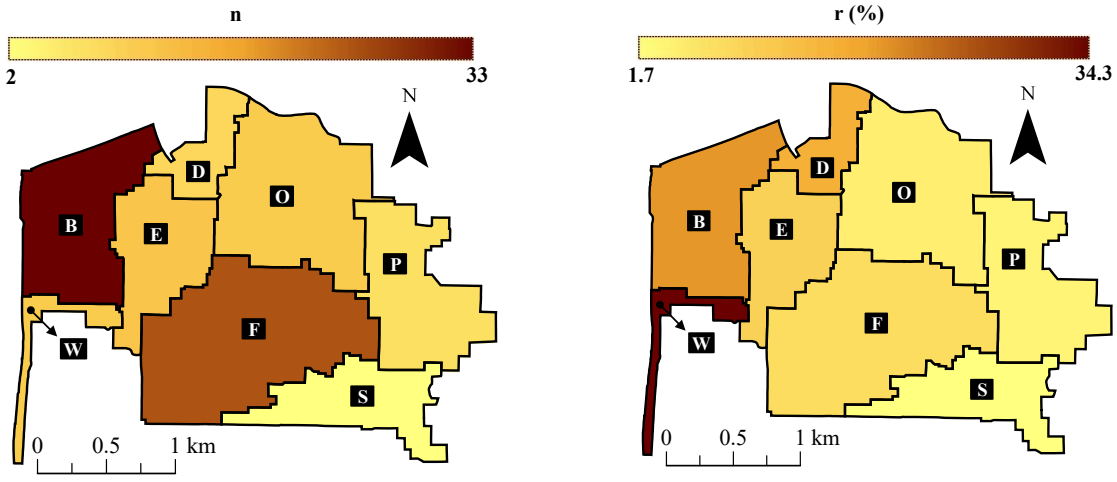

(a) (b)

Figure 4.11 Spatial distribution of survey responses across the city: (a) absolute number of responses in each watershed; (b) normalized number of responses using the area of watersheds.

Corresponding to Q1, 4, and 5 of the survey, Figure 4.12 illustrates the familiarity of IB's

residents with RWH and GI concepts as well as their specific examples of RB and RG systems. As shown, for all studied decentralization practices, homeowners have a higher level of familiarity and usage compared to renters. In addition, both IB's homeowners and renters are more aware of RB (and RG) compared to RWH (and GI). For example, about 10% (and 20%) of participants familiar with RB responded that they are not (and slightly) familiar with RWH. This point can imply that the public may have a deeper perception of an engineering application rather than the more general concept itself. Figure 4.12 also indicates that there is a higher level of public familiarity with RB (or RWH in general) compared to RG (or GI in general), which leads to higher rates of RB implementation and usage in both rented and owned houses. Thus, it can be concluded that an effective knowledge transfer among stakeholders (which can be achieved through public engagement programs) and sufficient considerations of ownership constraints are crucial for decentralized infrastructure to be successfully accepted and implemented by the community.

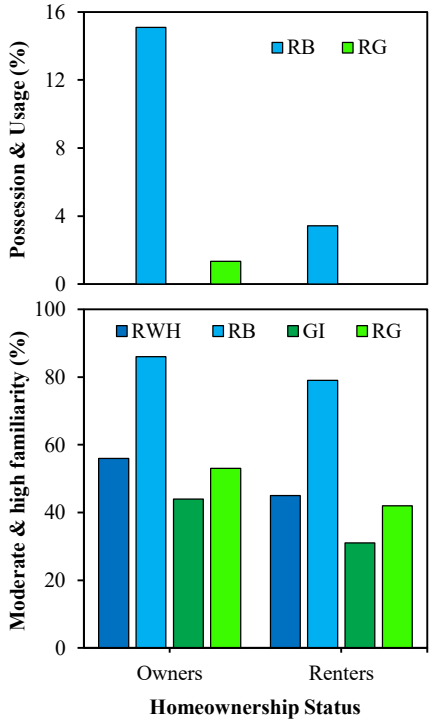

Figure 4.12 Public familiarity with decentralization practices and their usage in IB

Survey respondents showed higher interest in receiving an incentive for participating in RB practices (Figure 4.13) such that all participants interested in an RG incentive (Q9) already showed their interest in an RB incentive in Q7. It can be associated with the more familiarity of the residents with RB (Figure 4.12). The interactive analysis of responses to Q6, 7, 9, 11, and 12 of the survey (shown in Figure 4.14) indicates that people interested in receiving financial incentives for RB and RG installation have smaller water bills compared to others. It is probably because interested people are more likely to adopt practices (Figure 4.13), and adopters generally have more positive toward water resources than non-adopters (Maeda et al. 2018).

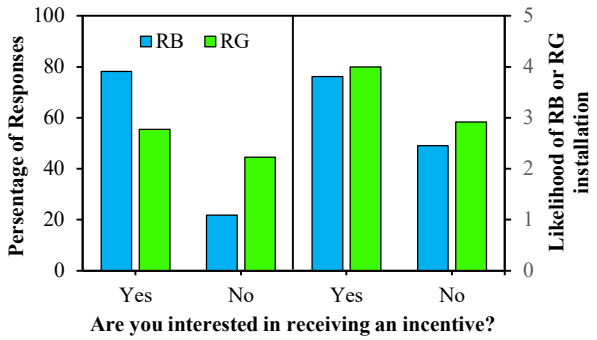

Figure 4.13 Residents' interest in receiving an incentive for RB and RG installation and its correlation with the likelihood of RB and RG adoption

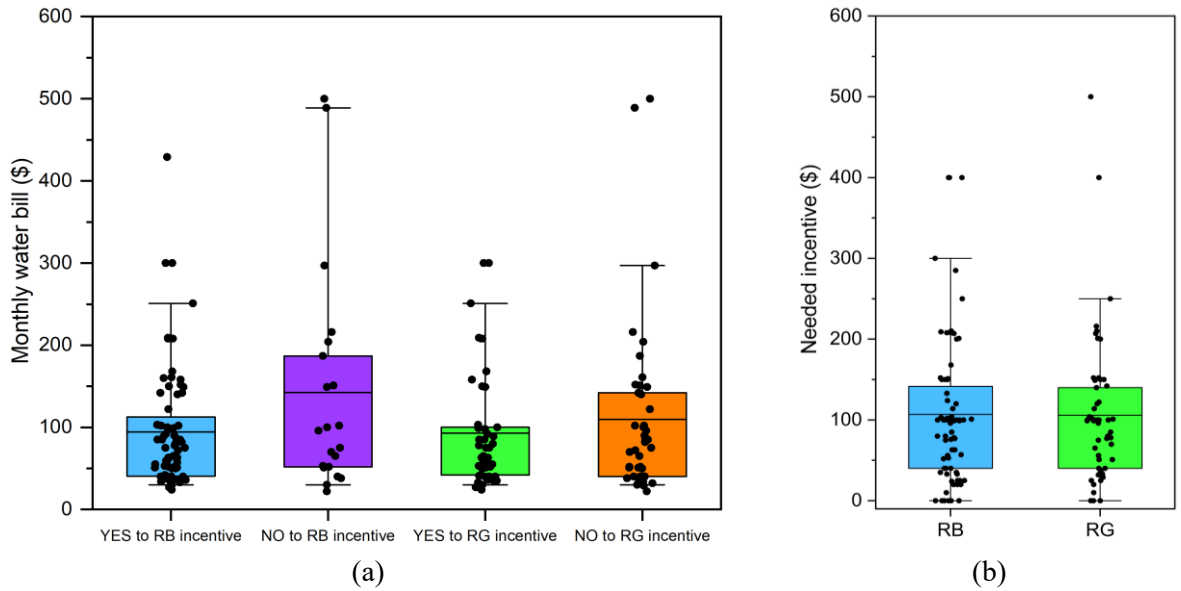

Figure 4.14 Variations of (a) monthly water bill of respondents with and without interest in RB and RG incentives; (b) needed incentives for RB and RG installation

County of San Diego Rain Barrel Tutorial (2022) recommends a 60-gallon volume of RB for each 100-ft^2 rooftop area receiving 1-inch rainfall (whose capability has been proven in the current study). While the estimated cost of a 60-gallon barrel system is \$100-\$120 (HomeAdvisor 2022; Lawn Love 2023), Figure 4.14(b) indicates that IB's residents need a financial incentive of \$115.10 on average (which is about the whole cost of RB installation). By assuming that (i) the catchment area of IB's nonpublic parcels is ~ 2.7 times of that of rooftop footprints (determined by GIS analysis on urban parcels and buildings shown in Figure 3.6 and Figure 4.4), (ii) RG surface area is 5% of the catchment area (Liu and Fassman-Beck 2017), and (iii) RG installation typically costs about \$10 a square foot (CostHelper 2023), the estimated cost for RG installation in a property with 100-ft^2 rooftop (equivalent to the catchment area for a 60-gallon RB) is \$135 [= 100 $ft^2 \times 2.7 \times 0.05 \times \$10/ft^2$]. With an average value of \$137.49, the needed financial incentive for RG installation also can be the whole cost of the practice. It is worth noting that 6% to 8% of interested participants in receiving an incentive (answering "Yes" to Q7 and 9) selected "0" as a needed financial incentive in Q11 and 12, for whom a different rebate program can be considered to incentivize RB and RG practices.

Figure 4.15 (corresponding to Q13 and 14) illustrates how different potential benefits of RB and RG practices may interest IB's residents. From Figure 4.15(a), garden watering by an RB system will be the most favorite benefit of decentralization, and gardeners with the intention of water usage reduction in their yards should be targeted as the most prevalent adopters of stormwater conservation practices. This finding is consistent with previous studies [i.e., Newburn et al. (2014) and Gao et al. (2016)] reporting that households with vegetable or flower gardeners have much higher awareness and adoption levels than those with no gardener.

The second, third, and fourth reported motivators for decentralization are respectively

helping the community in expensive pollution clean-up projects, water pollution reduction, and flood prevention using an RG system. Therefore, in addition to compound flooding control, water quality also should be addressed as a serious environmental issue and a strong motivation for RG adoption in IB. Figure 4.15(a) also shows that a "beautiful low-maintenance landscape" using RG interested about ninety percent of respondents. On average, people have shown more interest in RG benefits although they are generally less familiar with it compared to RB (Figure 4.12). Thus, it is crucial for future outreach activities to include clear descriptions of decentralization benefits.

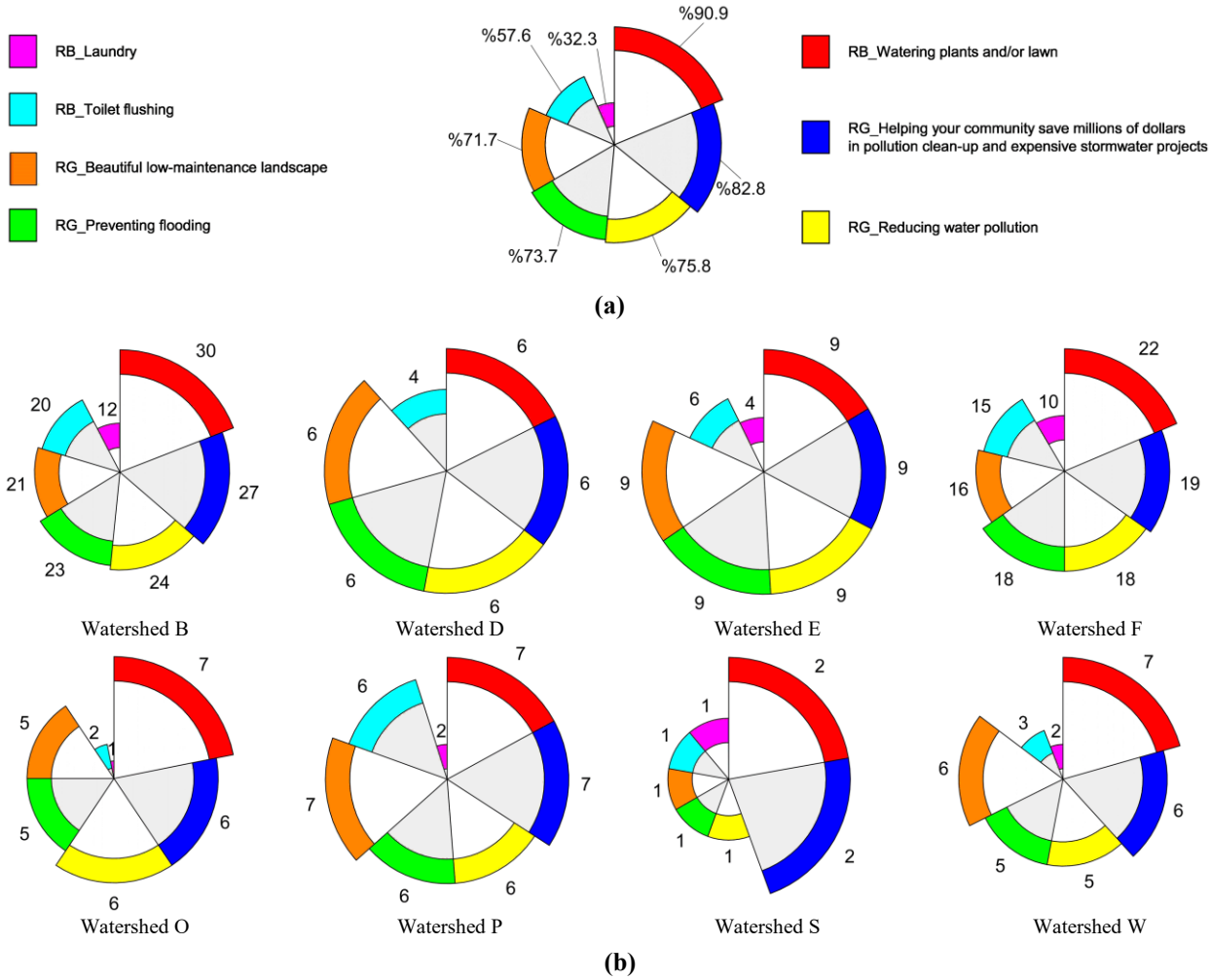

Figure 4.15 Residents' interests in potential benefits of RB and RG practices: (a) percentage of interested respondents in the city; (b) absolute number of interested respondents in each watershed

The start-up and maintenance difficulty of an RG system is listed as its top barrier in the

perception of people (mentioned in 31.3% of open-ended responses to Q10), which also should be addressed in future educational programs. This concern, however, is listed as a minimal barrier to RB and RWH adoption (mentioned in 3.2% and 6.5% of responses to Q8 to Q19, respectively). The first concern of respondents about RWH practices (mentioned in 35.5% of open-ended responses to Q19) is the infrastructure feasibility including installation and plumbing efforts (besides site-specific restrictions). Thus, compared to "watering plants and/or lawn", residents will be less likely to use an RB system for "toilet flushing" [Figure 4.15(a)]. The additional concern on the quality of harvested rainwater (including rooftop contaminants and attracting insects like mosquitos as mentioned in 12.9% of responses to Q19) makes people least interested in doing "laundry" by an RB. As a result, while IB's residents do laundry 38.8% more frequently than garden watering (respectively with the weighted averages of 2.29 and 1.65 times per week as shown in Figure 4.16), the former interests them ~3 times less [38.0% as mentioned in Figure 4.15(a)]. Figure 4.15(b) indicated that watering plants/lawn and doing laundry using harvested rainwater from an RB system are respectively the most and least favorite benefits of decentralization in all eight watersheds. With the highest number of respondents, the general order of motivators in two watersheds B and F is similar to that of the whole city.

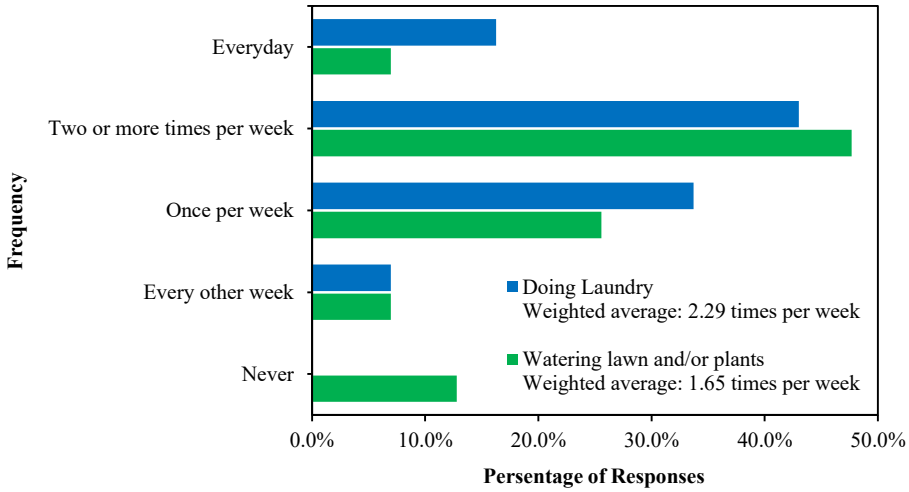

Figure 4.16 Frequency of laundry and garden watering (corresponding to Q15 and 16 of the survey)

From Table 4.4 and Table 4.5, while cost is the concern of 11.3% of respondents to Q19 for integrating RWH interventions, 81.3% of the respondents to Q17 said they are interested in "receiving a rain barrel for free". In addition, a high percentage of respondents to Q17 (77.9%) are interested in having educational resources on RWH practices, which is reflected in responses to the three open-ended questions of Q8, 10, and 19. Moreover, in the case of building their own RB or RG, people are more interested in receiving information on the latter (Q17), which requires more efforts for start-up and maintenance in their perception (Q8 and 10).

Survey participants are eventually asked in Q18 to scale the likelihood of RB or RG installation into their house or building from 1 (extremely unlikely) to 5 (extremely likely). Overall, the average value of 3.53, with a potential for improvement through public engagement and education, provides promising prospects for the adoption of decentralized water infrastructure by the community. However, this parameter is smaller for renters (3.23) with two-thirds of the city population, which can be attributed to their lower levels of familiarity with stormwater issues and decentralization practices (Figure 4.10 and Figure 4.12). Figure 4.17 illustrates the distribution of this parameter in different watersheds.

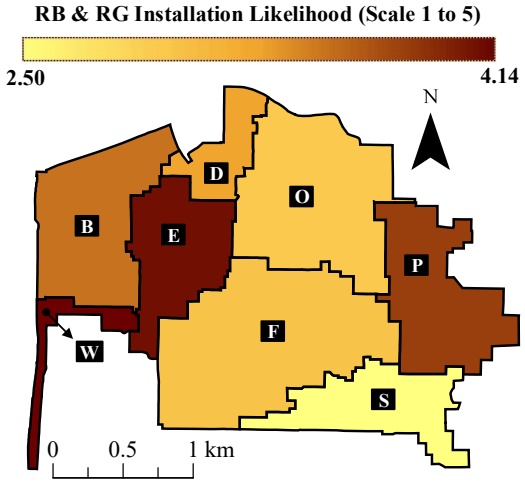

Figure 4.17 Distribution of the likelihood of decentralized infrastructure adoption across IB

As expected, the likelihood parameter is the most and least in watersheds of W and S, which are currently at the highest and lowest risk of flooding, respectively (discussed in the following section). This parameter is 3.04 (less the average) in watershed F, which will be substantially impacted by compound flooding in the future (discussed in the following section). Thus, appropriate outreach activities are needed to increase awareness of compound flooding impacts and mitigation solutions in the region.

4.3.2 Compound flood mitigation through decentralization

This section presents the effects of decentralization on compound flooding extent for both current and future conditions. The outputs of the conducted social studies for modeling and implementing decentralized infrastructure are mainly:

- confirming the general acceptability of decentralized infrastructure by the community (average value of the likelihood parameter = 3.53 out of 5.00);
- routing RB outflow to the pervious area (considering the high interest of residents in garden watering) with a 24-hour drain delay; and
- more importantly, estimating spatial distribution of adoption rates of decentralized infrastructure by combining the likelihood parameter for different stakeholders (Figure 4.10) with urban land-use units (Figure 4.18).

As pointed out previously, the County of San Diego Rain Barrel Tutorial (2022) recommends 60 gallons (or 271 liters) volume of RB for each 100-ft^2 (9.29 m^2) rooftop area receiving 1-inch (or 25.4 mm) rainfall, which covers almost all hourly rainfalls and the majority of daily rainfalls in IB (marked in Figure 2.3). Firstly, the capability of the above-mentioned recommendation has been verified for the City of Imperial Beach using sensitivity analysis

(performed by varying one independent variable at a time). Figure 4.19 indicates a sharp drop in the total peak runoff (i.e., summation of peak values of stormwater runoff over all subcatchments) from a rainfall with 1-year return period by implementing an RB system and increasing its volume to the recommended value ($V_{RB} \rightarrow V_{rec}$). However, larger RBs ($V_{RB} > V_{rec}$) lead to higher costs without any significant gains for capturing frequent rainfalls (i.e., a 1-year return period). From Figure 4.20, the stormdrain inflow and depth (at the data measurement location specified in Figure 2.1) also show the same trend with RB volume. In addition, RB impacts on peak values of flow characteristics are more remarkable compared to their average values.

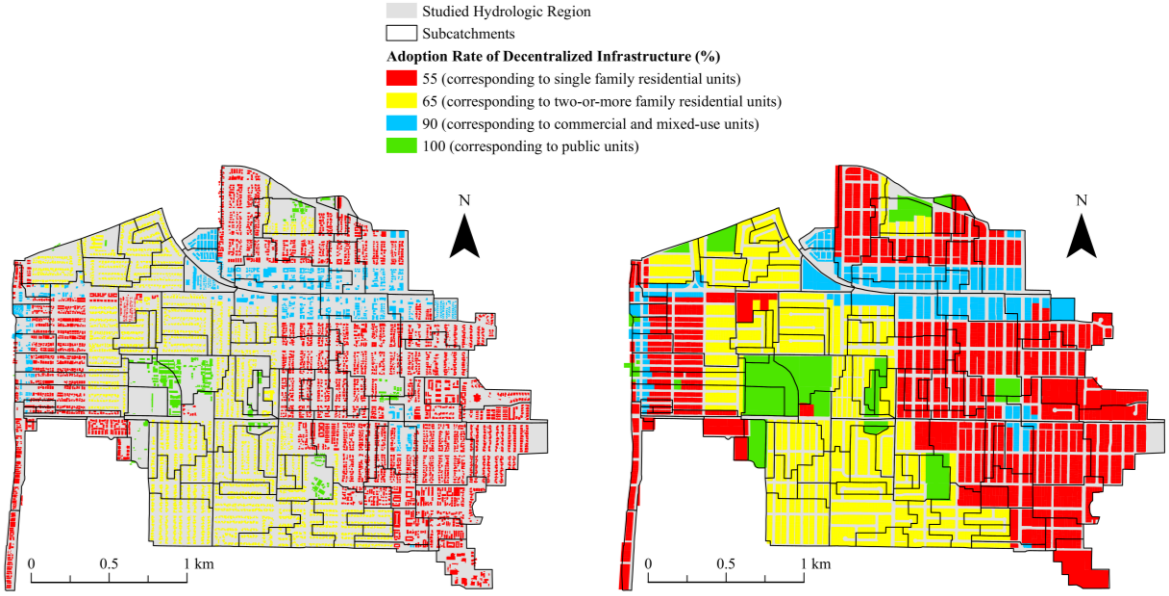

(a) (b)

Figure 4.18 Adoption rates for (a) RB system corresponding to urban buildings; (b) RG system corresponding to urban parcels

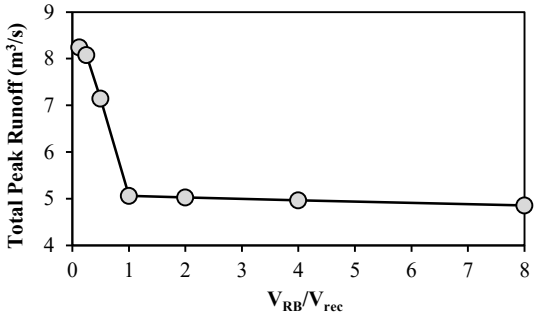

Figure 4.19 Variations of total peak runoff by changing RB volume from the recommended value

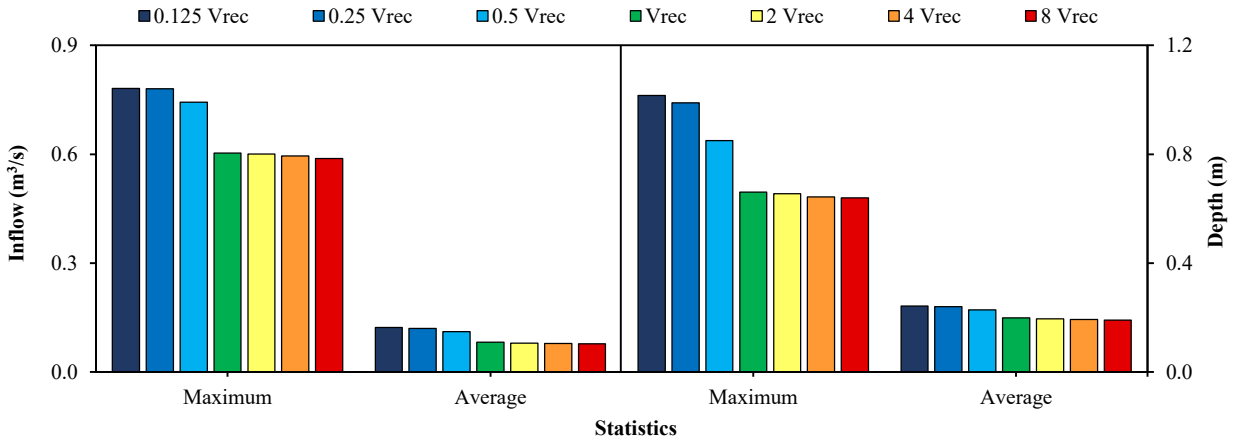

Figure 4.20 Stormdrain flow characteristics for different RB volumes (rainfall with 1-year return period; location specified with ★ in Figure 2.1)

Figure 4.21 shows that by implementing the RB system, the peak stormdrain depth at the mentioned location reduces by 31.2% and 4.6% during 1- and 10-year rainfall events, respectively. Thus, the benefits of RB installation are limited to more frequent (or less intense) rainfall events. This is because the contribution of an RB system in rainwater capturing is restricted to building rooftops, which consist of ~ 25% of IB's urbanized area (Figure 4.18). However, the mentioned percentages increase to 71.3% and 25.2% after adding the RG system. Therefore, for capturing rainfalls with higher return periods, the city may implement an RG and RB systems jointly.

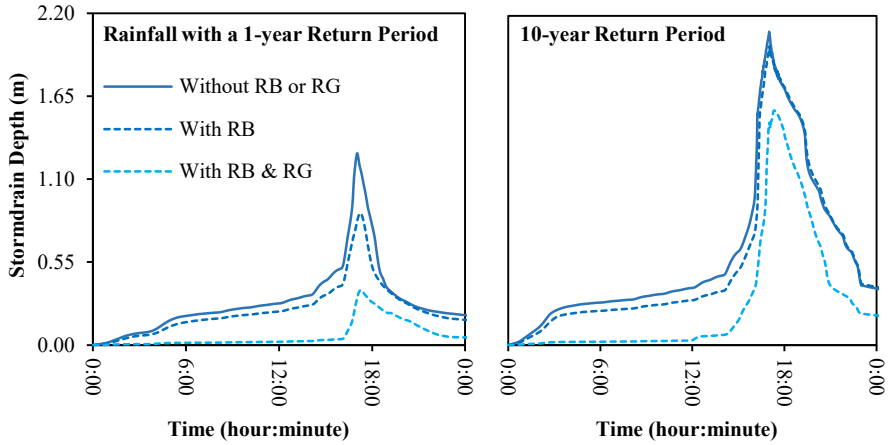

Figure 4.21 Stormdrain flow characteristics in the presence and absence of the RB system for rainfall events with (a) 1-year and (b) 5-year return periods (location specified with ★ in Figure 2.1)

The presented results in Figure 4.22 reveal that with a 2-m rise in the sea level, a slight system porosity of 0.25%, and the projected 25 percent uplift the intensity of a 1-year rainfall, the flood area (A) and volume (V) will grow up to 2.6 and 5.8 times, respectively. However, these parameters may reduce 31.4% and 51.8% by avoiding GWI into the stormdrain system (P = 0). While this figure confirms the capability of the RB system in flood mitigation for current conditions (47% and 56% reductions in A and V), the RB system implementation can reduce A and V only by 19% and 24% for the defective system at future conditions. By adding an RG system, the mitigation of future flood area and volume can be improved up to of 70% and 77% while and it can eliminate the current flooding.

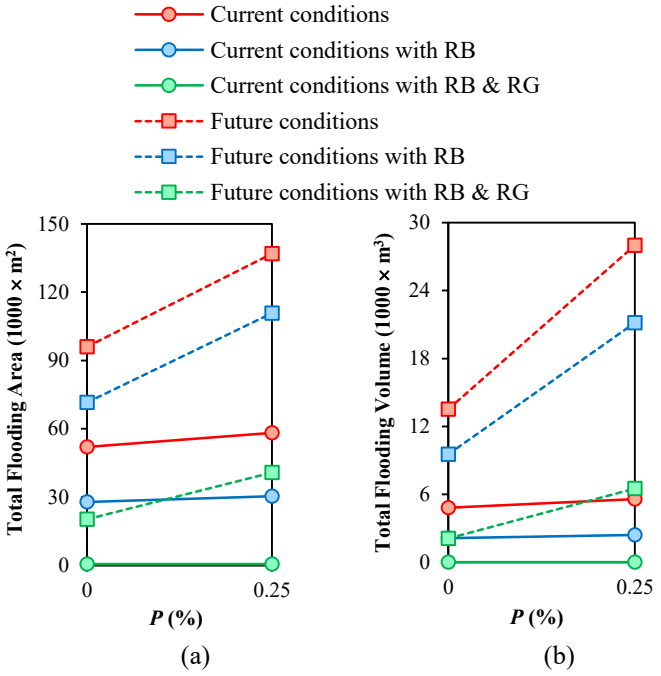

Figure 4.22 Effects of RB implementation on flood extent during a 1-year return period rainfall: (a) total flooding area; (b) total flooding depth; (c) relative flooding volume in the presence and absence of RBs

Figure 4.23 presents flood maps for some selective scenarios mentioned in Table 4.3. As shown in the first map, some areas are frequently flooding even in current conditions (mostly driven by rainfall), which can be confirmed by stormwater flooding observation across the city.

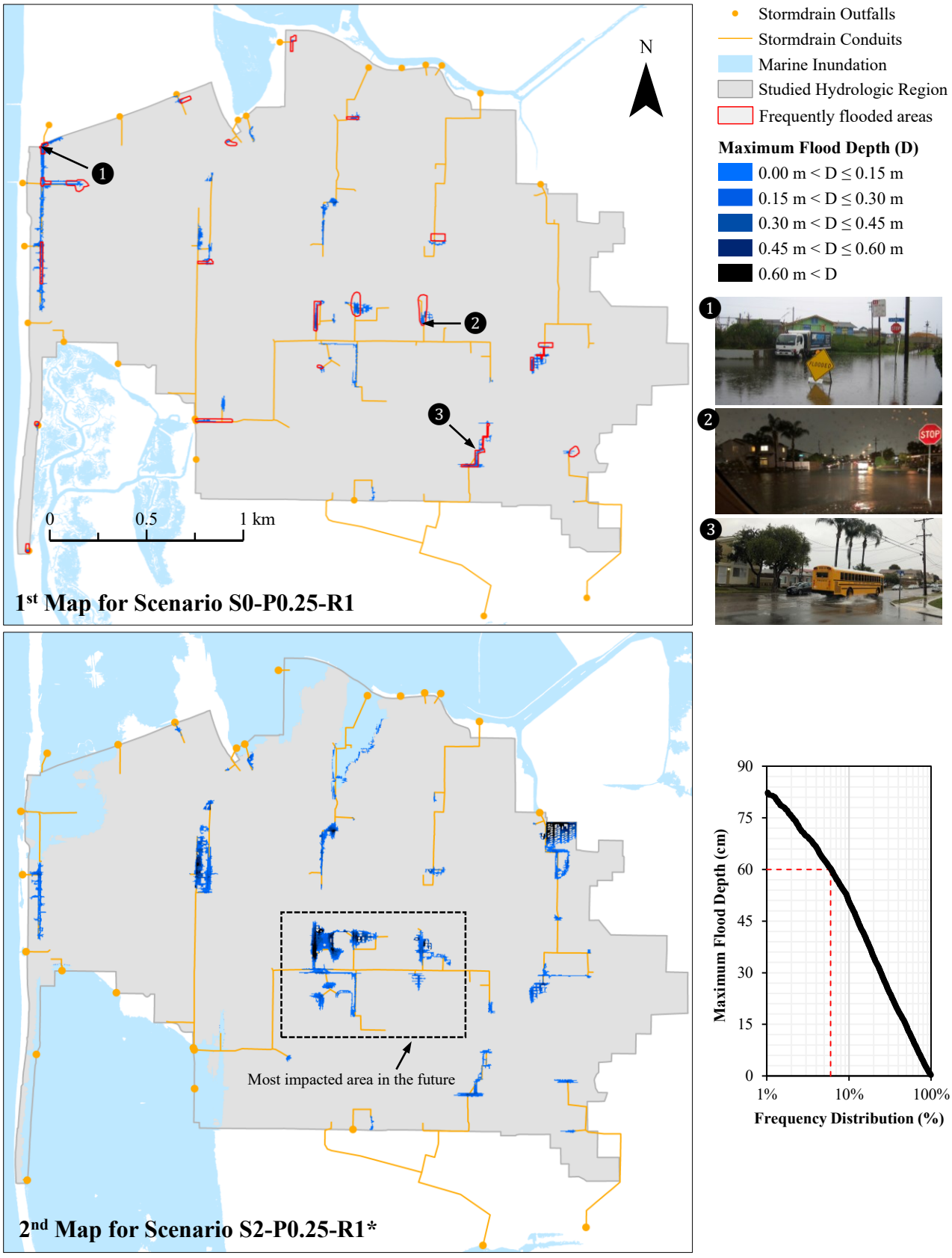

Figure 4.23 Compound flooding maps along with the frequency of future flood depth

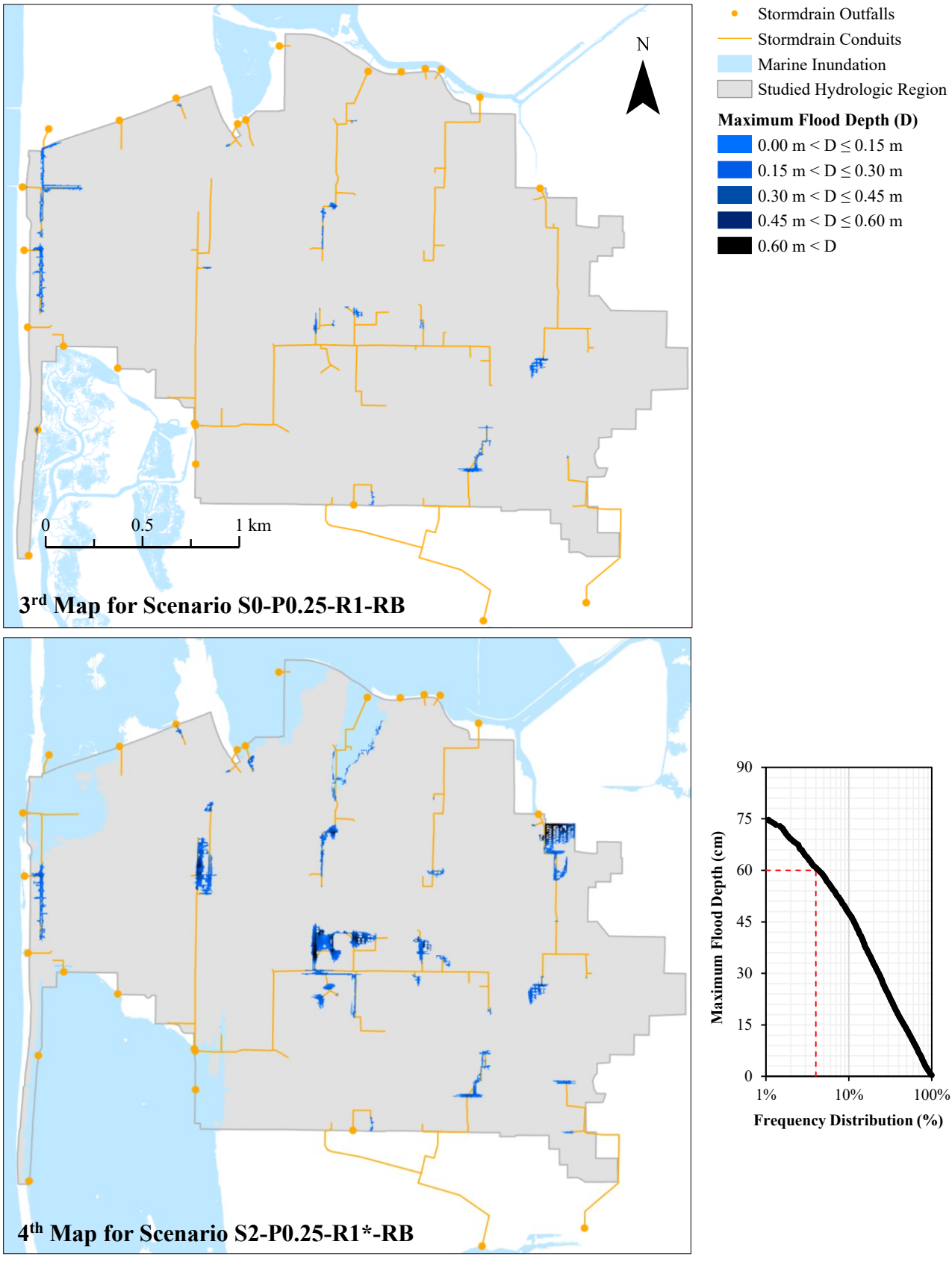

Figure 4.23 Continued…

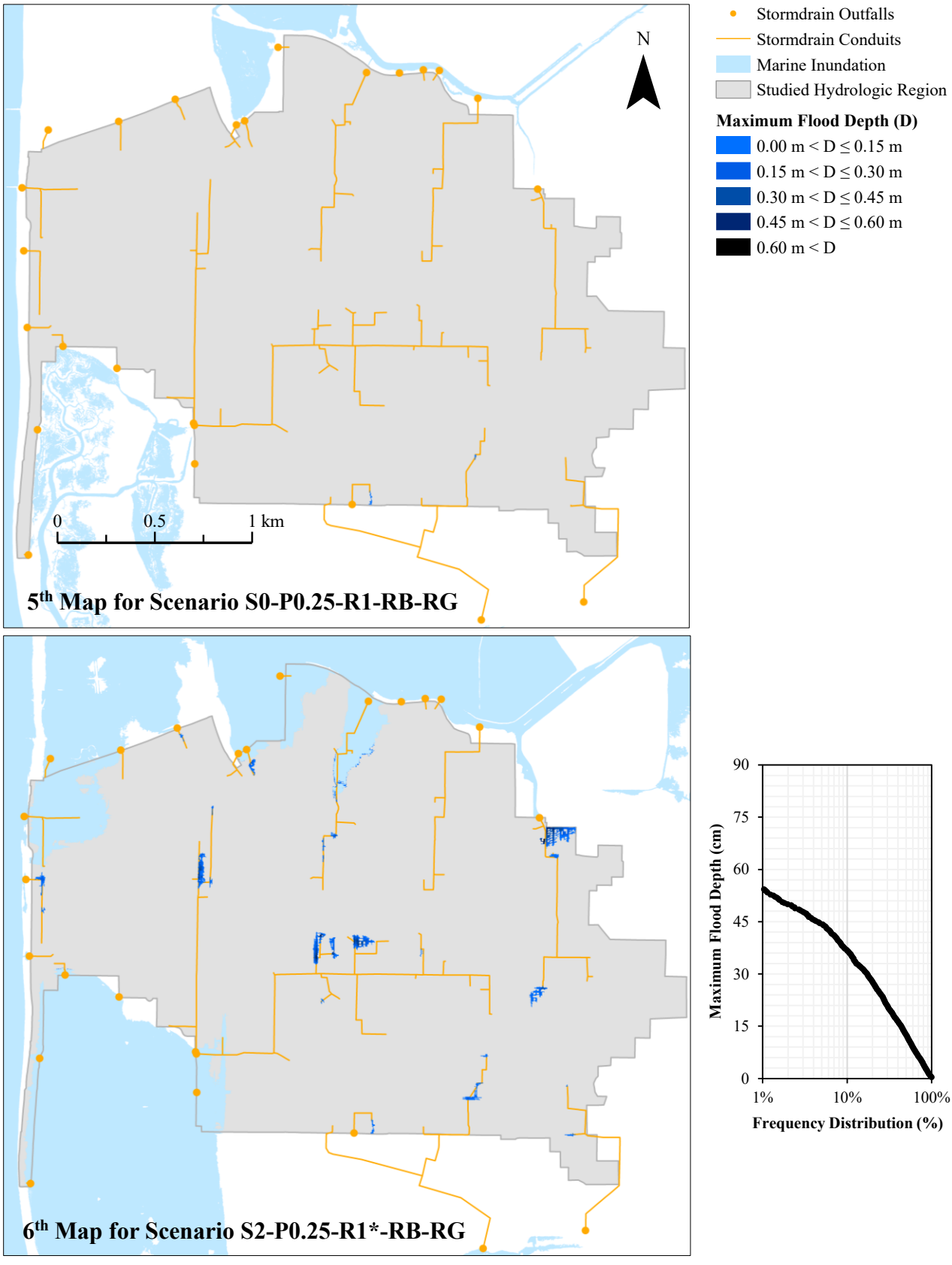

Figure 4.23 Continued…

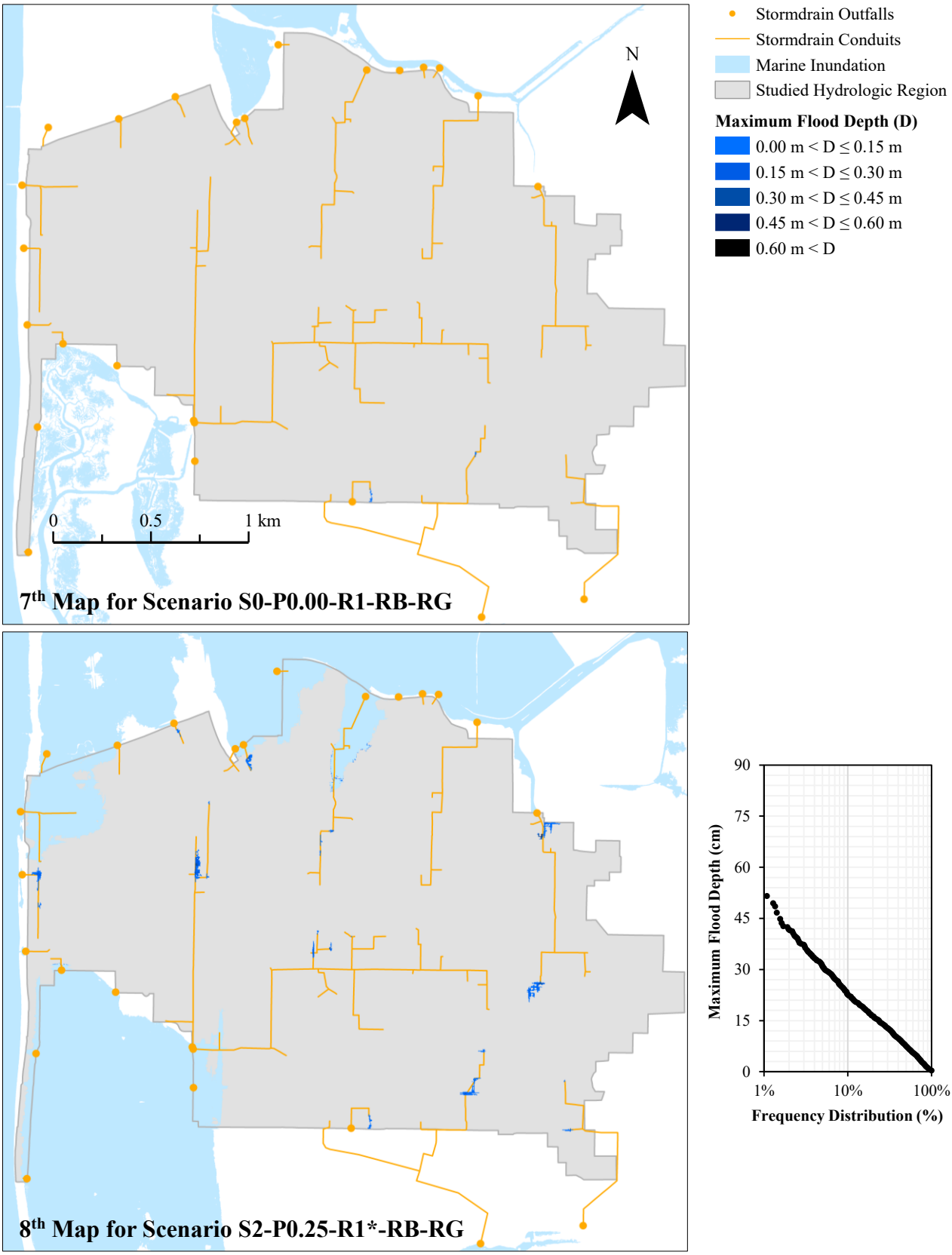

Figure 4.23 Continued…

By comparing the first two maps in Figure 4.23, it can be found that the compound coastal stressors (i.e., SWI, GWI, and stormwater runoff) can substantially increase the flood extent in the future conditions, in 6% of which the flood depth will be more than 60 cm (~ 2 feet) and a serious threat to urban buildings (FEMA 2020). Comparison of the 1st and 2nd maps with 3rd and 4th maps shows that the RB system can be only effective for mitigating the flood extent in current conditions (not future conditions, in which 4% of the flood depth will be still more than 60 cm in 4% of the impacted areas). From the 5th and 6th maps, the combination of RB and RG system can be effective for both current and future flood mitigation. The gains will be even more by avoiding GWI through an effective maintenance of the system ($P = 0$ in the 7th and 8th maps).

From the first two maps in Figure 4.23, the stormdrain line near/parallel to the coastline (located on Seacoast Dr. and Palm Ave.) is currently at a high risk of compound flooding. However, in the future conditions, some areas far from the surrounding water bodies will be substantially impacted by compound flooding due to emerging climate change effects on water resources (SLR, shallow groundwater, and more intense precipitation). The area shown by dashed-line rectangle (located near Imperial Beach Blvd.) will be mostly impacted, for which the flood extent is replotted in Figure 4.24 for different studied scenarios. Therefore, watershed F (shown in Figure 4.17) need special attention from the city to motivate the public for implementing decentralized infrastructure systems. However, SLR planning projects for the areas near the coast should be focused on marine-based stressors (e.g., living shorelines and revetments).

The benefit of implementing an RB system is twofold. Besides its contribution to flood mitigation, the captured rainwater by an RB system can adjust the water budget on a local scale (providing new sources of water supply for both outdoor and indoor end uses). RB cost and volume typically have a linear relation for nominal sizes such that the conservative prices of $100 and

$1000 can be considered for 60-gallon (or 271-liter) and 2000-gallon (or 7571-liter) barrels, respectively (Walsh et al. 2014). By combing these cost estimations with the recommendation of the County of San Diego Rain Barrel Tutorial (2022) on barrel sizing, one can obtain Equation (4-3) for estimating the cost of RB installation for a building with a given rooftop footprint. It should be noted that homeowners are assumed to undertake operation and maintenance efforts, which are negligible according to (Walsh et al. 2014).

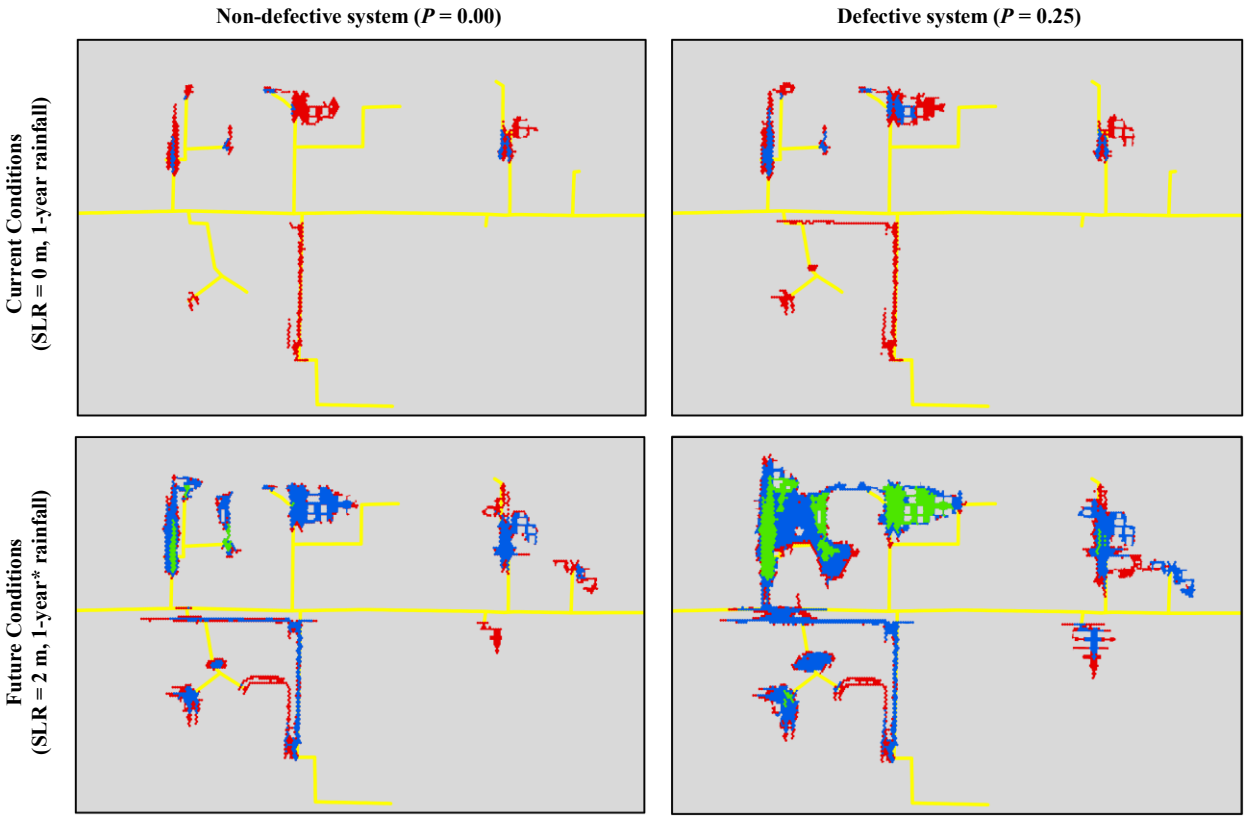

Figure 4.24 Flood extent in the selected area on the second map of Figure 4.23 (red, blue, and green polygons refer to the scenarios without RB/RG, with RG, and with RB and RG)

$$
\begin{cases}
Y = \left[0.464 \times (V_{RB} - 60)\right] + 100 \\
V_{RB} = 0.6 \times A_B; \\
A_B = \text{building rooftop footprint (ft}^2\text{)};\ V_{RB} = \text{rain barrel volume (gallon)}; \\
Y = \text{approximate cost of rain barrel installation (\$)}
\end{cases}
\tag{4-3}
$$

Using Equation (4-3) and RB adoption rates [Figure 4.18(a)], RB implementation cost in

IB is estimated to be ~ 3.3 million dollars (Table 4.6). Additionally, the expected life of RB units may exceed 50 years with proper maintenance (Coombes et al. 2000). Based on the continuous simulation of the stormdrain system (performed for the 4-year historical rainfall data shown in Figure 2.3), the city can harvest about 1 M cubic meters over a 4-year period. According to (Statistica 2023), one cubic meter of tap water costs an average of $6 in California. Thus, the value of harvested rainwater over the lifetime of the city-wide RB system (i.e., 50 years) can be ~ 63.4 million dollars, which is about 19 times larger than the implementation cost. From Table 4.7, it is also estimated that the RG system can occupy 2.4% of city area and cost about 15 million dollars.

The next chapter summarizes the main findings of this research and presents some topics for future studies.

Table 4.6 Estimated cost of a city-wide RB system and value of harvested rainwater

Row	Parameter	Value	Source/formula
r1	Harvested rainwater during the 4-year representative wet period (m^3)	1,014,490	Modeling output
r2	Harvested rainwater over the 50-year expected life of RB units (m^3)	12,681,124	r1 × 50/4
r3	Estimated cost of one cubic meter of tap water in San Diego ($)	5	Statistica (2023)
r4	Estimated Value of harvested rainwater over the 50-year expected life of RB units ($)	63,405,618	r3 × r2
r5	Estimated cost of RB implementation in the city ($)	3,315,358	Equation (4-3)

Table 4.7 Estimated cost and area of a city-wide RG system

Row	Parameter	Value	Source/formula
r1	Total area of urbanized region (m^2)	5,784,944	GIS mapping
r2	Total area of urban parcels (m^2)	4,120,476	GIS mapping
r3	Ratio of RG surface area to catchment area (or urban parcels)	0.05	Liu and Fassman-Beck (2017)
r4	Total area of the city-wide RG system (m^2)	137,273	r2, r3, and adoption rates
r5	Estimated cost of one square foot (or 0.093 m^2) of RG ($)	10	CostHelper (2023)
r6	Ratio of RG surface area to urbanized area (%)	2.4	r4/r1
r7	Estimated cost of the city-wide RG system ($)	14,776,000	r5 × r4/0.093

CONCLUSIONS AND FUTURE WORKS

This study evaluates compound impacts of seawater, groundwater, and stormwater stressors on the performance of coastal drainage infrastructure (i.e., stormdrain and sanitary sewer systems) under emerging climate change phenomena, i.e., sea-level rise, groundwater shoaling, and heavy rainfall intensification (Figure 1.5). Integrating engineering solutions with social survey responses in the City of Imperial Beach (IB; California, USA), the present research also aims to develop resilient measures for climate change adaptation aligned with communities' needs. The results lead to the following conclusions:

- The groundwater data from monitoring wells in IB (installed by the Oceanography part of the team) shows that although the groundwater table near the coast is influenced by ocean tides, it is almost stationary with signals < 0.1 m in the majority of the city. The collected data supports the development of a steady-state groundwater model for IB by the dissertation author.
- In the case of the high SLR scenario of 2 m, less than two percent of the urbanized area will be inundated by water bodies. However, the groundwater depth will be less than 2 m in about one-fourth of the city. In these circumstances, more than one-third of the sanitary sewer systems might be immersed in groundwater (susceptible to groundwater infiltration). In addition, about two-thirds of the stormdrain length could be susceptible to both SeaWater Intrusion (SWI) and GroundWater Infiltration (GWI).
- With the current sea level, defect flows increase hydraulic loads on the existing sanitary sewer system by 21% and 49% in dry- and wet-weather conditions, respectively. With 2-m SLR, GWI into the drainage infrastructure system grows approximately 4 times. For the sanitary sewer system, defect flows increase hydraulic loads by 84% and 120% in dry- and

wet-weather conditions, respectively. As a result, the additional ~2 million cubic meters of sewage will cost the city approximately three million dollars each year. For the stormdrain system (with 0.25 % porosity systemwide), GWI is estimated to consist of twenty percent of the system's hydraulic loads during annual rainfall events.

- Defect flows also increase the potential of sanitary sewer overflow events. With a 2-m rise in the sea level, there will be about 70% and 130% growth in the number of pressurized sewer junctions across the city in dry and wet-weather conditions, respectively. The number can increase up to 2.3 times during peak flow hours. Due to the contribution of SWI and GWI to stormdrain flow, the compound flooding extent may increase in all forms of flooding depth, area, and time. For example, the flooding volume increases up to 6 times by a 2 m increase in current sea level for a defective system (P = 0.25%) working under a 1-year rainfall event. However, by repairing system defects and avoiding GWI in the system, the flooding volume can be reduced to less than a third in these conditions.
- Besides a landward shift in the shoreline, SLR also can impact the performance of coastal drainage infrastructure kilometers away from the coastline. While the city of IB is currently paying most attention to the coast for its SLR planning projects, the results of this study reveal that the interactions of oceanographic, hydrological, and meteorological processes can impact some areas in the middle of the city by compound flooding of the stormdrain system and overflowing of the sanitary sewer system. Involving structural, hydrological, and hydraulic criteria, the proposed vulnerability index (SSVI) gives the highest rehabilitation priority to some parts of the sanitary sewer system kilometers far from the water bodies surrounding IB.
- The oceanographic and hydrological stressors of SWI and GWI can also increase the

frequency of flooding events in the region, while some low-lying areas with emergent-to-shallow groundwater may suffer sunny-day flooding. During extreme rainfall events (e.g., 100-year return period), the stormwater source dominates SWI and GWI, i.e., the system may fail solely by stormwater regardless of the other coastal stressors.

- The analysis of the social survey responses indicates that property ownership, familiarity with stormwater management practices, and residence in high-risk flood areas correlate with the likelihood of decentralized infrastructure adoption by the community. In addition, compared to RG, there is a higher level of public familiarity with RB leading to higher rates of its implementation and usage in both rented and owned houses. Moreover, "watering plants/lawn" and "doing laundry" using harvested rainwater from an RB system are respectively the most and least favorite benefits of decentralization in the study area. While the start-up and maintenance difficulties are listed as the top barrier in RG implementation, people's concerns about the quality of RB's harvested rainwater for indoor use need to be addressed.
- Based on the conducted social studies, more than 4/5 of respondents are interested in receiving a rain barrel for free, and the needed financial incentives for RB and RG installation can be the whole cost of the practice. While the results provide promising prospects for the community's adoption of decentralized water infrastructure, public's awareness and engagement still need to be improved through appropriate outreach activities, particularly in areas at risk of future flooding and sewer overflow (i.e., watershed F in Figure 4.17 corresponding to high-risk areas in Figure 4.23 and Figure 3.14).
- The spatial distribution of adoption rates of the decentralized infrastructure systems is obtained from the social survey analyses. In addition, for rain barrel sizing, the

recommendation of the County of San Diego Rain Barrel Tutorial (2022) was used and verified for the City of Imperial Beach. The outputs of RWH modeling reveal that the benefits of implementing a city-wide RB system is twofold. First, for current and future conditions (SLR = 0 and 2 m and rainfall with a 1-year return period), RB implementation may decrease the flood volume by 56%-57% and 24%-29% for defective (with 0.25% porosity) and non-defective (with 0.00% porosity) systems, respectively. Additionally, the value of harvested rainwater over the lifetime of the RB system (i.e., 50 years) can be about $63.4M while its implementation will only cost $3.3M.

- The model outputs also reveal that in the case of implementing both RB and RG systems, the flood volume may decrease 99% and 77% for a defective stormdrain system (with 0.25% porosity) respectively working under current conditions (SLR = 0 m rainfall with 1-year return period) and future conditions (SLR = 2 m and 25% increase in rainfall intensity). The latter can be improved up to 93% by avoiding GWI through an effective maintenance of the system. It is also estimated that the RG system can cost ~ $15 M for the city and occupy 2.4% of its area.

To improve our understanding of emerging climate change impacts and adaptation strategies, future studies are needed on the following topics:

- The recent field-based evidence demonstrates that wastewater exfiltration from defective sewer pipes above GWT is a source of groundwater quality degradation in urban coastal aquifers (McKenzie et al. 2021; Nguyen et al. 2021). While wastewater exfiltration processes (and possible interactions between GWT variations and aquifer contamination) are beyond the scope of this research, they should be considered in modeling procedures and comprehensive rehabilitation strategies.

- Considering the useful life expiration of almost all sewer pipelines by 2100 and the rapid development of sensing and communication technologies using Artificial Intelligence (AI) applications, a significant shift from reactive to real-time and smart monitoring of urban water infrastructure systems will be required for addressing climate change issues in a resilient and sustainable manner. By leveraging state-of-the-art computer vision techniques, preliminary studies in the literature [such as Tan et al. (2021) and Oh et al. (2022)] have provided promising prospects for implementing AI-based models for sewer defect detection. In this regard, other team members have started new studies on the detection of IB's sewer defects from the massive CCTV recorded videos (Figure 3.3). In addition, they have installed time-lapse cameras to capture the flood extent and duration in IB during rainfall events.
- While rainfall is the main contributor to urban flooding in today's climate, storm waves may become the future dominant stressor in downstream areas closer to the sea. In terms of temporal distribution, there also might be a shift in the dominant period from spring/autumn rain-induced flooding to winter sea-induced flooding due to energetic storm wave events originating in the North Pacific (Kunkel and Champion 2019; Laster Grip et al. 2021). By adding dynamic storm wave action and local wind-driven surge to coastal stressors, a new model can be developed for a better prediction of emerging compound floodplains near the shoreline, which will be helpful for SLR mitigation and adaptation.
- It is often easier in hydrogeology to measure model output (e.g., groundwater head) and then infer model inputs through "inverse problem" techniques (Su et al. 2022). However, modeling and analysis of transient groundwater near the coast (heavily influenced by ocean tides) requires the calibration of various parameters such as hydraulic conductivity and

storage coefficient, for which more groundwater monitoring wells are needed in this area.

- Besides exposure to flood events, socioeconomic factors (e.g., race, income, public health, and education level), also should be taken into account for assessing the overall vulnerability of a community (Bathi and Das 2016). In addition, the sustainability of mitigation solutions throughout their life cycles is needed to be determined by quantifying the consumption of resources and emissions (Tavakol-Davani et al. 2018). Thus, more studies are needed for identifying vulnerable population groups and prioritizing resources to sustainably protect them against climate change.
- While the focus of the present study was on the vulnerability of IB's drainage infrastructure systems to compound impacts of climate change, this community may have different environmental priorities and concerns. For example, some of the survey participants expressed that they have higher priorities for the three-decade problem of Tijuana sewage pollution, and some people refused to participate or talk to the survey team about anything else. Therefore, a bigger and richer picture needs to be painted regarding other ways that IB has been historically underserved.

REFERENCES

Ahiablame, L., and Shakya, R. (2016). "Modeling flood reduction effects of low impact development at a watershed scale." *Journal of Environmental Management*, 171, 81-91.

Ahiablame, L. M., Engel, B. A., and Chaubey, I. (2013). "Effectiveness of low impact development practices in two urbanized watersheds: Retrofitting with rain barrel/cistern and porous pavement." *Journal of Environmental Management*, 119, 151-161.

Anderson, T. R., Fletcher, C. H., Barbee, M. M., Romine, B. M., Lemmo, S., and Delevaux, J. M. S. (2018). "Modeling multiple sea level rise stresses reveals up to twice the land at risk compared to strictly passive flooding methods." *Scientific reports*, 8(1), 14484-14484.

Arkema, K. K., Guannel, G., Verutes, G., Wood, S. A., Guerry, A., Ruckelshaus, M., Kareiva, P., Lacayo, M., and Silver, J. M. (2013). "Coastal habitats shield people and property from sea-level rise and storms." *Nature Climate Change*, 3(10), 913-918.

Badaruddin, S., Werner, A. D., and Morgan, L. K. (2015). "Water table salinization due to seawater intrusion." *Water Resources Research*, 51(10), 8397-8408.

Bathi, J. R., and Das, H. S. (2016). "Vulnerability of Coastal Communities from Storm Surge and Flood Disasters." *International Journal of Environmental Research and Public Health*, 13(2).

Befus, K. M., Barnard, P. L., Hoover, D. J., Finzi Hart, J. A., and Voss, C. I. (2020). "Increasing threat of coastal groundwater hazards from sea-level rise in California." *Nature Climate Change*, 10(10), 946-952.

Bevacqua, E., Maraun, D., Vousdoukas, M. I., Voukouvalas, E., Vrac, M., Mentaschi, L., and Widmann, M. (2019). "Higher probability of compound flooding from precipitation and storm surge in Europe under anthropogenic climate change." *Science Advances*, 5(9), eaaw5531.

Boening-Ulman, K. M., Winston, R. J., Wituszynski, D. M., Smith, J. S., Andrew Tirpak, R., and Martin, J. F. (2022). "Hydrologic impacts of sewershed-scale green infrastructure retrofits: Outcomes of a four-year paired watershed monitoring study." *Journal of Hydrology*, 611, 128014.

California Water Boards (2020). "Sewage pollution within the Tijuana River watershed."

<https://tinyurl.com/yurtcn3b>. (January 2022).

Chelleri, L., Schuetze, T., and Salvati, L. (2015). "Integrating resilience with urban sustainability in neglected neighborhoods: Challenges and opportunities of transitioning to decentralized water management in Mexico City." *Habitat International*, 48, 122-130.

City of San Diego Sewer Design Guide (2015). <https://tinyurl.com/ywwc8r98>.

Coleman, S., Hurley, S., Rizzo, D., Koliba, C., and Zia, A. (2018). "From the household to watershed: A cross-scale analysis of residential intention to adopt green stormwater infrastructure." *Landscape and Urban Planning*, 180, 195-206.

Computational Hydraulics International, 2023. https://www.pcswmm.com (2023). "PCSWMM/SWMM5 Article: About Dual Drainage Systems." *Article No. 79149*, <www.pcswmm.com>. (April 2023).

Coombes, P. J., Argue, J. R., and Kuczera, G. (2000). "Figtree Place: a case study in water sensitive urban development (WSUD)." *Urban Water*, 1(4), 335-343.

Cooper, H. M., Zhang, C., and Selch, D. (2015). "Incorporating uncertainty of groundwater modeling in sea-level rise assessment: a case study in South Florida." *Climatic Change*, 129(1), 281-294.

CostHelper (2023). "Rain Garden Cost." <https://tinyurl.com/2p8dafvp>. (January 2023).

County of San Diego Hydrology Manual (2003). <https://tinyurl.com/pu7rtmne>.

County of San Diego Rain Barrel Tutorial (2022). <https://tinyurl.com/463dvzkd>.

County of San Diego Standard Urban Stormwater Mitigation Plan (2012). <https://tinyurl.com/y5v9ytdv>.

Davtalab, R., Mirchi, A., Harris, R. J., Troilo, M. X., and Madani, K. (2020). "Sea Level Rise Effect on Groundwater Rise and Stormwater Retention Pond Reliability." *Water*, 12(4).

Dawson, R. J., Dickson, M. E., Nicholls, R. J., Hall, J. W., Walkden, M. J. A., Stansby, P. K., Mokrech, M., Richards, J., Zhou, J., Milligan, J., Jordan, A., Pearson, S., Rees, J., Bates, P. D., Koukoulas, S., and Watkinson, A. R. (2009). "Integrated analysis of risks of coastal

flooding and cliff erosion under scenarios of long term change." *Climatic Change*, 95(1), 249-288.

Dirckx, G., Van Daele, S., and Hellinck, N. (2016). "Groundwater Infiltration Potential (GWIP) as an aid to determining the cause of dilution of waste water." *Journal of Hydrology*, 542, 474-486.

Elliott, A. H., and Trowsdale, S. A. (2007). "A review of models for low impact urban stormwater drainage." *Environmental Modelling & Software*, 22(3), 394-405.

Elvidge, C. D., Milesi, C., Dietz, J. B., Tuttle, B. T., Sutton, P. C., Nemani, R., and Vogelmann, J. E. (2004). "U.S. constructed area approaches the size of Ohio." *Eos, Transactions American Geophysical Union*, 85(24), 233-233.

Engineering ToolBox (2004a). "Fluid flow friction loss - Hazen-Williams coefficients." <https://tinyurl.com/6uamkz7b>. (October 2022).

Engineering ToolBox (2004b). "Manning's roughness coefficients." <https://tinyurl.com/56dwket5>. (October 2022).

FEMA (2020). "Shallow flooding analyses and mapping ", <https://tinyurl.com/mr2h3z7s>.

Ferreira, A., Sousa, V., Pinheiro, M., Meireles, I., Silva, C. M., Brito, J., and Mateus, R. (2023). "Potential of rainwater harvesting in the retail sector: a case study in Portugal." *Environmental Science and Pollution Research*, 30(14), 42427-42442.

Finewood, M. H., Matsler, A. M., and Zivkovich, J. (2019). "Green Infrastructure and the Hidden Politics of Urban Stormwater Governance in a Postindustrial City." *Annals of the American Association of Geographers*, 109(3), 909-925.

Fischer, E. M., Sedláček, J., Hawkins, E., and Knutti, R. (2014). "Models agree on forced response pattern of precipitation and temperature extremes." *Geophysical Research Letters*, 41(23), 8554-8562.

Frost, W. H. (2006). "Minor Loss Coefficients for Storm Drain Modeling with SWMM." *Journal of Water Management Modeling*, R225-23, 517-546.

Fung, A., and Babcock, R. (2020). "A Flow-Calibrated Method to Project Groundwater Infiltration

into Coastal Sewers Affected by Sea Level Rise." *Water*, 12(7).

Gallien, T. W. (2016). "Validated coastal flood modeling at Imperial Beach, California: Comparing total water level, empirical and numerical overtopping methodologies." *Coastal Engineering*, 111, 95-104.

Gao, Y., Babin, N., Turner, A. J., Hoffa, C. R., Peel, S., and Prokopy, L. S. (2016). "Understanding urban-suburban adoption and maintenance of rain barrels." *Landscape and Urban Planning*, 153, 99-110.

Giacalone, K., Mobley, C., Sawyer, C., Witte, J., and Eidson, G. (2010). "Survey Says: Implications of a Public Perception Survey on Stormwater Education Programming." *Journal of Contemporary Water Research & Education*, 146(1), 92-102.

Gold, A. C., Brown, C. M., Thompson, S. P., and Piehler, M. F. (2022). "Inundation of Stormwater Infrastructure Is Common and Increases Risk of Flooding in Coastal Urban Areas Along the US Atlantic Coast." *Earth's Future*, 10(3), e2021EF002139.

Guo, S., and Zhu, D. Z. (2017). "Soil and Groundwater Erosion Rates into a Sewer Pipe Crack." *Journal of Hydraulic Engineering*, 143(7), 06017008.

Haaland, O., and Ortiz, P. (2022). "Disadvantaged communities nomenclature within the state of California: findings and conclusions." California Department of Water Resources.

Habel, S., Fletcher, C. H., Anderson, T. R., and Thompson, P. R. (2020). "Sea-Level Rise Induced Multi-Mechanism Flooding and Contribution to Urban Infrastructure Failure." *Scientific reports*, 10(1), 3796-3796.

Habel, S., Fletcher, C. H., Rotzoll, K., and El-Kadi, A. I. (2017). "Development of a model to simulate groundwater inundation induced by sea-level rise and high tides in Honolulu, Hawaii." *Water Research*, 114, 122-134.

Harbaugh, A. W. (2005). "MODFLOW-2005 : the U.S. Geological Survey modular ground-water model−the ground-water flow process." *Techniques and Methods*, USGS, USA.

Hauer, M. E., Evans, J. M., and Mishra, D. R. (2016). "Millions projected to be at risk from sea-level rise in the continental United States." *Nature Climate Change*, 6(7), 691-695.

Hernandez Rosales, B., and Lutz, A. (2023). "Assessing the feasibility of rooftop rainwater harvesting for food production in Northwestern Arizona on the Hualapai Indian Reservation." *Sustainability*.

HomeAdvisor (2022). "How much does a rainwater collection system cost to install?", <https://tinyurl.com/etprmrcf>. (2022 January).

Hoover, D. J., Odigie, K. O., Swarzenski, P. W., and Barnard, P. (2017). "Sea-level rise and coastal groundwater inundation and shoaling at select sites in California, USA." *Journal of Hydrology: Regional Studies*, 11, 234-249.

IBM (2023). "IBM SPSS Statistics." <https://tinyurl.com/5ynzthbr>. (January 2023).

Jang, J.-H., and Chang, T.-H. (2022). "Flood risk estimation under the compound influence of rainfall and tide." *Journal of Hydrology*, 606, 127446.

Karamouz, M., Zahmatkesh, Z., Goharian, E., and Nazif, S. (2015). "Combined Impact of Inland and Coastal Floods: Mapping Knowledge Base for Development of Planning Strategies." *Journal of Water Resources Planning and Management*, 141(8), 04014098.

Karpf, C., and Krebs, P. (2011). "Quantification of groundwater infiltration and surface water inflows in urban sewer networks based on a multiple model approach." *Water Research*, 45(10), 3129-3136.

Keeley, M., Koburger, A., Dolowitz, D. P., Medearis, D., Nickel, D., and Shuster, W. (2013). "Perspectives on the Use of Green Infrastructure for Stormwater Management in Cleveland and Milwaukee." *Environmental Management*, 51(6), 1093-1108.

Khanam, M., Sofia, G., Koukoula, M., Lazin, R., Nikolopoulos, E. I., Shen, X., and Anagnostou, E. N. (2021). "Impact of compound flood event on coastal critical infrastructures considering current and future climate." *Nat. Hazards Earth Syst. Sci.*, 21(2), 587-605.

Khodadad, M., Aguilar-Barajas, I., and Khan, A. Z. (2023). "Green infrastructure for urban flood resilience: a review of recent literature on bibliometrics, methodologies, and typologies." *Water*.

Kirezci, E., Young, I. R., Ranasinghe, R., Muis, S., Nicholls, R. J., Lincke, D., and Hinkel, J. (2020). "Projections of global-scale extreme sea levels and resulting episodic coastal flooding over the 21st Century." *Scientific Reports*, 10(1), 11629.

Kunkel, K. E., and Champion, S. M. (2019). "An Assessment of Rainfall from Hurricanes Harvey and Florence Relative to Other Extremely Wet Storms in the United States." *Geophysical Research Letters*, 46(22), 13500-13506.

Langevin, C. D., Hughes, J. D., Banta, E. R., Niswonger, R. G., Panday, S., and Provost, A. M. (2017). *Documentation for the MODFLOW 6 Groundwater Flow Mode*, United States Geological Survey (USGS), Book 6, Chapter A55.

Laster Grip, I., Haghighatafshar, S., and Aspegren, H. (2021). "A methodology for the assessment of compound sea level and rainfall impact on urban drainage networks in a coastal city under climate change." *City and Environment Interactions*, 12, 100074.

Lawn Love (2023). "How much does a rain barrel cost in 2023?", <https://tinyurl.com/bd8a9j4c>. (January 2022).

Lincoln Stormwater Program (2022). "Rain Barrel." <https://tinyurl.com/2p87fz9w>. (January 2022).

Little, J. (2021a). "Looking to Keep Imperial Beach Above Water." *NBC 7 San Diego*, <https://tinyurl.com/mr4ww876>. (September 1, 2021).

Little, J. (2021b). "Researchers Work to Keep Imperial Beach Above Water." *NBC 7 San Diego*, <https://tinyurl.com/mr4ww876>. (December 2, 2021).

Liu, R., and Fassman-Beck, E. (2017). "Hydrologic response of engineered media in living roofs and bioretention to large rainfalls: experiments and modeling." *Hydrological Processes*, 31(3), 556-572.

Liu, T., Ramirez-Marquez, J. E., Jagupilla, S. C., and Prigiobbe, V. (2021). "Combining a statistical model with machine learning to predict groundwater flooding (or infiltration) into sewer networks." *Journal of Hydrology*, 603, 126916.

Liu, T., Su, X., and Prigiobbe, V. (2018). "Groundwater-sewer interaction in urban coastal areas." *Water*, 10(12), 1774.

Lu, C., Chen, Y., Zhang, C., and Luo, J. (2013). "Steady-state freshwater–seawater mixing zone in stratified coastal aquifers." *Journal of Hydrology*, 505, 24-34.

Maeda, P. K., Chanse, V., Rockler, A., Montas, H., Shirmohammadi, A., Wilson, S., and Leisnham, P. T. (2018). "Linking stormwater Best Management Practices to social factors in two suburban watersheds." *PLOS ONE*, 13(8), e0202638.

Mason, L. R., Ellis, K. N., and Hathaway, J. M. (2019). "Urban flooding, social equity, and "backyard" green infrastructure: An area for multidisciplinary practice." *Journal of Community Practice*, 27(3-4), 334-350.

Masson-Delmotte, V., Zhai, P., Pirani, A., Connors, S. L., Péan, C., Berger, S., Caud, N., Chen, Y., Goldfarb, L., and Gomis, M. (2021). "Climate change 2021: the physical science basis." *Contribution of working group I to the sixth assessment report of the intergovernmental panel on climate change*, 2.

Mayer, P. W. (2016). "Water Research Foundation Study Documents Water Conservation Potential and More Efficiency in Households." *Journal AWWA*, 108(10), 31-40.

McDowell, R. (2022). "Anaylsis of bioretention capability in removing microplastic particles from stormwater." MS Thesis, San Diego State University, USA.

McKenzie, T., Habel, S., and Dulai, H. (2021). "Sea-level rise drives wastewater leakage to coastal waters and storm drains." *Limnology and Oceanography Letters*, 6(3), 154-163.

Meder, I. A., and Kouma, E. (2010). "Low Impact Development for the Empowered Homeowner: Incentive Programs for Single Family Residences." *Low Impact Development 2010*, 1144-1159.

Meerow, S. (2020). "The politics of multifunctional green infrastructure planning in New York City." *Cities*, 100, 102621.

Mehdizadeh, S. S., Werner, A. D., Vafaie, F., and Badaruddin, S. (2014). "Vertical leakage in sharp-interface seawater intrusion models of layered coastal aquifers." *Journal of Hydrology*, 519, 1097-1107.

Merrifield, M. (2021). "Collaborative Research: Sustainable Water Infrastructure for Adapting to Coastal Climate Change." National Science Foundation (Award Number: 2113984).

Merrifield, M. A., Johnson, M., Guza, R. T., Fiedler, J. W., Young, A. P., Henderson, C. S., Lange, A. M. Z., O'Reilly, W. C., Ludka, B. C., Okihiro, M., Gallien, T., Pappas, K., Engeman, L., Behrens, J., and Terrill, E. (2021). "An early warning system for wave-driven coastal

flooding at Imperial Beach, CA." *Natural Hazards*, 108(3), 2591-2612.

Miller, S. M., and Montalto, F. A. (2019). "Stakeholder perceptions of the ecosystem services provided by Green Infrastructure in New York City." *Ecosystem Services*, 37, 100928.

Moftakhari, H., Schubert, J. E., AghaKouchak, A., Matthew, R. A., and Sanders, B. F. (2019). "Linking statistical and hydrodynamic modeling for compound flood hazard assessment in tidal channels and estuaries." *Advances in Water Resources*, 128, 28-38.

Moghimi, S., Myers, M., Pe'eri, S., Zhang, Y. J., and Fei, Y. (2021). "Forecasting compound floods in complex coastal regions." *Eos (102)*, <https://doi.org/10.1029/2021EO210604>.

Newburn, D. A., Alberini, A., Rockler, A., and Karp, A. (2014). "Adoption of household stormwater best management practices."

Newell, J. P., Seymour, M., Yee, T., Renteria, J., Longcore, T., Wolch, J. R., and Shishkovsky, A. (2013). "Green Alley Programs: Planning for a sustainable urban infrastructure?" *Cities*, 31, 144-155.

Nguyen, H. H., Peche, A., and Venohr, M. (2021). "Modelling of sewer exfiltration to groundwater in urban wastewater systems: A critical review." *Journal of Hydrology*, 596, 126130.

Nicholls, R. J. (2011). "Planning for the Impacts of Sea Level Rise." *Oceanography*, 24.

Nicholls, R. J., and Cazenave, A. (2010). "Sea-Level Rise and Its Impact on Coastal Zones." *Science*, 328(5985), 1517.

O'Donnell, E., Maskrey, S., Everett, G., and Lamond, J. (2020). "Developing the implicit association test to uncover hidden preferences for sustainable drainage systems." *Philosophical Transactions of the Royal Society A: Mathematical, Physical and Engineering Sciences*, 378(2168), 20190207.

Oh, C., Dang, L. M., Han, D., and Moon, H. (2022). "Robust Sewer Defect Detection With Text Analysis Based on Deep Learning." *IEEE Access*, 10, 46224-46237.

Pacific Institute (2018). "Urban water use data." <www.pacinst.org>. (October 2022).

Paul, M. J., and Meyer, J. L. (2001). "Streams in the urban landscape." *Annual Review of Ecology*

and Systematics, 32(1), 333-365.

Persaud, A., Alsharif, K., Monaghan, P., Akiwumi, F., Morera, M. C., and Ott, E. (2016). "Landscaping practices, community perceptions, and social indicators for stormwater nonpoint source pollution management." *Sustainable Cities and Society*, 27, 377-385.

Piratla, K. R., and Goverdhanam, S. (2015). "Decentralized water systems for sustainable and reliable supply." *Procedia Engineering*, 118, 720-726.

Plane, E., Hill, K., and May, C. (2019). "A Rapid Assessment Method to Identify Potential Groundwater Flooding Hotspots as Sea Levels Rise in Coastal Cities." *Water*.

Porse, E. C. (2013). "Stormwater Governance and Future Cities." *Water*, 29-52.

Project Clean Water (2019). "San Diego County Rainfall Station Map." <https://tinyurl.com/2uuuewpn>.

Qi, J., and Barclay, N. (2021). "Social barriers and the hiatus from successful green stormwater infrastructure implementation across the US." *Hydrology*.

Qi, J., and Barclay, N. (2022). "Addressing the social barriers to green stormwater infrastructure in residential areas from a socio-ecological perspective." *Journal of Environmental Management*, 313, 114987.

Qualtrics (2022). "Online Survey Software - Digital Survey Management Tool." <https://tinyurl.com/ync7akk8>. (January 2022).

Rahimi, R., Tavakol-Davani, H., Graves, C., Gomez, A., and Fazel Valipour, M. (2020). "Compound Inundation Impacts of Coastal Climate Change: Sea-Level Rise, Groundwater Rise, and Coastal Precipitation." *Water*, 12(10).

Rangari, V., Gonugunta, R., Umamahesh, N., Patel, A., and Bhatt, C. (2018). "1d-2d modeling of urban floods and risk map generation for the part of hyderabad city." *The International Archives of Photogrammetry, Remote Sensing and Spatial Information Sciences*, 42, 445-450.

Reitz, M., Sanford, W. E., Senay, G. B., and Cazenas, J. (2017). "Annual Estimates of Recharge, Quick-Flow Runoff, and Evapotranspiration for the Contiguous U.S. Using Empirical

Regression Equations." *JAWRA Journal of the American Water Resources Association*, 53(4), 961-983.

Rezaee, M., and Tabesh, M. (2022). "Effects of inflow, infiltration, and exfiltration on water footprint increase of a sewer system: A case study of Tehran." *Sustainable Cities and Society*, 79, 103707.

Rossi, R. J., and Toran, L. (2019). "Exploring the potential for groundwater inundation in coastal US cities due to interactions between sewer infrastructure and global change." *Environmental Earth Sciences*, 78(8), 258.

Rossman, L. A. (2015). "Storm Water Management Model User's Manual Version 5.1."

Rotzoll, K., and Fletcher, C. H. (2013). "Assessment of groundwater inundation as a consequence of sea-level rise." *Nature Climate Change*, 3(5), 477-481.

Saharia, A. M., Zhu, Z., and Atkinson, J. F. (2021). "Compound flooding from lake seiche and river flow in a freshwater coastal river." *Journal of Hydrology*, 603, 126969.

Sangsefidi, Y., Bagheri, K., Davani, H., and Merrifield, M. (2023). "Data analysis and integrated modeling of compound flooding impacts on coastal drainage infrastructure under a changing climate." *Journal of Hydrology*, 616, 128823.

Sangsefidi, Y., Mehraein, M., Ghodsian, M., and Motalebizadeh, M. R. (2017). "Evaluation and analysis of flow over arced weirs using traditional and response surface methodologies." *Journal of Hydraulic Engineering*, 143(11), 04017048.

Shuster, W. D., Morrison, M. A., and Webb, R. (2008). "Front-loading urban stormwater management for success–a perspective incorporating current studies on the implementation of retrofit low-impact development." *Cities and the Environment (CATE)*, 1(2), 8.

Sidek, L. M., Chua, L. H. C., Azizi, A. S. M., Basri, H., Jaafar, A. S., and Moon, W. C. (2021). "Application of PCSWMM for the 1-D and 1-D–2-D Modeling of Urban Flooding in Damansara Catchment, Malaysia." *Applied Sciences*, 11(19), 9300.

Smith, J. S., Winston, R. J., Wituszynski, D. M., Tirpak, R. A., Boening-Ulman, K. M., and Martin, J. F. (2023). "Effects of watershed-scale green infrastructure retrofits on urban stormwater quality: A paired watershed study to quantify nutrient and sediment removal." *Ecological Engineering*, 186, 106835.

Smyth, K., Drake, J., Li, Y., Rochman, C., Van Seters, T., and Passeport, E. (2021). "Bioretention cells remove microplastics from urban stormwater." *Water Research*, 191, 116785.

Snir, O., Friedler, E., and Ostfeld, A. (2022). "Optimizing the control of decentralized rainwater harvesting systems for reducing urban drainage flows." *Water*.

Statistica (2023). "Prices of tap water in selected cities in the United States." <https://tinyurl.com/4r5dxtmf>. (February 2023).

Stuart, S. L. (2008). "Groundwater and surface water interactions at the Tijuana Estuary, San Diego, California." MS Thesis, San Diego State University, USA.

Su, X., Belvedere, P., Tosco, T., and Prigiobbe, V. (2022). "Studying the effect of sea level rise on nuisance flooding due to groundwater in a coastal urban area with aging infrastructure." *Urban Climate*, 43, 101164.

Swamee, P. K., and Swamee, N. (2010). "Discharge equation of a circular sharp-crested orifice." *Journal of Hydraulic Research*, 48(1), 106-107.

Sweet, W. V., Hamlington, B. D., Kopp, R. E., Weaver, C. P., Barnard, P. L., Bekaert, D., Brooks, W., Craghan, M., Dusek, G., Frederikse, T., Garner, G., Genz, A. S., Krasting, J. P., Larour, E., Marcy, D., Marra, J. J., Obeysekera, J., Osler, M., Pendleton, M., Roman, D., Schmied, L., Veatch, W., White, K. D., and Zuzak, C. (2022). "Global and Regional Sea Level Rise Scenarios for the United States: Updated Mean Projections and Extreme Water Level Probabilities Along U.S. Coastlines." *NOAA Technical Report NOS 01*, National Oceanic and Atmospheric Administration, National Ocean Service, Silver Spring.

Tahvildari, N., Abi Aad, M., Sahu, A., Shen, Y., Morsy, M., Murray-Tuite, P., Goodall Jonathan, L., Heaslip, K., and Cetin, M. (2022). "Quantification of Compound Flooding over Roadway Network during Extreme Events for Planning Emergency Operations." *Natural Hazards Review*, 23(2), 04021067.

Tan, Y., Cai, R., Li, J., Chen, P., and Wang, M. (2021). "Automatic detection of sewer defects based on improved you only look once algorithm." *Automation in Construction*, 131, 103912.

Tavakol-Davani, H., Burian Steven, J., Butler, D., Sample, D., Devkota, J., and Apul, D. (2018). "Combining hydrologic analysis and life cycle assessment approaches to evaluate sustainability of water infrastructure." *Journal of Irrigation and Drainage Engineering*, 144(11), 05018006.

Tavakol-Davani, H., Goharian, E., Hansen, C. H., Tavakol-Davani, H., Apul, D., and Burian, S. J. (2016). "How does climate change affect combined sewer overflow in a system benefiting from rainwater harvesting systems?" *Sustainable Cities and Society*, 27, 430-438.

Tavakol-Davani, H., and Welsh, M. (2021). "Collaborative Research: Sustainable Water Infrastructure for Adapting to Coastal Climate Change." National Science Foundation (Award Number: 2113987).

Teimoori, S., O'Leary, B. F., and Miller, C. J. (2021). "Modeling Shallow Urban Groundwater at Regional and Local Scales: A Case Study in Detroit, MI." *Water*, 13(11), 1515.

The City of Imperial Beach (2021). "Sewer service charge and capacity fee study."

The City of San Diego Stormwater Standards (2021). <https://tinyurl.com/ysyjujb5>.

The City of San Diego Whitebook (2018). <https://tinyurl.com/3bthawzh>.

Thomas, R. B., Kirisits, M. J., Lye, D. J., and Kinney, K. A. (2014). "Rainwater harvesting in the United States: a survey of common system practices." *Journal of Cleaner Production*, 75, 166-173.

Thompson, P. R., Widlansky, M. J., Hamlington, B. D., Merrifield, M. A., Marra, J. J., Mitchum, G. T., and Sweet, W. (2021). "Rapid increases and extreme months in projections of United States high-tide flooding." *Nature Climate Change*, 11(7), 584-590.

Trenberth, K. E. (2011). "Changes in precipitation with climate change." *Climate Research*, 47, 123-138.

United States Census Bureau (2022a). "Income in the United States: 2021." <https://tinyurl.com/bddn653k>. (October 2022).

United States Census Bureau (2022b). "QuickFacts: Imperial Beach city, California; San Diego County, California; California; United States." <https://tinyurl.com/2jvpryre>. (October 2022).

United States Department of Agriculture (2019). "Web soil survey." <http://websoilsurvey.sc.egov.usda.gov/>. (October 2022).

United States Environmental Protection Agency (2022). "Green Infrastructure." <https://tinyurl.com/ywc6ckf4; https://tinyurl.com/2mnp292a>. (January 2022).

Vitousek, S., Barnard, P. L., Fletcher, C. H., Frazer, N., Erikson, L., and Storlazzi, C. D. (2017). "Doubling of coastal flooding frequency within decades due to sea-level rise." *Scientific Reports*, 7(1), 1399.

Wahl, T., Jain, S., Bender, J., Meyers, S. D., and Luther, M. E. (2015). "Increasing risk of compound flooding from storm surge and rainfall for major US cities." *Nature Climate Change*, 5(12), 1093-1097.

Walsh, T. C., Pomeroy, C. A., and Burian, S. J. (2014). "Hydrologic modeling analysis of a passive, residential rainwater harvesting program in an urbanized, semi-arid watershed." *Journal of Hydrology*, 508, 240-253.

Water Environment Federation (2010). *Design of Municipal Wastewater Treatment Plants: WEF Manual of Practice No. 8*, McGraw-Hill Education, New York.

Waterloo Hydrogeologic (2021). "Visual MODFLOW Flex 7.0 Integrated Conceptual & Numerical Groundwater Modeling Software." Waterloo, ON, Canada.

Watson, T. A., Werner, A. D., and Simmons, C. T. (2010). "Transience of seawater intrusion in response to sea level rise." *Water Resources Research*, 46(12).

Willis, R. M., Stewart, R. A., Panuwatwanich, K., Williams, P. R., and Hollingsworth, A. L. (2011). "Quantifying the influence of environmental and water conservation attitudes on household end use water consumption." *Journal of Environmental Management*, 92(8), 1996-2009.

Zamani Sabzi, H., Rezapour, S., Fovargue, R., Moreno, H., and Neeson, T. M. (2019). "Strategic allocation of water conservation incentives to balance environmental flows and societal outcomes." *Ecological Engineering*, 127, 160-169.

Zhao, Z., Yin, H., Xu, Z., Peng, J., and Yu, Z. (2020). "Pin-pointing groundwater infiltration into urban sewers using chemical tracer in conjunction with physically based optimization model." *Water Research*, 175, 115689.

APPENDIX

The social survey questions, framed and distributed by the Social-Science part of the research team, are mentioned in the following.

English

IB Project- Perceptions on Water Sustainability

Introduction .

Hello Imperial Beach residents and/or business owners!

We are conducting a survey to better understand your perspectives on flooding in Imperial Beach (IB) and potential solutions. As you may know, IB is at high risk of a type of flooding called compound flooding, which happens when sea-level rise due to climate change interacts with an already-saturated groundwater table. Compound flooding also carries additional risks because the stormwater that can't be absorbed into the ground contains pollutants. The survey takes 10-15 minutes to complete. If you are interested in receiving more information and educational resources on rainwater harvesting (RWH) and Rain Gardens, you will have the option to access a link to resources at the end of the survey. Thank you for your time!

Informed consent.

SDSU | San Diego State University

Perceptions of flooding and resilience approaches in Imperial Beach, CA

San Diego State University

Who should I contact if I have questions?

Project's Principal Investigators (lead researchers):

Dr. Hassan Davani
College of Engineering
San Diego State University
Email: **hdavani@sdsu.edu**

Dr. Megan Welsh Carroll
School of Public Affairs
San Diego State University
Email: **mwelsh@sdsu.edu**

This project is funded by the National Science Foundation (grant # 2113987), overall project title: Sustainable Water Infrastructure for Adapting to Coastal Climate Change.

The purpose of the research study is to gain a better understanding of the ongoing flooding in Imperial Beach and the barriers to uptake such as usage of sustainability measures (e.g., rainwater harvesting through rain barrels). Rainwater harvesting practices are an adequate solution to capture rainwater and help prevent flooding from occurring. We hope to have about 400 IB residents and business owners complete our brief survey, and from those responses, our objective is to obtain valuable information on ways to improve the flooding issue in IB.

How long will this take? This brief survey should take you no more than 10-15 minutes to complete.

What do I need to do? This study is anonymous. If you choose to participate by clicking "yes" at the bottom of this page, you will be asked to complete a brief survey. You can print a copy of this consent form to keep for your records.

At the end of this consent page, you will be asked to acknowledge that your participation is fully voluntary and that you understand you do not have to answer any of the questions. We value your input, but you are not required to answer every question, and you are free to not answer questions and/or stop participating at any time.

What are the risks? If you choose to participate in this study, the risks to you are no greater than those that occur in everyday life. You might feel some frustration or other negative emotions based on some of our questions – we're going to ask you about your opinions about the ongoing flooding issues in your community. This may remind you of a negative experience that you, or someone you know, had.

Do I get anything? There are no direct benefits to you for participating in this research; however, you may appreciate having your voice heard on these issues.

Will my information be private? We are collecting no data that can be traced back to you or used to identify you in any way. Your information will not be shared with other researchers. All data collected for this project will be stored in secure, password-protected electronic files that only the research team can access. These files will be stored for a period of five years and will then be destroyed.

Will I be told about study results? We will not contact you with the results of this study. However, we will summarize our results in policy research briefs as well as peer-reviewed manuscripts, which will be publicly available within 5 years of the conclusion of the study at **https://www.hassanh2o.com/**.

Will it cost me anything to participate? No.

Will I be paid anything to participate? No.

Who can I contact if I have questions? Please contact project leads Hassan Davani (Email: **hdavani@sdsu.edu**) and/or Megan Welsh Carroll (Email: **mwelsh@sdsu.edu**) with any questions. You may also contact the Division of Research Affairs at San Diego State University: **(619) 594-6622** or **irb@sdsu.edu**.

Electronic consent: Please select your choice below. You may print a copy of this consent form for your records. Clicking on the "Yes" button indicates that

- You have read the above information,
- You voluntarily agree to participate, and
- You are 18 years of age or older.

- ○ Yes
- ○ No

Q1. Which of the following do you identify with? (check all that apply)

- ☐ I am a IB homeowner
- ☐ I am a IB renter
- ☐ I am a IB business owner

Q2. Are you familiar with the city's ongoing **storm water issues** such as stormwater pollution?

- ○ Yes
- ○ No

Watersheds/Cuencas. Please help us identify which watershed(s) your residence or business is located at (please choose all that apply if you have multiple residences or businesses within the City of IB):

Watersheds/Cuencas.

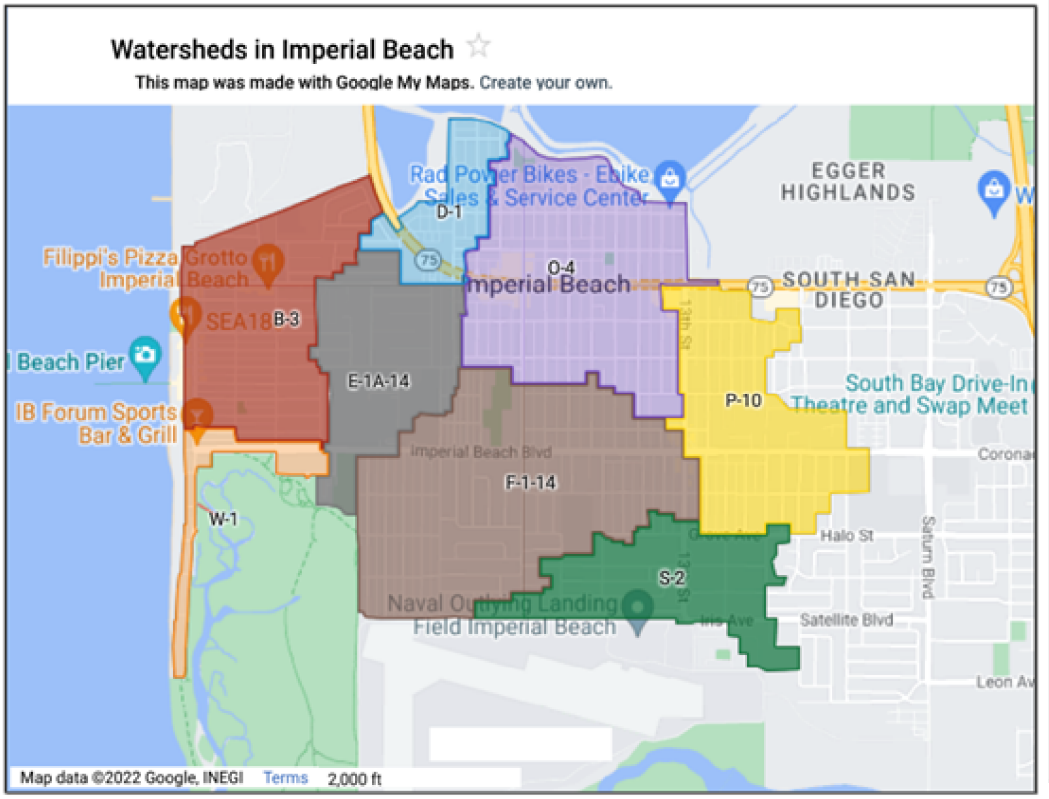

Q3. Based on the above picture, which part of IB does your residence or business reside at (please choose all that apply if you have multiple residences or businesses within the City of IB):?

- [ ] B-3= red area
- [ ] E-1A-14= light green area
- [ ] D-1= light blue area
- [ ] O-4= purple area
- [ ] P-10= yellow area
- [ ] S-2= dark geen area
- [ ] W-1= orange area
- [ ] F-1-14= brown area

Q4. Are you familiar with any of the following terms? (select all that apply)

	Not at all familiar	Slightly familiar	Moderately familiar	Very familiar
Rain Water Harvesting (RWH)	○	○	○	○
Green Infrastructure	○	○	○	○

Q5. Are you familiar or currently using any of the following terms green infrastructure interventions? (select all that apply)

	Not at all familiar	Moderately familiar	Familiar but currently not using	I already have one and currently using
Rain Barrel	○	○	○	○
Rain Garden	○	○	○	○

Rain Barrels.
According to the United States Environmental Protection Agency (EPA), rain barrels are a rainwater harvesting system that can reduce stormwater pollution by halting runoff and collecting rainfall for later use.

Did you know?

Rain barrels are one of the best ways to save money and water by cutting back potable water used for irrigation. You can capture about **312 gallons of water** for every half-inch of rain that falls on a 1,000-square-foot roof. Rain barrels collect rainwater which is especially good for plants because it is free of the additives that tap water has for sanitation. Your plants and garden will thrive by being watered with rainwater. -San Mateo

-Countywide Water Prevention Program

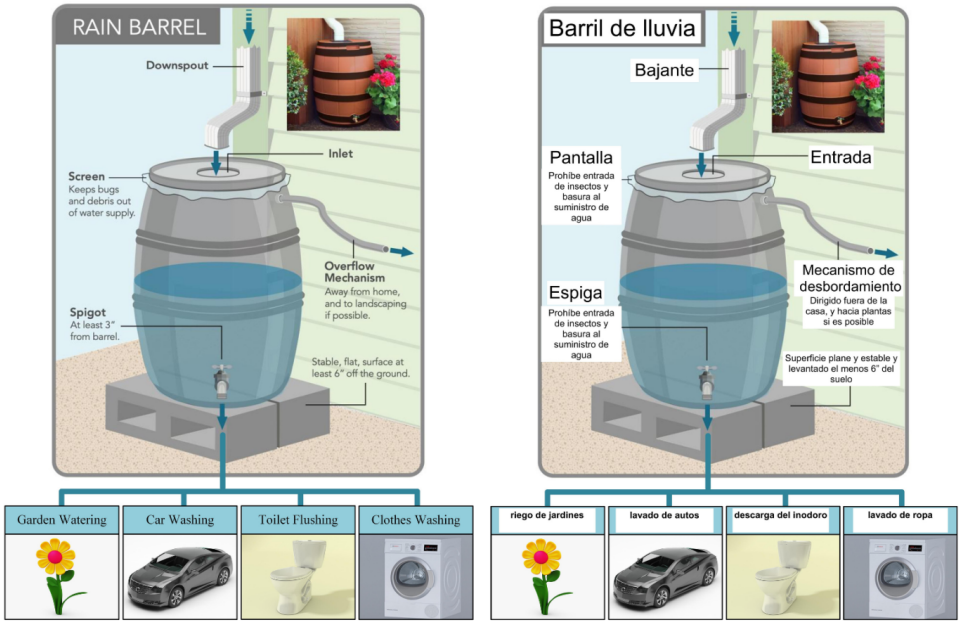

Rain Gardens.
Rain gardens are small, shallow, sunken areas of plantings that collect stormwater runoff from roofs, streets, and sidewalks. Also known as Bioretention cells, they are created to imitate the natural ways water flows over and absorbs into the land to reduce stormwater pollution.
-United States Environmental Protection Agency (EPA)

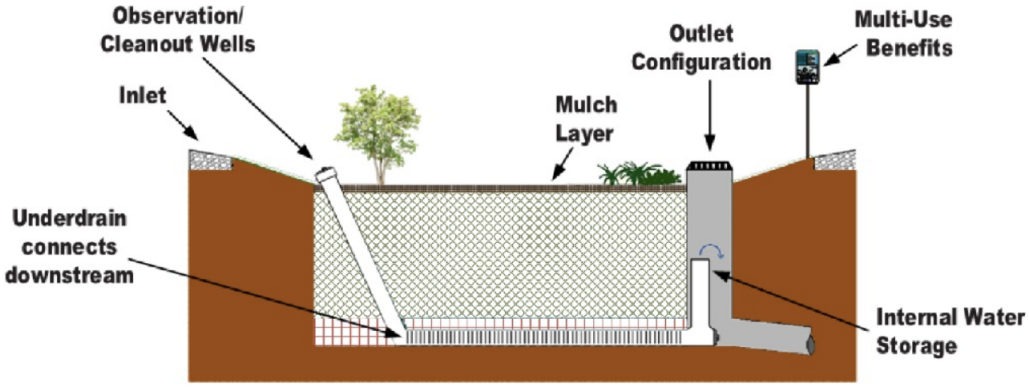

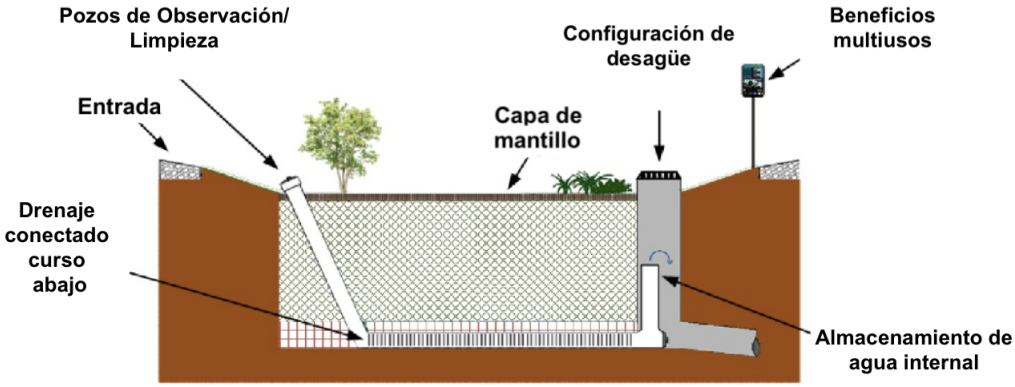

Q6. Please guesstimate your **monthly water bill** in U.S dollars:

Low High

0 50 100 150 200 250 300 350 400 450 500

Monthly water bill:

Q7. Would you be interested in receiving an **incentive** (such as a rebate on your water bill) for participating in rain barrel practices?

- Yes
- No

Q8. Please tell us why you chose your prior response:

Q9. Would you be interested in receiving an **incentive** (such as a rebate on your water bill) for participating in rain garden practices?

- Yes
- No

Q10. Please tell us why you chose your prior response:

Q11. How much of a **financial incentive** would you need to install a rain barrel in your residence and/or business in U.S dollars:

0 40 80 120 160 200 240 280 320 360 400

Financial incentive:

Q12. How much of a **financial incentive** would you need to install a rain garden in your residence and/or business in U.S dollars:

0 40 80 120 160 200 240 280 320 360 400

Financial incentive:

Q13. If you were to start using a rain barrel, which of the following would you use the harvested water for? (select all that apply)

	Yes	No	Maybe
Watering plants and/or lawn	○	○	○
Laundry	○	○	○
Toilet flushing	○	○	○

Q14. If you were to start using a rain garden, which of the following potential benefits interest you? (select all that apply)

	Yes	No	Maybe
Reducing water pollution	○	○	○
Preventing flooding	○	○	○
Beautiful low-maintenance landscape	○	○	○
Helping your community save millions of dollars in pollution clean-up and expensive stormwater projects	○	○	○

Q15. At your residence or business, how many times per week do you **water your lawn and/or plants**?

- ○ Everyday
- ○ Once per week
- ○ 2 or more times per week
- ○ Every other week
- ○ Never

Q16. At your residence or business, how many times per week do you do **laundry**?

- ○ Everyday
- ○ Once per week
- ○ 2 or more times per week
- ○ Every other week

○ Never

Q17. Do any of the following interest you? (select all that apply)

	Yes	No	Maybe
Learning how to make my own rain barrel	○	○	○
Receiving a rain barrel for free	○	○	○
Information on building your own rain garden	○	○	○
Educational resources on RWH practices	○	○	○

Q18. After reviewing the previous questions, on a scale of 1-5 (1 being extremely unlikely and 5 being extremely likely), how likely are you to install a rain barrel or rain garden into your house or building?

Likelihood: ☐

Q19. Do you have any concerns about integrating rain water harvesting interventions into your residence and/or business?

Q20. Is there anything else you would like to share with us about your views on flooding and prevention in IB?

Video.
Interested in learning more about storm water pollution and prevention? Here is a quick 2 minute video!

Block 1

Thank you. By pressing the arrow button below, you will have completed our survey.

Powered by Qualtrics